EXAMINING THE ROLE OF PRDM13 IN DORSAL INTERNEURON SPECIFICATION

APPROVED BY SUPERVISORY COMMITTEE

_____
Jane Johnson, Ph.D.

_____
Raymond MacDonald, Ph.D.

_____
Sean Morrison, Ph.D.

_____
Jiang Wu, Ph.D.

I dedicate this work to my family,

mom, dad, Adriana, Eduardo, Scott, Patricia and Lily,

for their support, advice, sacrifice and unconditional love.

I could not have done it without you.

And to Abuela,

I know you were with me every step of the way.

EXAMINING THE ROLE OF PRDM13 IN DORSAL INTERNEURON SPECIFICATION

by

ANA CRISTINA URUENA

DISSERTATION

Presented to the Faculty of the Graduate School of Biomedical Sciences

The university of Texas Southwestern Medical Center at Dallas

In Partial Fulfillment of the Requirements

For the Degree of

DOCTOR OF PHILOSOPHY

The University of Texas Southwestern Medical Center

Dallas, Texas

August, 2016

EXAMINING THE ROLE OF PRDM13 IN DORSAL INTERNEURON SPECIFICATION

ANA CRISTINA URUENA, Ph.D.

The University of Texas Southwestern Medical Center at Dallas, 2016

JANE JOHNSON, Ph.D.

PTF1A is a transcription factor transiently expressed as neural progenitor cells become post-mitotic and begin to express neuronal specific genes. PTF1A specifies these cells to become GABAergic (inhibitory) neurons while suppressing the glutamatergic (excitatory) program. A fundamental principle in bipotential fate decisions is the necessity to repress gene programs in the alternative fate. Our lab identified PRDM13, a zinc finger transcription factor and direct downstream target of PTF1A that may serve this function in the inhibitory/excitatory neuron fate choice. Overexpression of PRDM13 in chick neural tube shows it represses markers of the excitatory neuronal lineage. To explore PRDM13 function *in vivo* and expand these findings to regions outside the neural tube, a $Prdm13^{GFP\_KI}$ and $Prdm13^{\Delta ZF}$ mutant mouse strains was generated and are null for PRDM13 expression. These mice die neonatally and at E10.5 show an

increase in the dorsal neural tube excitatory neuron population at the expense of the inhibitory neurons. These phenotypes recapitulate that seen in *Ptf1a* null mice. These models have revealed additional insights into the function of PRDM13 in the developing spinal cord. First, PRDM13 negatively regulates *Ptf1a* providing a mechanism for downregulating PTF1A as development progresses. Second, in contrast to the phenotype seen with *Ptf1a* mutants, late stage mutant embryos show only a partial loss of the inhibitory interneuron population, possibly due to the higher levels of PTF1A in these mutants. Finally, ChIP-Seq and RNA-Seq analysis of heterozygote vs homozygote *Prdm13* mutants revealed a novel function of PRDM13 to keep neuronal subtype specification genes for the ventral neural tube suppressed in the dorsal region. These mouse models has placed PRDM13 in a pivotal role in the specification of neuronal subtypes in the spinal cord, a function that will likely extend to the retina and cerebellum where PRDM13 is also present.

TABLE OF CONTENTS

LIST OF FIGURES/TABLES/APPENDICES

LIST OF ABBREVIATIONS

AML	acute myeloid leukemia
ASCL1	achaete-scute homolog 1
ATOH1	atonal homolog 1
BAT	brown adipose tissue
bHLH	basic helix-loop-helix
BMP	bone morphogenic protein
Cas9	CRISPR associated protein 9
ChIP	chromatin immunoprecipitation
CNS	central nervous system
co-IP	co-immunoprecipitation
CRE	cis-regulatory elements
CRISPR	clustered regularly interspaced short palindromic repeats
CRX	cone-rod homeobox
D-V	dorsal-ventral
dI	dorsal interneuron
DLL1	deltalike1
DLL3	deltalike3
DNA	deoxyribonucleic acid
dP	dorsal progenitor
E	embryonic day
FACS	fluorescent-activated cell sorting
GAD	glutamic acid decarboxylase
GFP	green fluorescent protein
GLI	glioblastome protein
HD	homeodomain
HDAC	histone deacetylases
HMT	histone methyltransferase
IHC	immunohistochemistry
IP	immunoprecipitation
ISH	in situ hybridization
ISL	insulin gene enhancer protein
LBX1	ladybird homeobox 1
LHX	LIM/homeobox protein
LMX1B	LIM homeobox transcription factor 1-beta
MDS	myelodysplasic syndrome
MED	mediator complex subunit
MEF	myocyte enhancer factor
mRNA	messenger ribonucleic acid
MYOD	myogenic differentiation
MZ	mantle zone
NEUROG1/2	neurogenin1/2
NKX	NK homeobox protein
OLIG	oligodendrocyte transcription factor
OTX	orthodenticle homeobox

PAX2	paired box gene 2
PBS	phosphate buffered saline
PCR	polymerase chain reaction
POU	pituitary specific, octamer, Unc transcription factor
PRDM	PRD1-BF1 and RIZ homology domain containing protein
PTF1A	pancreatic transcription factor 1a
PTF1	PTF1A forms a transcriptional complex with an E-protein and RBPJ
RBPJ	recombining binding protein suppressor of hairless
SET	suppressor of variegation 3-9, enhancer of zeste and trithorax
SHH	sonic hedgehog
SOX	SRY (sex determining region Y)-box 2
TF	transcription factor
TLX	T-cell leukemia homeobox protein
Ucp1	uncoupling protein 1
vGLUT2	vesicular glutamate transporter 2
VZ	ventricular zone
WAT	white adipose tissue
Wnt	wingless-type MMTV integration site family member
ZF	zinc-finger
ZFN	zinc-finger nuclease

CHAPTER ONE

Introduction

I. Role of the dorsal spinal cord in signal processing and somatosensation

The spinal cord serves as the integration center for sensory signals from the periphery. Inputs such as touch, pain and proprioception arrive at the dorsal horn of the spinal cord and are relayed to the supraspinal brain regions or processed locally as a reflex (Liu and Ma, 2011; Ross, 2011). The neuronal populations residing within the dorsal horn play an essential role in modulating these inputs through a system of inhibitory and excitatory neurons receiving sensory stimuli from primary sensory neurons innervating different regions throughout the body. While the excitatory interneuron population serves an amplifying effect, the inhibitory population attenuates these signals, and the interplay of these populations allows proper interpretation of sensory inputs from the periphery. Changes in the balance of excitatory/inhibitory interneurons within the spinal cord can lead to detrimental effects and a variety of disorders such as allodynia and hyperalgesia (Fitzgerald, 2005; Tavares and Lima, 2007). Given the importance of maintaining proper balance of the excitatory/inhibitory interneurons, much effort has been invested in understanding the genetic pathways that regulate specification of these populations during neurogenesis. While studies have focused on the key roles played by individual basic helix-loop-helix (bHLH) transcription factors (TFs) and homeodomain (HD) TFs in determining the cell fate of the multipotent progenitors residing within the spinal cord, it remains challenging to gain a comprehensive understanding of the wide range of effects these may have on the populations in which they are expressed. Here, I characterize the role of PRDM13, a member of

the PRDM family of proteins, on the specification of the dorsal interneuron populations of the spinal cord. PRDM13 plays a crucial role in providing precision to the interneuron populations of the dorsal spinal cord through broad suppression of genes specifying alternative cell fates.

II. Multiple signals govern developmental fate decisions

Decades of work have been invested in understanding the process by which naïve progenitors are driven to a specific cellular identity. Initial patterns of body and organ axis are determined by the expression of morphogens from a specific source outside of the affected cell populations. Morphogens are diffusible molecules produced by a specific source and affect individual cells differently depending on their distance from the source, due to the concentration of the morphogen they are exposed to (Green and Smith, 1991; Lewis et al., 1977; Wolpert, 1996). The number of receptors activated by the graded signal influences the gene expression programs of individual cells, allowing for determination of morphogen-dependent patterns within specific tissues. Moreover, temporal restriction of morphogen expression also affects the number and types of receptors activated during this process (Ashe and Briscoe, 2006; Balaskas et al., 2012; Dyson and Gurdon, 1998; Junker et al., 2014; Shimizu and Gurdon, 1999; Stamataki et al., 2005; Wilson et al., 1997; Zecca et al., 1996). While these inputs determine initial tissue patterning, their importance lays within their capacity to regulate expression of distinct sets of transcription factors, causing a regulatory cascade that determines cell identity.

Recent work has focused on gaining a deeper understanding of how the cell interprets morphogen signals and how graded signals affect gene regulation. Studies performed in *Drosophila melanogaster* and spinal cord patterning have highlighted two important functions of morphogens: activation of gene sets for specific cell programs, while repressing genes for the

opposite “default” programs within a specific tissue (Briscoe and Small, 2015; Chiang et al., 1996; Litingtung and Chiang, 2000; Wijgerde et al., 2002). One confounding finding to this straightforward understanding of morphogens has been the fact that their absolute concentration thresholds do not seem to strictly define the gene sets they regulate. This becomes clear when heterozygotes expressing only half the protein product as compared to wild-type counterparts are capable of surviving and developing normally (Driever and Nusslein-Volhard, 1988; Liu et al., 2013; Struhl et al., 1989). This suggests the sensitivity to morphogen inputs is flexible and other factors must be important in regulating their activity.

Studies seeking to clarify how morphogen concentration affects gene expression have found that multiple TFs, functioning as transcriptional activators, are capable of binding to cis-regulatory elements (CREs) and modulate the response to morphogen signaling (Liang et al., 2008; Oosterveen et al., 2012; Peterson et al., 2012; Xu et al., 2014). Moreover, precise cellular identity appears to come from expression of local repressing transcription factors under the control of morphogens or other downstream TFs counteracting broad activating signals (Clyde et al., 2003; Kraut and Levine, 1991; Kutejova et al., 2016; Nishi et al., 2015; Novitch et al., 2001; Vallstedt et al., 2001). Analysis of the transcriptional profile of several ventral factors found that SOX2 and GLI1, direct targets of the ventral neural tube morphogen SHH, function as broad activators for transcriptional programs specifying multiple progenitor domains. Specificity is only gained through activity of repressors, which suppress alternative fates in their expression domains. SHH stimulates expression of the transcriptional repressors NKX2.2, NKX6.1 and OLIG2, which suppress the alternative fates within their specific domains, allowing for specification of the p2, p3 and pMN domains (Kutejova et al., 2016; Nishi et al., 2015).

Additionally, broadly expressed activators can be directed to specific CREs by the action of tissue-specific co-factors. These broadly expressed factors can be re-directed from their canonical binding sites to regulate tissue specific genes by action of these associated co-factors, revealing a mechanism by which they can now function in specification of particular cell types through combinatorial regulation of tissue specific enhancers (Andzelm et al., 2015). In the developing retina, the ubiquitously expressed TF MEF2D is recruited away from canonical MEF2 binding sites by the retina-specific TF CRX. MEF2D is now directed to bind at enhancer sites for genes essential for retinal development, and can only be recruited to these regions by action of CRX, given that these sites lack canonical MEF2 binding sites. Together, these factors form a co-activator complex that allow transcription of these genes and, therefore, proper retinal development (Andzelm et al., 2015).

Once patterning has been established, the combinatorial action of morphogens, broadly expressed transcriptional activators, tissue specific co-factors and local repressors determine the transcriptional profile of individual cell populations. This allows for establishment of a particular cellular identity that will activate downstream genetic cascades and see a particular population to its ultimate fate during embryogenesis. One interesting aspect of the differentiation process is the accuracy with which these identities are established. Overexpression studies and development of numerous knockout models in a variety of tissues have found that a multipotent progenitor is rarely specified to a "mixed" fate upon loss or ectopic expression of particular factors. Most often, these factors serve as cell fate switches that push progenitors towards one defined identity, which is reinforced through positive feedback networks for factors determining a particular lineage (Bertrand, 2016; Cau and Blader, 2009; Chang et al., 2013; Costamagna et al., 2014; Dalton, 2013; Ferrell, 1999; Graham et al., 2010; Sunadome et al., 2014).

A class of factors that play a pivotal role in cell fate decision have been determined to be "master regulators". This term has evolved since its initial conception to include a particular subset of factors with the capacity to restrict cells to a lineage through regulation of a battery of genetic targets and is capable of reprogramming another cell type to this lineage upon misexpression (Chan and Kyba, 2013). Specificity is further achieved by the convergence of multiple gene expression programs allowing for specific cell identities to be achieved (Pimanda et al., 2007; Trompouki et al., 2011). One "master regulator" that has been studied extensively is the bHLH TF MyoD. Absence of MyoD expression leads to a complete loss of myogenesis, while ectopic expression of MyoD leads to transdifferentiation of fibroblasts to myoblasts (Davis et al., 1987; Rudnicki et al., 1993). Its initial expression is influenced by several morphogen signals such as BMP4, Sonic hedgehog (Shh) and Wnt. In order to be capable of driving the myogenic program, MyoD has been found to bind to DNA in a sequence specific manner to control cell cycle regulation, activate a feed-forward program to promote sustained MyoD expression, mediate broad changes in histone modifications and activate/repress numerous genes to specify the myogenic program (Blackwell and Weintraub, 1990; Gustafsson et al., 2002; Tapscott, 2005; Teboul et al., 2003; Thayer et al., 1989; Weintraub et al., 1991). Several studies have found that cooperative binding and interaction with co-factors grant specificity to MyoD binding throughout the genome directing it to particular gene targets (Biesiada et al., 1999; de la Serna et al., 2001; Knoepfler et al., 1999; Molkentin et al., 1995; Puri et al., 1997). These principles have been found to be common with many master regulators, providing insight on how it is possible for one factor to drive a bimodal fate decision, such as whether or not to become a myoblast.

III. Multiple transcription factors direct cell fate decisions in the dorsal spinal cord

During neurogenesis, following neural tube closure, initial dorsal-ventral (D-V) patterning in the spinal cord is established through opposing morphogen signals, Wnt and BMP dorsally from the roof plate, and Shh ventrally from the floor plate and the notochord (Cauthen et al., 2001; Hollyday et al., 1995; Parr et al., 1993). Each morphogen plays a specific role in establishing D-V cell identities within the spinal cord. Loss of Wnt signaling leads to a loss of dorsal identities and alteration of cell cycle regulation (Megason and McMahon, 2002; Muroyama et al., 2002). BMP antagonizes Shh signaling from the ventral spinal cord, while also influencing progenitor proliferation and dorsal identities (Barth et al., 1999; Mekki-Dauriac et al., 2002; Wine-Lee et al., 2004). Lastly, Shh is required for specification of ventral subtypes and stimulates progenitor proliferation (Ahn and Joyner, 2005; Ericson et al., 1997; Lai et al., 2003; Machold et al., 2003; Palma et al., 2005). During this process, two distinct populations are established within the spinal cord, proliferating progenitors in a region named the ventricular zone, and post-mitotic neurons in an area named the mantle zone. The progenitor population gives rise to neurons, oligodendrocytes and astrocytes at different temporal windows throughout neurogenesis (Merkle and Alvarez-Buylla, 2006). Initial pattern establishment by the morphogen factors allow for expression of several bHLH TFs within the progenitors of the ventricular zone in a restricted fashion, which stimulate specific progenitor subpopulations to their ultimate fate. The restricted manner in which the bHLH TFs are expressed allow for further classification of the ventricular zone progenitors into dorsal progenitor (dP) domains 1-6. Once the cells become postmitotic and move into the mantle zone, they are divided into dorsal interneuron (dI) populations 1-6 (Helms and Johnson, 2003; Murre et al., 1994).

1. ASCL1 specifies the excitatory program within the dorsal spinal cord

ASCL1 is a member of the bHLH family of TFs. These proteins are categorized by their characteristic structure, containing two alpha helices joined together by a polypeptide loop, and a basic amino acid chain essential for interaction with DNA. Within this superfamily, several classes have been defined depending on their interacting partners and ability to bind DNA. Class I bHLH proteins are E-proteins that are expressed ubiquitously and homodimerize or heterodimerize with Class II bHLH factors. Class II factors are expressed in a tissue-specific fashion, form heterodimers with Class I bHLH proteins, bind to the E-box sequence "CANNTG", and regulate a host of genetic targets to exert their function (Murre et al., 1994). ASCL1 is an ortholog of the *Drosophila* Achaete-scute genes, which interacts with the Class I bHLH E12 and interacts with DNA binding to the preferred motif "CAGCTG" through its basic domain activating its transcriptional targets (Fig. 1-1) (Borromeo et al., 2014; Castro et al., 2006; Johnson et al., 1992).

During the onset of neurogenesis at E10.5, ASCL1 expression is constrained to the dP3-dP5 domains of the dorsal spinal cord (Fig. 1-2). At this time, further expression can be found in multiple regions of the CNS such as the diencephalon, telecephalon, mesencephalon and myencephalon (Johnson et al., 1990; Kim et al., 2008; Lo et al., 1991; Verma-Kurvari et al., 1996). Gain of function studies performed through chick electroporation assays found that overexpression of ASCL1 causes the progenitor population to move out of the ventricular zone into the mantle zone. Additionally, these cells become postmitotic and begin to express markers for mature neurons (Nakada et al., 2004).

Additionally, ASCL1 plays a crucial role in maintaining the proportion of progenitor cells within the ventricular zone through activation of the Notch pathway. ASCL1 directly activates expression of the genes encoding the Notch ligands Delta1 and Delta3 (DLL1 and

DLL3), which are transcribed in ASCL1-expressing cells. DLL1 interacts with Notch receptors on the cell surface of adjacent cells, resulting in cleavage of the Notch intracellular domain, which in turn activates expression of *Hes* genes. HES proteins such as HES1 bind to regulatory regions controlling proneural gene expression, such as *Ascl1*, suppressing their expression and maintaining these cells as progenitors (Castro et al., 2006; Henke et al., 2009; Kageyama et al., 2005).

Consistent with its role in neuronal differentiation, ASCL1 is a "master regulator" for specification of the neuronal fate. Ectopic expression of ASCL1 in terminally differentiated cells leads to direct reprogramming to neurons (Marro et al., 2011; Vierbuchen et al., 2010). The mechanism by which this ASCL1 function occurs is thought to be through its capability as a pioneering factor. Analysis of ASCL1 binding through the use of ChIP-Seq found it is capable of binding its genomic targets regardless of whether the chromatin state hinders accessibility (Wapinski et al., 2013). Thus, in some cases ASCL1 is capable of displacing nucleosomes to activate transcriptional targets and stimulate conversion to the neuronal fate.

Aside from its role in interneuron differentiation, loss of function studies have found ASCL1 plays a role in dorsal spinal cord interneuron specification. Even though ASCL1 is expressed in progenitors to the dI3 through dI5 populations, absence of ASCL1 causes a decrease in the number of TLX1/3+ (dI3/5) cells within the dorsal spinal cord, suggesting ASCL1 is required for specification of the dI3 and dI5 populations, and not dI4. This loss is accompanied by an expansion of the dI4 population, as seen by the increase of PAX2+ (dI4) neurons. Moreover, ASCL1 overexpression causes ectopic expression of TLX1/3 in electroporated cells in the chick neural tube at the expense of the PAX2+ population (Chang et al., 2013; Helms et al., 2005; Mizuguchi et al., 2006; Wildner et al., 2006). TLX1, TLX3 and

PAX2 are HD TFs required for subtype specification of the postmitotic dorsal interneuron populations. TLX1 and TLX3 are essential for specification of the excitatory fate in the dI3/5 interneurons, while PAX2 is necessary for specification of the dI4 inhibitory interneurons. Further studies have determined *Tlx3* is directly regulated by ASCL1 and *Pax2* is directly regulated by another bHLH TF, PTF1A (Fig 1-2, 1-4). Loss of the HD TFs leads to hindering specification of the dI populations to their ultimate excitatory or inhibitory fates (Cheng et al., 2004; Cheng et al., 2005; Glasgow et al., 2005).

2. PTF1A specifies the inhibitory lineage in the CNS

PTF1A is a member of the Class II bHLH TFs with transient expression during embryonic development in multiple regions of the central nervous system (CNS). Unlike ASCL1, PTF1A forms a functional trimer, the PTF1-J complex, along with an E-protein and the TF RBPJ. The trimer requires not only the presence of an E-box sequence, but also an adjacent TC-box (TTTCCCA), with a spatially constricted separation between both sequences (Fig. 1-1) (Beres et al., 2006; Cockell et al., 1989; Henke et al., 2009; Hori et al., 2008; Krapp et al., 1996; Masui et al., 2007; Obata et al., 2001; Rose and MacDonald, 1997). Loss of the PTF1A interaction with RBPJ through a point mutation in PTF1A phenocopies the *Ptf1a* null mouse model, suggesting trimer formation is required for PTF1A function in the development of the spinal cord (Hori et al., 2008). PTF1A is expressed in the dorsal neural tube, cerebellum, diencephalon and retina during neurogenesis. Additionally, a 2.3 kb autoregulatory enhancer for directing PTF1A expression in all positive tissues was identified by testing evolutionarily conserved regions surrounding the *Ptf1a* gene. Loss of PTF1A binding to this enhancer causes

ablation of PTF1A expression, demonstrating this region is required for autoregulatory activity (Meredith et al., 2009).

PTF1A is expressed in the ventricular zone of the developing cerebellum, giving rise to the GABAergic lineage in this tissue. Mice lacking PTF1A expression causes ablation of the Purkinje, Golgi and deep cerebellar nuclei neurons, all of which are from the GABAergic lineage. Moreover, *Ptf1a* mutants show ectopic expression of glutamatergic neurons in the cerebellum (Hoshino et al., 2005; Millen et al., 2014; Pascual et al., 2007). Lineage trace experiments show these ectopic glutamatergic cells are produced from the *Ptf1a* lineage; therefore, PTF1A expression is required for suppression of the glutamatergic fate in these cells. The GABAergic neurons produced from PTF1A expressing progenitors are also positive for PAX2 expression, which is lost in the *Ptf1a* null mouse cerebellum (Millen et al., 2014; Pascual et al., 2007).

In the E10.5 neural tube, PTF1A is localized to newly post-mitotic cells exiting the ventricular zone in a subset of dorsally restricted cells. Moreover, absence of PTF1A results in a decrease in PAX2+ and an increase in TLX1/3+ neurons within the dI4 domain (Fig. 1-4). Additionally, examination of *Ptf1a* null neural tubes at E16.5 shows a loss of the GABAergic population, as observed through *in situ* hybridization with a probe against *Gad1*. Conversely, there is an increase in the glutamatergic population, as seen in the increase in cells positive for V*glut2* (Glasgow et al., 2005). Further studies found PAX2 to be a direct downstream target activated by PTF1A (Fig. 1-2, 1-4) (Borromeo et al., 2014; Meredith et al., 2013). These results are the converse of the ASCL1 phenotype, suggesting these bHLH TFs specify opposite developmental programs for the excitatory and inhibitory interneuron populations within the dorsal spinal cord.

In E14.5 retina, lineage trace experiments find the *Ptf1a* lineage contributes to the amacrine and horizontal cells of the outer neuroblastic layer of this tissue. PTF1A expression is detected within post-mitotic cells in the retinal ventricular zone within the developing retina. Absence of PTF1A expression shows a dramatic loss of inhibitory neurons in retina including the horizontal neurons and GABAergic and glycinergic amacrine neurons. PTF1A overexpression resulted in an increase in GABAergic horizontal and amacrine cells, with a corresponding decrease in the number of excitatory ganglion cells. Lastly, *Ptf1a* null cells undergo a fate switch and become ganglion cells upon in mice lacking PTF1A (Dullin et al., 2007; Fujitani et al., 2006; Nakhai et al., 2007). These data suggest that as in the spinal cord and cerebellum, PTF1A functions to specify a particular cell fate program in the retina while suppressing the alternative fate. Moreover, PTF1A is required for specification of the inhibitory interneuron lineages within the retina, as it does in the spinal cord and cerebellum.

PTF1A expression in the pancreas is restricted to progenitors that give rise to both endocrine and exocrine cells as well as differentiated cells of the acinar lineage (Burlison et al., 2008; Fukuda et al., 2008; Kawaguchi et al., 2002; Krapp et al., 1998). This dual function of PTF1A in the pancreas is due to differential expression levels of the protein. While low levels of PTF1A seem to be required for the maintenance of the progenitor population, high levels are necessary for exocrine lineage specification (Dong et al., 2008; Fukuda et al., 2008). Absence of PTF1A causes a loss of the exocrine lineage, suggesting it is required for differentiation of this cell type. Interestingly, *Ptf1a* knockout mice show the endocrine progenitors are specified to spleen, suggesting PTF1A is required for specification of the endocrine lineage as well (Krapp et al., 1998; Zecchin et al., 2004). Moreover, PTF1A loss causes the pancreatic progenitor cells to adopt a duodenal fate (Fukuda et al., 2008; Kawaguchi et al., 2002). Upon birth, PTF1A

expression is sustained in the acinar lineage of the mature pancreas (Krapp et al., 1996). PTF1A binds to genes required for specification of the exocrine acinar pancreas cells and activates their expression (Cockell et al., 1989; Masui et al., 2007; Rose et al., 2001). Mutations in human *Ptf1a* lead to pancreatic and cerebellar agenesis and this phenotype was recapitulated in a PTF1A knockout mouse model as well (Kawaguchi et al., 2002; Krapp et al., 1998; Sellick et al., 2004; Sellick et al., 2003; Tutak et al., 2009). While PTF1A requires trimer formation in order to exert its function, in pancreas it is capable of interacting with both RBPJ and the related factor, RBPJL. Dynamic interactions with these factors add another layer of complexity in PTF1A function. Early in pancreatic development PTF1A interacts with RBPJ allowing for its function in pancreatic progenitors. This complex binds to the promoter of the *Rbpjl* gene activating its transcription and upon accumulation of the RBPJL protein, RBPJL substitutes for RBPJ within the trimer, and it is this complex that functions in acinar specification (Masui et al., 2007; Masui et al., 2010). Through these mechanisms, PTF1A is capable of functioning in both neuronal and pancreatic specification.

3. PRDM13 is a downstream target of PTF1A required for antagonizing ASCL1 activity in the dP4 population

While ASCL1 is present in the dP3, dP4 and dP5 progenitor domains, PTF1A expression is restricted to the dP4 population cells. These factors activate gene programs specifying opposing cell fates. Ultimately, the dP4 progenitors will become inhibitory interneurons while the dP3/5 populations become excitatory. This leads to a model in which progenitors expressing both ASCL1 and PTF1A must be capable of repressing expression of the genes specifying the excitatory fate while activating the inhibitory gene program (Beres et al., 2006; Borromeo et al., 2014; Glasgow et al., 2005; Helms et al., 2005; Hori et al., 2008; Krapp et al., 1996; Krapp et al.,

1998; Masui et al., 2008; Mizuguchi et al., 2006). *In vivo* analysis using ChIP-Seq and RNA-Seq of transcriptional targets for PTF1A identified a novel factor, PRDM13, as the downstream effector of PTF1A functioning to suppress the excitatory program within the dP4 population (Fig. 1-4) (Chang et al., 2013).

PRDM13 is a member of the PRDM family of proteins, characterized by a PR domain followed by a variable number of zinc-finger (ZF) domains. This family is composed of 16 orthologs in mice and 17 in humans (Fig. 1-3). PRDM11 is the only member that does not contain zinc-finger domains. These regions play important roles in mediating interaction with DNA and other proteins. The PR domain is 30% homologous to the catalytic SET domains found in *Drosophila,* which has histone methyltransferase activity (HMT) to mediate transcriptional silencing. The catalytic SET domains contain a conserved H/RxxNHxC domain and when mutated the intrinsic HMT activity is abolished (Rea et al., 2000). The PR domain of the PRDM family of TFs does not possess this conserved sequence, which is interesting given some members have been reported to have intrinsic HMT activity mediated through their PR domain. The PRDM factors function in a variety of cell types to promote cell proliferation or cell type specification (Di Zazzo et al., 2013; Fog et al., 2012; Hohenauer and Moore, 2012). Of all members, PRDM2, PRDM3, PRDM6, PRDM8, PRDM9 and PRDM16 have been reported to have intrinsic HMT activity mediated through the PR domain of the protein (Eom et al., 2009; Eram et al., 2014; Huang et al., 1998; Pinheiro et al., 2012; Wu et al., 2013; Wu et al., 2008). Additional variability is added by the generation of alternative isoforms with distinct functions and activity through alternative splicing or use of alternate promoters (Di Zazzo et al., 2013). Those PRDM members that lack intrinsic HMT activity depend on the recruitment of co-factors that are necessary for their function (Bikoff et al., 2009; Chittka et al., 2012; Ross et al., 2012).

An interesting example of the complexity of structure and function of the PRDM protein family is PRDM16. PRDM16 has been extensively studied for its role in brown fat specification (Chi and Cohen, 2016; Cohen et al., 2014; Fruhbeck et al., 2009; Harms et al., 2014; Kajimura et al., 2008; Kinameri et al., 2008; Seale et al., 2011; Seale et al., 2007). This process requires interaction with MED1 at specific sites for brown fat selector genes and changes the chromatin architecture to regulate gene expression (Harms et al., 2015; Iida et al., 2015). Specifically, regulation of *Ucp1* is essential for the PRDM16 specification function in brown fat cells (Iida et al., 2015). Although PRDM16 has been found to have intrinsic HMT activity (Pinheiro et al., 2012), deletion of the PR domain does not affect its function in brown fat specification (Kajimura et al., 2009; Kajimura et al., 2008; Ohno et al., 2012; Seale et al., 2008), demonstrating the significance of its HMT activity *in vivo* is not well understood. Aside from its role in development, PRDM16 has been implicated in acute myeloid leukemia (AML) and myelodysplastic syndrome (MDS) (Shing et al., 2007). Interestingly, study of these diseases in mouse models has found that of the four potential PRDM16 isoforms, only expression of those lacking the PR domain seem to harbor pathogenic properties (Du et al., 2005; Nishikata et al., 2003). Moreover, studies performed in human tissue have found that PRDM16 translocations are capable of generating a number of PRDM16 chimeric proteins lacking the PR domain, and patients with AML/MDS positive for these translocations have a poor prognosis (Duhoux et al., 2012; Shing et al., 2007; Xinh et al., 2003). Therefore, depending on whether PRDM16 is being studied in the context of development or disease, its different domains take on specific functions that cannot be translocated to a different cellular setting, adding a layer of complexity to the study of this protein and forcing caution on how the data are interpreted.

Within the nervous system, there are several PRDM family members that play roles in specification of distinct cell types. In the developing retina, PRDM1 is required for specification of the photoreceptor over bipolar cell fate. While absence of PRDM1 in the developing photoreceptors causes an increase in the bipolar cell population, ectopic protein expression caused an increase in the number of photoreceptor cells at the expense of the bipolar cell population. Moreover, a regulatory feedback loop controlled by PRDM1 and OTX2, a marker for both bipolar and photoreceptor cells, is required for formation of a balanced population of both cell types (Brzezinski et al., 2010; Brzezinski et al., 2013; Katoh et al., 2010; Wang et al., 2014). PRDM8 plays multiple roles within the CNS. In the dorsal telencephalon, BHLHB5 binds to specific DNA regions and recruits PRDM8 to form a repressor complex. Absence of expression of either protein causes axonal mistargeting and loss of neuronal circuits (Ross et al., 2012). PRDM8 is expressed in multipolar neocortical neurons and absence of PRDM8 in this tissue causes an increase in the number of these cells, which fail to acquire the bipolar morphology characteristic of more mature cells of the developing cortical plate (Inoue et al., 2014). Within the developing retina, PRDM8 is required for bipolar cell subspecification. Mice lacking PRDM8 show the bipolar cell population is unable to differentiate into rod and cone bipolar cells, resulting in a phenotype similar to congenital stationary night blindness (Jung et al., 2015). Lastly, within the developing spinal cord, PRDM12 has restricted expression in the ventral p1 progenitor domains and is required for specification of the v1 interneurons. It functions by recruiting the methyltransferase protein G9a to form a suppressor complex that represses genes specifying alternative neuronal fates (Thelie et al., 2015; Yang and Shinkai, 2013; Zannino et al., 2014). While a variety of PRDM family members had been characterized for their function within the spinal cord, the role of PRDM13 remained largely unknown.

In an attempt to identify the downstream target of PTF1A capable of actively suppressing the excitatory program in the dP4 progenitors, ChIP-Seq was performed for PTF1A and the list of binding sites was intersected with differentially expressed genes identified by RNA-Seq of mutant versus heterozygote *Ptf1a* lineage cells. Through this analysis PRDM13 was identified as a downstream target of PTF1A in the neural tube. Absence of PTF1A leads to a decrease in PRDM13 expression in PTF1A lineage cells (Chang et al., 2013).

Chick electroporation experiments were used to demonstrate PRDM13 function within the dorsal spinal cord. Ectopic expression of PRDM13 led to an increase in the PAX2+ population at the expense of the TLX1/3+ neurons, and recapitulated the phenotype seen in overexpression of PTF1A. To elucidate the epistatic relationship between PRDM13 and PTF1A, PRDM13 was knocked down as PTF1A was overexpressed. Under these conditions, the PTF1A phenotype was suppressed, consistent with PRDM13 function being downstream of PTF1A. Overexpression of truncated versions of the PRDM13 protein identified the zinc-finger domains as the minimal region required for PRDM13 function (Fig. 1-2, 1-4). Full-length PRDM13 was fused to either a VP16 activator or an Engrailed repressor sequence and electroporated into chick neural tubes. Engrailed-PRDM13 phenocopied the expansion of the PAX2+ population and a loss of the TLX1/3+ population observed during overexpression of PRDM13. These data suggested PRDM13 functions as a transcriptional repressor downstream of PTF1A to suppress the excitatory program in the dP4 population (Chang et al., 2013).

PRDM13 was also shown to repress ASCL1's ability to induce TLX1/3 in the chick electroporation assays (Chang et al., 2013). ChIP-Seq for PRDM13 and ASCL1 identified a common binding site upstream of *Tlx3*. A *eTlx3::GFP* construct is activated by ASCL1 and this activation is repressed by PRDM13 (Fig. 1-4). In addition, *in vitro* experiments found PRDM13

and ASCL1 are capable of interacting, suggesting they form a complex on the *Tlx3* enhancer in order to suppress ASCL1 activity. Taken together, these data suggest PRDM13 is the factor downstream of PTF1A capable of suppressing the ASCL1 program within the dP4 domain (Chang et al., 2013).

A separate study performed in *Xenopus* supported the model put forth in Chang et. al, 2013. In order to assess whether PRDM13 has intrinsic histone methyltransferase activity, *in vitro* assays were performed assessing the ability of PRDM13 to induce incorporation of radiolabeled S-adenosyl methionine, a methyl donor for this assay. PRDM13 was immunoprecipitated with antibodies against FLAG following expression of a FLAG-PRDM13 construct in HEK293 cells. Through this assay, expression of PRDM13 induced incorporation of the radiolabeled donor into the H3 subunit of core histones. This analysis lacked an assessment to determine if the PR domain of the protein was necessary for this activity, which would suggest this HMT activity to be intrinsic to PRDM13, and not the activity of an associate cofactor (Hanotel et al., 2014).

While the previous studies began to shed some light over the function of PRDM13 within the dorsal spinal cord, its function in other regions of the CNS remains unclear. Like PTF1A, PRDM13 is present in the developing cerebellum, diencephalon and retina as well (Chang et al., 2013). Recently, a function for PRDM13 in the retina was reported (Watanabe et al., 2015). Characterization of PRDM13 in the retina found it is restricted to GABAergic and glycinergic amacrine cells of the developing retina. In order to analyze its function within these cells, a mutant PRDM13 mouse model was generated through targeted deletion of the second and third exons of *Prdm13*. This model exhibited a lack of PRDM13 protein expression as detected through immunohistochemistry and Western blot analysis of retinal tissue. *Prdm13* mutant

retinas had an overall decrease of GABAergic and glycinergic amacrine cells. Moreover, *in vivo* electroporation of a construct encoding for *Prdm13* into the developing mouse retina found it is capable of inducing differentiation into the amacrine neuronal lineage. This activity is dependent on the expression of the zinc-finger domain of the protein, as expression of the PR domain alone could not recapitulate the phenotype observed with the full-length protein. These data suggest PRDM13 is required for specification of the amacrine lineage within the developing retina, sharing properties to that seen in the spinal cord (Watanabe et al., 2015).

IV. Remaining questions for PRDM13

While the studies discussed above begin to reveal the roles for PRDM13 in the CNS, several questions remain. The studies performed for PRDM13 in the neural tube made use of overexpression and knockdown assays. While informative, these findings would be more compelling with confirmation from alternative *in vivo* experiments. Here, *Prdm13* mutant mice were generated to allow the study of PRDM13 function in its endogenous domains. A group studying PRDM13 function in retina developed one mouse model, but determination of the phenotypes in the developing neural tube was not explored. It is necessary to examine this model and compare the results presented here with the potential effects seen in the neural tubes of these mice.

How PRDM13 functions mechanistically to influence cell fate, such as whether PRDM13 is capable of interacting directly with DNA to regulate its gene targets is unknown. Direct binding of PRDM13 to DNA is one possible mode of PRDM13 activity. An alternative model is PRDM13 recruitment to its targets by one or several co-factors, indicating a higher order transcriptional complex. In addition, it is still unclear whether PRDM13 possesses intrinsic HMT as suggested from *in vitro* assays. *In vitro* experiments found PRDM13 is capable of interacting

with ASCL1. It remains to be seen if this interaction occurs *in vivo* and whether PRDM13 can interact with other factors. Furthermore, identification of the protein domains required for interaction between PRDM13 and ASCL1 may be informative in understanding its mechanism of action. Here, I find PRDM13 can interact *in vitro* with another bHLH factor, PTF1A, which is expressed in the dorsal neural tube. Although these interactions have not been confirmed *in vivo*, I do find PRDM13 binding to a number of sites throughout the genome where PTF1A and ASCL1 bind. While no unique binding motif for PRDM13 was identified in this study, it is enriched at E-box motifs, where PTF1A and ASCL1 are known to bind. Additionally, we find PRDM13 enriched at SOX, RFX and NKX motifs, and we find a number of members of these families of factors expressed throughout the dorsal neural tube. Taken together, these results suggest a model in which PRDM13 is recruited to its genomic targets by interaction with ASCL1, PTF1A and, potentially, other transcription factors expressed within the neural tube.

PRDM13 expression is enriched in the dP4 domain, but there is broader expression of this protein within the progenitors to dP2-dP6 regions. The studies exploring PRDM13 function within the spinal cord focused on its role within the dP4 progenitors for specification of the inhibitory interneurons. *Prdm13* mouse mutants are used here to gain a broader understanding of the function of PRDM13 within the dorsal neural tube outside of its function in inhibitory neuronal fate decisions and how it may serve to specify other interneuron populations. I find *Prdm13* nulls present upregulation of ventral transcription factors in the dorsal neural tube, demonstrating it plays an essential role in restricting the expression of these factors to their appropriate domains. The mechanism by which PRDM13 exerts this variety of functions is still elusive, but through the data presented here I gain some insight on potential modes of function.

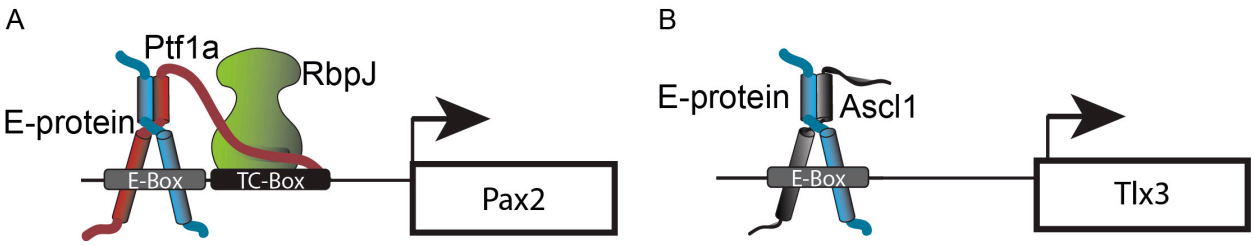

Figure 1-1. Class II bHLH factors form heterodimers with Class I bHLH factors
A. PTF1A forms the PTF1 trimer complex by interacting with E-protein and RBPJ to activate its transcriptional targets, such as *Pax2*.
B. ASCL1 forms a heterodimer with E-protein to activate its transcriptional target *Tlx3*.

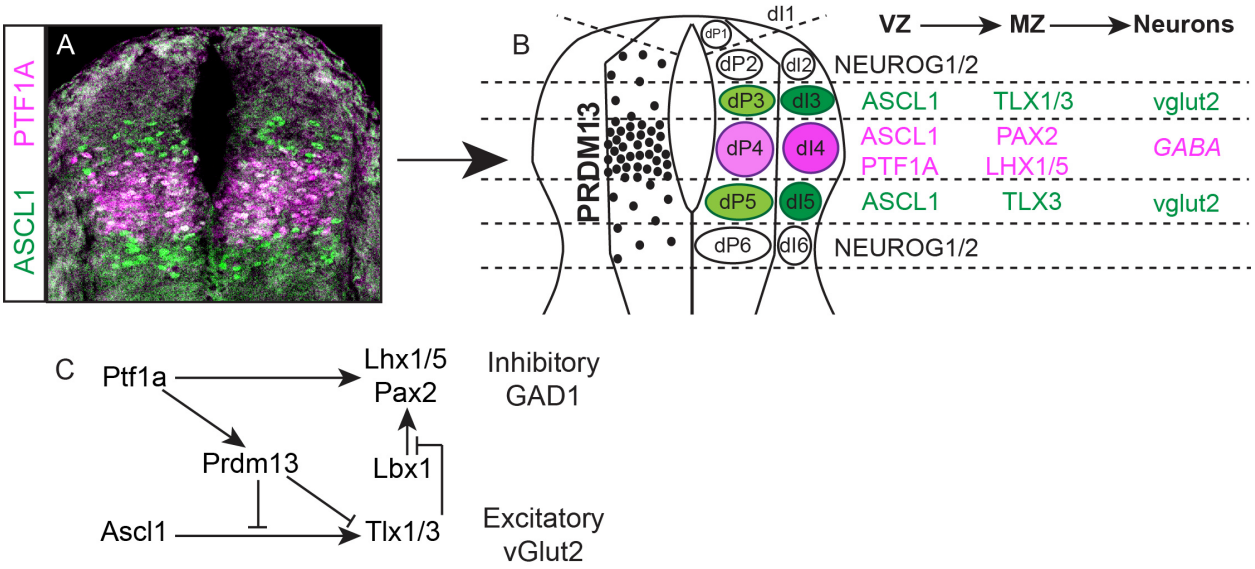

Figure 1-2. bHLH and HD transcription factor network controlling the inhibitory/excitatory neuron populations in the dorsal neural tube

A. Immunohistochemistry with antibodies against ASCL1 and PTF1A demonstrating the endogenous expression pattern of these factors within the dorsal spinal cord.

B. Diagram illustrating the domains for the dorsal progenitors (dP) and the dorsal interneurons (dI), along with the bHLH and HD transcription factors that define the populations.

C. Diagram illustrating the genetic relationships governing the specification of the excitatory and inhibitory interneuron populations in the dorsal spinal cord.

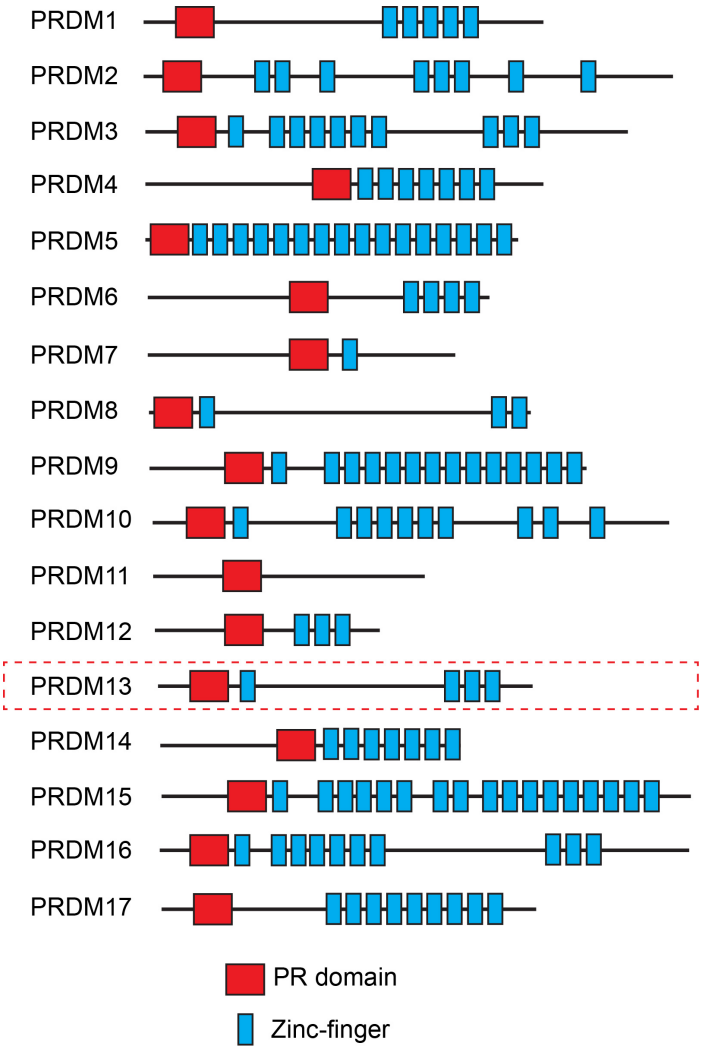

Figure 1-3. PRDM family of proteins
The PRDM proteins are characterized by an N-terminal PR domain and a varying number of zinc-finger domains. PRDM13 possesses four zinc-finger domains and is structurally most closely related to PRDM8 (Hohenauer and Moore, 2012).

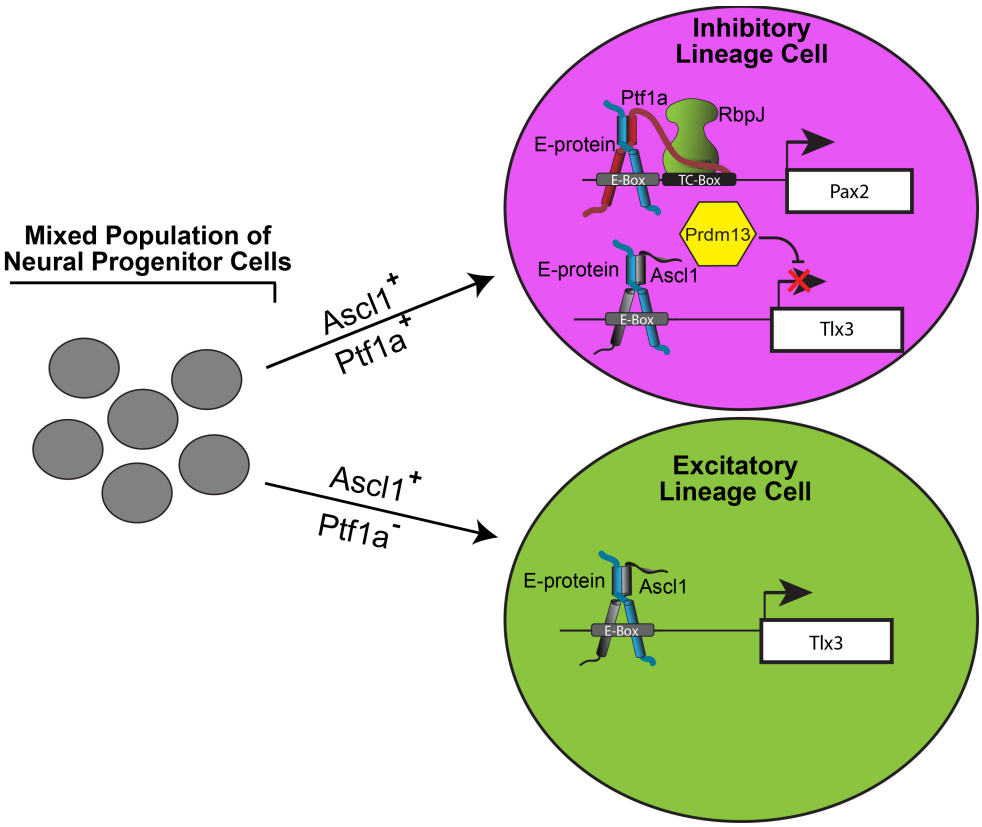

Figure 1-4. Specification of dorsal neural tube progenitors
The current model for dorsal interneuron specification involves a mixed progenitor population in the ventricular zone that gives rise to the excitatory and inhibitory neuronal populations. Progenitors in domains dP3 and dP5 expressing ASCL1 are specified to the excitatory lineage through activity of TLX3. Progenitors in dP4 expressing both ASCL1 and PTF1A are specified to the inhibitory lineage through PTF1A activation of genes for the inhibitory neuronal program, such as *Pax2*, and suppression of the excitatory program by PRDM13, which antagonizes ASCL1 activation of *Tlx3*.

CHAPTER TWO

Materials and Methods

Mouse strains

The *Prdm13*$^{GFP\_KI}$ and *Prdm13*$^{GFP\text{-}FUS}$ mutant mouse models were developed using zinc-finger nuclease technology (Fig. 3-1 and Appendix One). mRNA encoding two zinc-finger nuclease (ZFN) proteins targeting within the first exon of the *Prdm13* gene (CACCAGCGTGAACGCTGActgctGCATCCCGGCTGGCT) were purchased from Sigma-Aldrich and delivered by pronuclear injection into fertilized mouse eggs along with a donor plasmid. A first donor plasmid encoding GFP followed by a stop codon was co-injected with a second donor plasmid encoding GFP, each containing homology regions of 750 bp in length to allow for homologous recombination of the insert into the *Prdm13* locus (Figures 3-1). For *Prdm13*$^{GFP\_KI}$, out of 35 potential founders, 8 integrated the GFP coding region at the designed site. Two independently generated strains were bred and upon initial analysis were seen to have the same phenotype. These strains were interbred for all experiments shown here. For *Prdm13*$^{GFP\text{-}FUS}$ (PRDM13 with GFP fused near the N-terminus), out of 71 potential founders, 8 integrated the GFP coding region at the designed site. Two independently generated strains were bred and upon initial analysis were seen to have the same phenotype. These strains were interbred for all experiments shown here. Mice for both strains were genotyped by PCR with 5' -GCTGCTCCTGGTTCTGTCA- 3', 5' -CCTTTTCTCTGCTGCTCGTC- 3' and 5' -GCTGGAGTACAACTACAACAGCCA- 3' for wild-type (313 bp band size) and mutant (549 bp band size).

The *Prdm13*$^{\Delta 115}$ mutant line is a 115 bp deletion generated within the first exon of *Prdm13* upon injection of the same ZFN mRNA as described above. PCR genotyping used primers 5' -GCTGCTCCTGGTTCTGTCA- 3' and 5' -CCTTTTCTCTGCTGCTCGTC- 3' for both wild-type (313 bp band size) and mutants (200 bp band size). Other indel strains were generated and multiple lines with a frame shift mutation were bred (*Prdm13*$^{\Delta 34}$, *Prdm13*$^{\Delta 82}$ and *Prdm13*$^{\Delta 22}$). Similar to the *Prdm13*$^{\Delta 115}$ mutant line, all survived to adulthood. Only the *Prdm13*$^{\Delta 115}$ mutant line was maintained in the laboratory.

The *Prdm13*$^{\Delta ZF}$ and *Prdm13*^{V5} mutant mouse lines were generated by pronuclear injection of CAS9 mRNA, two sgRNA targeting the 3' end of *Prdm13*, and a 200bp ssOligo encoding for V5 with 76bp and 79bp homology on either arm. Out of 39 potential founders we obtained two lines of interest. One line has a 454 bp deletion in the fourth exon of *Prdm13*, that results in a protein truncated at amino acid 602 and deletes the three terminal zinc-fingers of the PRDM13 protein, adding 25 nonsense amino acids in the terminal portion of the protein. The second line was positive for homologous integration of the V5 sequence in the C-terminus of the PRDM13 protein. Once bred to homozygocity *Prdm13*$^{\Delta ZF}$ mice die at P0 and phenocopy all changes observed in the *Prdm13*$^{GFP\_KI/GFP\_KI}$ mutants at all developmental stages evaluated. Mice were PCR genotyped with 5' –GATCGCCATGCACACACAGC- 3' and 5' –CAATGAAGCCCTTCTTGT- 3' for both wild-type (617 bp band size) and mutants (207 bp band size). *Prdm13*^{V5} mutants survive to adulthood with no observable phenotypes as expected. Mice were PCR genotyped with 5' –GCCTATCCCTAACCCTCTCCTC- 3' and 5' –GTGATCCTGAACCTCAAGGCCAG- 3' for mutants (313 bp band size). The *Ptf1a*^{CRE} mouse line replaces the coding sequence for *Ptf1a* with that for *Cre* recombinase (Kawaguchi et al., 2002). Genotyping for this line was performed as previously described (Glasgow et al., 2005).

Tissue preparation, immunohistochemistry and *in situ* hybridization

All tissue (E10.5-E16.5) was dissected in ice-cold 0.1M sodium phosphate buffer pH 7.4 and fixed in 2% paraformaldehyde for 1 hour at 4° C. E16.5 spinal cords were dissected before fixing. Tissue was then washed three times in ice-cold 0.1M sodium phosphate buffer pH 7.4 for 15 minutes each and sunk overnight in 30% sucrose in PBS for E10.5 and E11.5 embryos, 15% sucrose in PBS for E12.5 embryos and 30% sucrose in water for E16.5 embryos. Tissue was embedded in Tissue-Plus O.C.T. compound (Fisher Healthcare) and cryosectioned at 20μm (E10.5-E11.5 tissue) and 30μm (E12.5-E16.5 tissue).

Immunofluorescence was performed using the following antibodies: guinea pig anti-PRDM13 (1:1000, gift from T. Furukawa), mouse anti-LHX1/5 (1:100, Developmental Studies Hybridoma Bank, CAT#4F2-s), rabbit anti-PAX2 (1:500, Invitrogen, CAT#71-6000), guinea pig anti-TLX1/3 (1:10000, gift from T. Müller and C. Birchmeier), guinea pig anti-PTF1A (TX507 1:10000, Johnson Lab), rabbit anti-OLIG2 (1:1000, Millipore, CAT#AB9610) and guinea pig anti-ASCL1 (TX518 1:10000, Johnson Lab). Imaging was performed with ZEISS LSM 510 confocal microscope. Cell quantification was performed with assistance of ImageJ software.

In situ hybridization was performed per standard protocols (Lai et al., 2011). Probes used were mouse *Prdm13* (Chang et al., 2013), mouse *Ptf1a* (gift from R. MacDonald), mouse *Prdm12* (gift from E. Bellefroid), mouse *Gad1* (gift from Qiu fu Ma) and mouse *Vglut2* (gift from Qiu fu Ma). Digoxygenin (DIG)-labeled antisense RNA probes (1-5 mg/mL) were hybridized overnight at 65° C, with the exception of the probe for *Vglut2* which was incubated at 60° C and that for *Gad1* incubated at 70° C. Sections were incubated with anti-digoxygenin AP antibody (Roche), and incubated with NBT/BCIP (Roche) for developing. Imaging was performed with a Hamamatsu Nanozoomer 2.0HT digital slide scanner.

mRNA isolation and RNA-Sequencing

Mouse neural tubes were dissected from E11.5 *Prdm13*$^{GFP\_KI}$ embryos either heterozygous or homozygous for GFP and placed into DMEM/F12 on ice and dissociated in 0.25% trypsin for 15 minutes at 37 degrees C. Trypsin activity was quenched with 2% fetal bovine serum, and GFP positive cells were purified from the resulting single cell suspension by fluorescence activated cell sorting (FACS). Total RNA from FACS isolated cells were extracted and purified with Zymo's Mini RNA Isolation Kit. mRNA was purified, reverse transcribed and amplified for sequencing with Illumina's mRNA-Seq kit according to manufacturer's instructions. Two independent libraries were sequenced for each cell population.

Chromatin isolation, immunoprecipitation and sequencing

Detailed descriptions of PTF1A and ASCL1 ChIP-Seq protocols were previously published (Castro et al., 2011; Meredith et al., 2013). 18 neural tubes from E11.5 mice were collected, as were telencephalon from the same embryos as a negative control. All ChIP buffers are listed below. Dissections were performed in ice cold PBS. Tissue was collected and placed into tubes with 1mL of buffer A. Tissue was dounce homogenized in buffer A then transferred to a 15mL tube with 10 mL of a 1:1 mixture of buffer A and buffer B and centrifuged at 10000rpm for 10min at 4° C. Supernatant was poured off and pellet was resuspended in 1mL of buffer C. Tissue was fixed by adding 27μL of 37% PFA and incubated for 10min at 30° C while shaking. Fixation was stopped by addition of 50 μL of 2.5M glycine and incubated on rotator for 2min at room temperature (RT). Tissue was incubated on ice for an additional 5min, moved to a fresh 15mL tube with 10 mL of a 1:1 mixture of buffer A/B and centrifuged at 3000rpm for 10min at 4° C. Supernatant was discarded and pellet was resuspended in ChIP sonication buffer with protease inhibitors (Roche) and incubated on ice for 30min. Samples were split into 300μL

aliquots per 1.5mL tube and sonicated on high for 7min (30sec on/30 sec off) using a Diagenode Inc Bioeruptor. Procedure was repeated 5 more times for a total of 42mins. Sample was spun down at the maximum speed at 4° C for 10min. Supernatant was placed in 1.5mL siliconized tube. 300µg of chromatin, measured with a Nanodrop, were placed into fresh siliconized tubes containing ChIP Sonication Buffer with a final volume of 1.3mL. 10 µg of chromatin were saved as an input sample at -20° C. 10µL of PA6659 Rabbit anti-PRDM13 antibody were added to each sample as well as 50µL of Protein A/G agarose beads (Thermo). Samples were incubated on a rotator at 4° C overnight. Samples were spun down at 350xg at 4° C for 2min. Supernatant was discarded and beads were washed three times with high salt buffer, twice with LiCl buffer and once with TE buffer. 500µL of Elution buffer were added to each sample and placed in 65° C shaker overnight. Beads are centrifuged at maximum speed in a microcentrifuge, and supernatants were placed in fresh tubes. 500µL of Elution buffer were now added to input samples. 11µL of 5M NaCl and 5µL of 10mg/mL Proteinase K (Roche) were added to each sample. Samples were placed on shaker at 55° C for 4 hours, followed by shaking at 65° C overnight. Samples were purified with Qiagen PCR cleanup kit by adding 2.5mL of PB binding buffer, followed by standard manufacturer protocol and eluted in 60µL of water. Rabbit polyclonal antibodies against PRDM13 were lab generated (PA6659, rabbit anti-PRDM13). The antigen used to generate the antibodies was a bacterially expressed C-terminal domain of PRDM13 including amino acids 622 to 755.

ChIP Buffers	
Buffer A	15mM HEPES-HCl, pH 7.6 60mM KCl 15mM NaCl 0.2mM EDTA 0.5mM EGTA 0.34M Sucrose

Buffer B	15mM HEPES-HCl, pH 7.6 60mM KCl 15mM NaCl 2.4M Sucrose
Buffer C	15mM HEPES-HCl, pH 7.6 60mM KCl 15mM NaCl 0.34M Sucrose 0.34M $MgCl_2$
Sonication Buffer	1% Triton X-100 0.1% Deoxycholate 50mM Tris pH 8.1 150mM NaCl 5mM EDTA
High Salt Buffer	1% Triton X-100 0.1% Deoxycholate 50mM Tris pH 8.1 500mM NaCl 5mM EDTA
LiCl Buffer	80mM LiCl 0.1% IGEPAL (NP-40) 0.1% Deoxycholate 3mM Tris pH 8.1 0.3mM EDTA
1X TE Buffer	10mM Tris pH 8.1 1mM EDTA
Elution Buffer	10mM Tris pH 8 1% SDS

Generation of reporter constructs

Regulatory elements bound by PRDM13 were cloned into the MCSIII GFP reporter cassette. These reporter cassettes contain the β-globin minimal promoter, a nuclear localized fluorescence reporter, and the 3' cassette from the human growth hormone. Mammalian conservation from the UCSC genome browser was used to identify boundaries of the elements cloned. All regions were PCR amplified from ICR mouse tail DNA. The 1.2 kb regulatory region R7 (chr2: 19458547-19459713) is located 11 kb 3' of the *Ptf1a* gene (Mona et al., submitted). *e1Prdm12* (chr2:31,609,785-31,610,285) and *e2Prdm12* (chr2:31,640,634-31,641,503) are located 30kb

upstream and within an intron of *Prdm12*, respectively. *e1Olig2* (chr16:91,245,790-91,246,877) and *e2Olig2* (chr16:91,333,568-91,335,428) are located 17 kb and 104 kb downstream of *Olig2*, respectively. Genomic coordinates for the homologies used are based on the mouse mm10 genome build. SalI and BamHI restriction sites were introduced on each end for the R7 reporter construct, while KpnI and SpeI restriction sites were introduced on each end for all other regions cloned. Products were cloned adjacent to the β-globin minimal promoter in the reporter cassettes. All constructs were sequence verified.

***In ovo* chick electroporation assays**

Fertilized White Leghorn eggs were obtained from the Texas A&M Poultry Department (College Station, TX, USA) and incubated for 48 hours at 37^{o}C. The supercoiled reporter plasmids described above were diluted to 1.5 mg/ml in H_20/1X loading dye and injected individually into the lumen of the closed neural tube of chick embryos at stages HH13-15. A pMiWIII-Myc epitope tagged vector was injected along with reporter plasmids as an electroporation control. The injected embryos were then electroporated with 5 pulses of 25 mV each for 50 msec with intervals of 100 msec. Embryos were harvested 48 hours later at stages HH22-23, fixed with 4% paraformaldehyde for 45 minutes, and processed for cryosectioning and immunofluorescence.

Co-immunoprecipitation assays

HEK293 cells were transfected using FuGENE 6 reagent (Promega) with expression vectors for pMiWIII-myc-HOOK3, pMiWIII-myc-PTF1A or pCIG-FLAG-PRDM13 and collected after 48 hours of incubation. A/G beads conjugated with anti-FLAG antibodies (Sigma, CAT#A2220) were used to immunoprecipitate, and membrane was blotted with anti-c-myc (1:1000, Santa Cruz, CAT#sc-789) or anti-FLAG M2 (1:1000, Sigma, CAT#F3165) to determine successful interactions.

ChIP-seq analysis

Sequence reads for each sample were mapped to the mm10 genome assembly by using Bowtie2 (v.2.2.6) (Langmead and Salzberg, 2012). Mapped reads were filtered to remove low quality reads using samtools (v.1.2) (Li et al., 2009). Duplicate reads were removed using picard tools (v.1.119), and the remaining unique reads were normalized to 10 million reads. Peak calling was performed by HOMER (v.4.7) (Heinz et al., 2010) using an FDR cutoff of 0.001, a cumulative Poisson p-value of <0.0001, and required a 4-fold enrichment of normalized sequence reads in the treatment sample over the control/input sample. Distance to gene and gene annotations for ChIP-Seq peaks were obtained using GREAT v3.0 (McLean et al., 2010).

RNA-seq analysis

Sequence reads from RNA-seq were assembled using mm10 refSeq gene annotation with tophat2 (v.2.1.0) (Kim et al., 2013). Gene expression abundance was estimated by counting the number of reads that mapped to any exon of a given gene using featureCounts (v.1.5.0-p1) from subread package (Liao et al., 2014). Counted reads were normalized using the TMM method (Robinson and Oshlack, 2010) and differential expression analysis was performed using the edgeR package (v.3.6.8) (Robinson et al., 2010).

CHAPTER THREE

Generation and initial characterization of *Prdm13* mutant mouse lines

Introduction

PRDM13 is at the center of the bimodal fate decision for dP4 progenitors to become excitatory or inhibitory. An important caveat to the previous studies is they were performed through overexpression and knockdown assays through *in ovo* chick electroporations. These assays can lead to false results given they are based on overexpression of protein-encoding chick expression vectors or shRNA containing-constructs, hindering the scope of their conclusions. Additionally, PRDM13 is expressed throughout other regions of the CNS, such as the cerebellum and the developing retina. In order to expand on these initial findings, it became clear that it would be necessary to generate a *Prdm13* knockout mouse model. This model would allow for determination of whether PRDM13 is capable of functioning as the downstream effector of PTF1A suppression of alternative cell fate programs in other regions of the CNS, as it does in the developing spinal cord.

In this study, we generate three *Prdm13* mouse models that allow us to address different questions about its function *in vivo*. I used zinc-finger nuclease technology to generate $Prdm13^{GFP\_KI}$ and $Prdm13^{\Delta 115}$ and CRISPR/Cas9 technology to generate $Prdm13^{\Delta ZF}$. $Prdm13^{GFP\_KI}$ is a GFP knockin/knockout for PRDM13, while in $Prdm13^{\Delta ZF}$ the terminal three zinc-fingers of the protein were specifically deleted. $Prdm13^{\Delta 115}$ features a 115bp deletion within the first exon of *Prdm13*, which leads to an early stop codon in the second exon, and a predicted loss of most of the PRDM13 protein. $Prdm13^{GFP\_KI}$ and $Prdm13^{\Delta ZF}$ are null for PRDM13 protein

and die shortly after birth, while *Prdm13*$^{\Delta 115}$ unexpectedly makes a mutant PRDM13 protein that appears to be a functional hypomorph with increased levels of PRDM13 protein but no discernable phenotypes in dorsal interneuron specification or effects on survival. All models show an increase in *Prdm13* mRNA transcript levels, while only *Prdm13*$^{GFP\_KI}$ and *Prdm13*$^{\Delta ZF}$ but not *Prdm13*$^{\Delta 115}$ show absence of PRDM13 protein. PRDM13 protein is undetectable in *Prdm13*$^{\Delta ZF}$ given that the antibody was developed against a region of the protein that is deleted in this model. Due to the lack of an antibody to detect the N-terminal portion of the protein, it is not known whether a truncated protein is produced in this model. Taken together, these results show presence of either the full-length protein or, at minimum the zinc-finger domains, are necessary for survival. Moreover, the *Prdm13*$^{\Delta 115}$ mice suggest the existence of an alternate isoform of PRDM13 in this mutant that encodes for the C-terminal region of the protein and is expressed in the dorsal spinal cord of this mouse line.

Results

Use of zinc-finger nuclease technology for generation of *Prdm13*$^{GFP\_KI}$ and *Prdm13*$^{\Delta 115}$ mouse models

Previous findings placed PRDM13 as an essential player in determining dorsal interneuron fates by functioning as the downstream effector of PTF1A in the spinal cord (Fig. 1A-B). These studies largely used ectopic expression of PRDM13 in the chick neural tube through *in ovo* chick electroporation assays (Chang et al., 2013). To test the requirement for PRDM13 in the developing nervous system *in vivo*, a ZNF strategy with a GFP donor plasmid was used to generate a GFP knock-in to disrupt *Prdm13 (Prdm13*$^{GFP\_KI}$*)* (Fig. 2-1). From the same experiment, a 115 bp deletion in the first exon of *Prdm13* was generated (*Prdm13*$^{\Delta 115}$*)* resulting in a frame shift mutant predicted to terminate within the second of four exons.

Intercrossing heterozygous animals of the *Prdm13* $^{GFP\_KI}$ resulted in no live pups by weaning (four litters, 36 pups). I traced two litters of newborn pups through their first 24 hours of birth. Each newborn pup was numbered and tailed for genotyping. Out of 21 pups, 4 were genotyped as *Prdm13* $^{GFP\_KI/\ GFP\_KI}$ homozygous mutants, all or which died within the first 24 hours after birth. This would be predicted if PRDM13 is an essential factor downstream of PTF1A, because *Ptf1a* knockout mice also die within 24 hours of birth (Glasgow et al., 2005). Surprisingly, *Prdm13*$^{\Delta 115}$ homozygotes survived into adulthood with no obvious phenotype. These mice presented no differences in weight, lifespan, appearance or behavior when compared to heterozygous littermates. Potential explanations for these results are further discussed below.

CRISPR/Cas9 technology was used to generate the *Prdm13*$^{\Delta ZF}$ mouse model

Because there was a discrepancy in survival phenotype in the *Prdm13*$^{GFP\_KI}$ and *Prdm13*$^{\Delta 115}$ mutants, and a report of a *Prdm13* mutant with exons 2 and 3 deleted that also survived into adulthood (Watanabe et al., 2015), we generated an additional *Prdm13* mutant allele. We used CRISPR/Cas9 technology to delete sequence in exon 4 that codes for the three terminal zinc-fingers. This domain has the same activity as the full-length protein when expressed in chick neural tube through *in ovo* chick electroporation assays, suggesting this domain is essential for PRDM13 function (Chang et al., 2013). *Prdm13*$^{\Delta ZF}$ homozygous mutant mice recapitulate the early postnatal death of the *Prdm13*$^{GFP\_KI/GFP\_KI}$ mice (Fig. 2-2).

***Prdm13*$^{GFP\_KI}$ and *Prdm13*$^{\Delta ZF}$ are null for PRDM13 and upregulate *Prdm13* mRNA**

In order to assess absence of PRDM13 protein expression in all these lines, I performed immunohistochemistry (IHC) and *in situ* hybridization (ISH) experiments on E11.5 neural tubes. Although nonsense mediated RNA decay would be predicted in the *Prdm13* mutants, *in situ* hybridization for *Prdm13* mRNA reveals an increased level of *Prdm13* mRNA transcripts in

Prdm13$^{GFP\_KI/GFP\_KI}$ and *Prdm13*$^{\Delta ZF/\Delta ZF}$ relative to wild-type (Fig. 3-3). This indicates RNA in each case is still made, but when protein is absent, feedback inhibition of the *Prdm13* locus is lost, consistent with reports from morpholino knockdown of *Prdm13* performed in *Xenopus* (Hanotel et al., 2014). Interestingly, IHC with an antibody directed towards the C-terminal portion of the protein (aa 685-754), revealed *Prdm13*$^{GFP\_KI/GFP\_KI}$ and *Prdm13*$^{\Delta ZF/\Delta ZF}$ showed a complete absence of PRDM13 protein within the dorsal neural tube. Taken together, these data suggest that lack of PRDM13 protein expression leads to an increase in transcription of *Prdm13* mRNA, demonstrating the existence of a negative feedback mechanism regulating the transcription of *Prdm13*.

Prdm13$^{\Delta 115}$ is a functional hypomorph for PRDM13

In situ hybridization for *Prdm13* in *Prdm13*$^{\Delta 115/\Delta 115}$ revealed, as with the previous two lines, there was an increase in *Prdm13* mRNA transcription. Surprisingly, IHC with the antibody recognizing the C-terminal portion of the protein revealed *Prdm13*$^{\Delta 115/\Delta 115}$ neural tubes still produce at least the C-terminal region of the PRDM13 protein, a finding not predicted from the frame shift mutation. This protein product seems to be present at higher levels than the wild-type control and is expressed within the VZ of the neural tube as well as the lateral early post-mitotic cells. This may indicate the existence of a PRDM13 protein isoform which includes the C-terminal domain and may function as a hypomorph, inducing higher levels of PRDM13 protein production to compensate for suboptimal protein function. Moreover, unlike the wild-type protein, this mutant PRDM13 localizes to both the nucleus and the cytoplasm, as seen by double staining for PRDM13 and DAPI (Fig. 3-4). These data indicate the mutant form of PRDM13 where at least the C-terminal domain is made, is apparently sufficient to overcome lethality due to absence of PRDM13.

To follow up on these results, I performed IHC with antibodies against PAX2 and LHX1/5 (markers for dI4) and TLX3 (markers for dI3/5) in order to evaluate if any changes occur in specification of dI3-dI5 interneurons. Results show no significant changes in the number of cells positive for expression of these proteins between homozygotes versus wild-type neural tubes (Fig. 3-4). These data contrast the results seen for *Prdm13*$^{GFP\_KI/GFP\_KI}$ and *Prdm13*$^{\Delta ZF/\ \Delta ZF}$, which show a complete absence of PAX2+/LHX1/5+ cells, accompanied by and increase in the TLX1/3+ population within the dI4 (see Chapter Four). Given the increase in *Prdm13* mRNA transcription levels, these data suggest *Prdm13*$^{\Delta 115/\Delta 115}$ mice produce an alternative protein product that contains the C-terminus of the protein and functions as a hypomorph.

Discussion

Here, I developed three *Prdm13* mutant mouse models *Prdm13*$^{GFP\_KI/GFP\_KI}$, *Prdm13*$^{\Delta ZF/\ \Delta ZF}$ and *Prdm13*$^{\Delta 115/\ \Delta 115}$. Neural tubes from these lines show increased levels of *Prdm13* mRNA transcripts, but lack PRDM13 protein to reveal a negative feedback loop regulating PRDM13 levels. *Prdm13*$^{\Delta 115/\Delta 115}$ surprisingly produced a putative mutant form of PRDM13 containing the C-terminal region. Moreover, although *Prdm13*$^{\Delta 115/\Delta 115}$ mice have increase expression from the *Prdm13* locus, no changes in dorsal interneuron populations are detected, suggesting the mutant form of the PRDM13 protein produced in these mice is sufficient to function in dorsal interneuron specification.

The available *Prdm13* mutant mouse models highlight the possibility of different PRDM13 protein domains having context-dependent functions. Here, we generated three *Prdm13* mutants. While both *Prdm13*$^{GFP\_KI}$ and *Prdm13*$^{\Delta ZF}$ mutants lose PRDM13 protein expression and show the predicted phenotype for loss of dI4 interneurons (see Chapter Four), the *Prdm13*$^{\Delta ZF}$ suggests a possible requirement for the terminal ZF domain for PRDM13 function.

Although confirmation of this possibility must wait for the generation of antibodies specific to the N-terminal domain of the protein, overexpression experiments in the chick neural tube through *in ovo* chick electroporation experiments demonstrated the ZF domain was sufficient for PRDM13 function (Chang et al., 2013). The homozygous progeny from both $Prdm13^{GFP\_KI}$ and $Prdm13^{\Delta ZF}$ mutant lines die within the first 24 hours after birth. Both mutants lose PRDM13 protein, therefore, both are functional nulls. The $Prdm13^{\Delta 115}$ mutant, which generates a frameshift mutation and an early stop codon due to a 115 bp deletion within exon 1 of *Prdm13*, produces homozygous offspring that live to adulthood with no notable phenotypes or defects. Notably, immunohistochemistry with an antibody targeting the C-terminus of the protein on these spinal cords shows PRDM13 protein at higher levels than wild-type. If the protein product was functioning as efficiently as the full-length wild-type PRDM13 protein, one would expect these mice to recapitulate the phenotype obtained through *in ovo* chick electroporation experiments for full-length PRDM13 protein, showing an increase in the number of PAX+/LHX1/5+ dI4 cell, with a corresponding decrease in the number of TLX1/3+ expressing cells. It is important to note the 115 bp deletion occurs upstream of the region encoding the PR domain, but due to the frame-shift is predicted to produce a non-functional truncated protein. Thus, it is not clear what is included in this mutant protein for the PR domain but a protein that includes the ZF domain is produced.

Additional insight is provided by a *Prdm13* mutant mouse line reported by Watanabe and colleagues in which exons 2 and 3, encoding most of the PR domain were deleted (Watanabe et al., 2015). We refer to this allele as $Prdm13^{\Delta 2/3}$ here. Although this mutant was found to present a phenotype in the specification of retinal amacrine interneurons, these mice survive to adulthood, similar to the $Prdm13^{\Delta 115}$ mutant. This suggests the possibility that the ZF domain encoded

within exon 4 is produced in tissues that support survival even though it is not sufficient for normal retina development. It will be interesting to evaluate what the neural tube phenotype is in the *Prdm13*$^{\Delta 2/3}$ and whether they produce a protein with the ZF domain in this region of the nervous system. Overall, the aggregate analysis of these mutant mouse lines suggests an isoform of PRDM13 lacking the PR domain is sufficient to provide at least some of PRDM13 activity necessary for survival outside the womb.

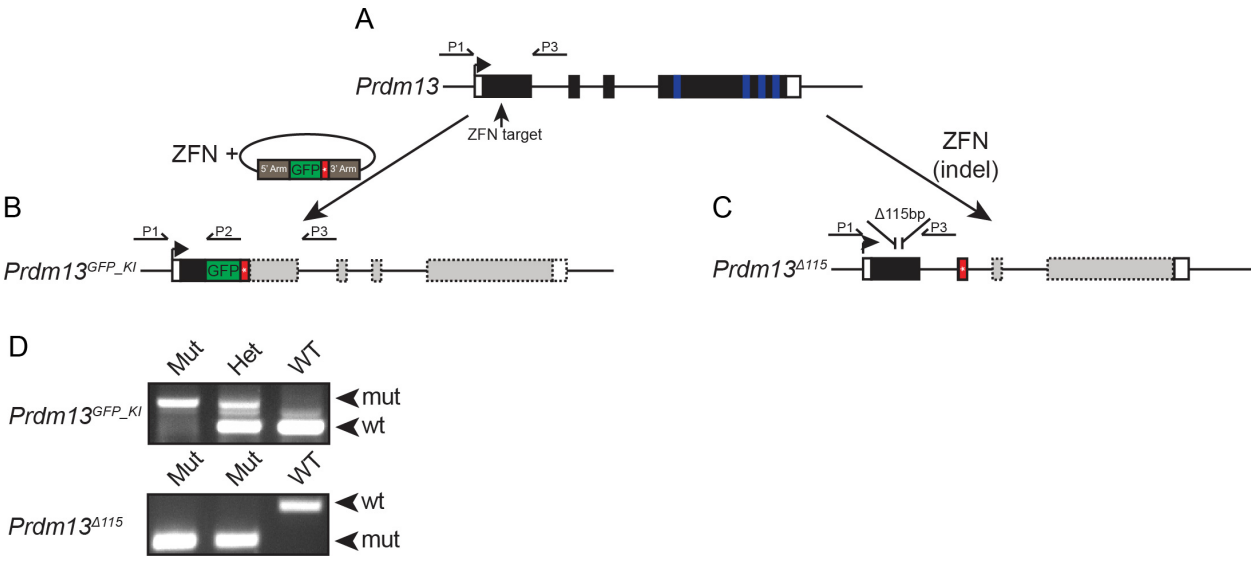

Figure 3-1. Generation of *Prdm13*$^{GFP\_KI}$ and *Prdm13*$^{\Delta 115}$ mutant mice with ZFN technology

A. *Prdm13* genomic locus containing four exons, and primers for genotyping are shown along with zinc-finger nuclease targeting region within the first exon.

B. *Prdm13*$^{GFP\_KI}$ locus after integration of GFP coding sequence followed by a stop codon within the first exon of *Prdm13* generates a GFP knockin-knockout mouse model.

C. *Prdm13*$^{\Delta 115}$ locus with a 115 bp deletion within the first exon of *Prdm13*. This frameshift mutation generates an early stop codon within the second exon (Red *).

D. PCR genotyping for both *Prdm13*$^{GFP\_KI}$ and *Prdm13*$^{\Delta ZF}$ mutant mice. Primers for each line are shown within the diagrams in B and C. Sequence of PCR products and their size are in Chapter 2.

Blue indicates genomic region encoding for zinc-finger domain.

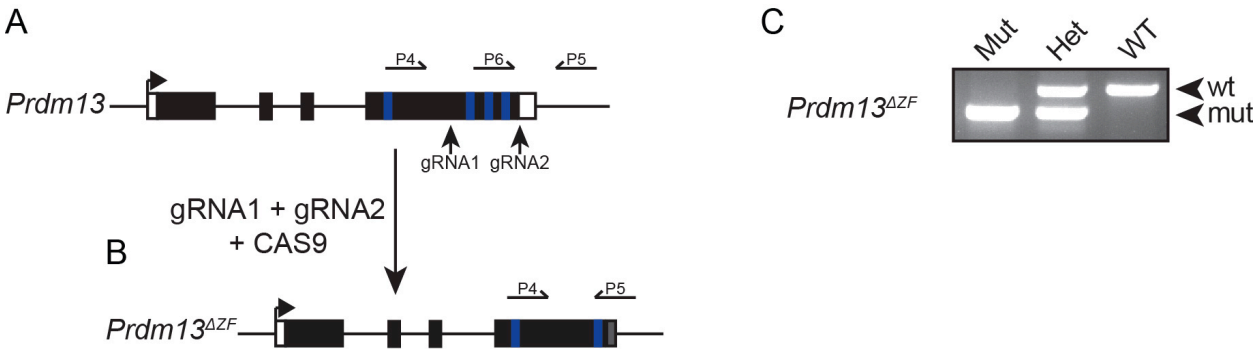

Figure 3-2. Generation of *Prdm13*$^{\Delta ZF}$ mutant mice with CRISPR/Cas9 technology

A. *Prdm13* genomic locus containing four exons, primers for genotyping shown along with two sgRNAs targeting region within the fourth exon.

B. *Prdm13*$^{\Delta ZF}$ locus following deletion of the region between the two sgRNAs, generating a truncation within the 3' region of the gene that results in loss of the three terminal zinc fingers.

C. PCR genotyping for *Prdm13*$^{\Delta ZF}$ mutant mice. Primers are shown within the diagram in B. Blue indicates genomic region encoding for zinc-finger domain.

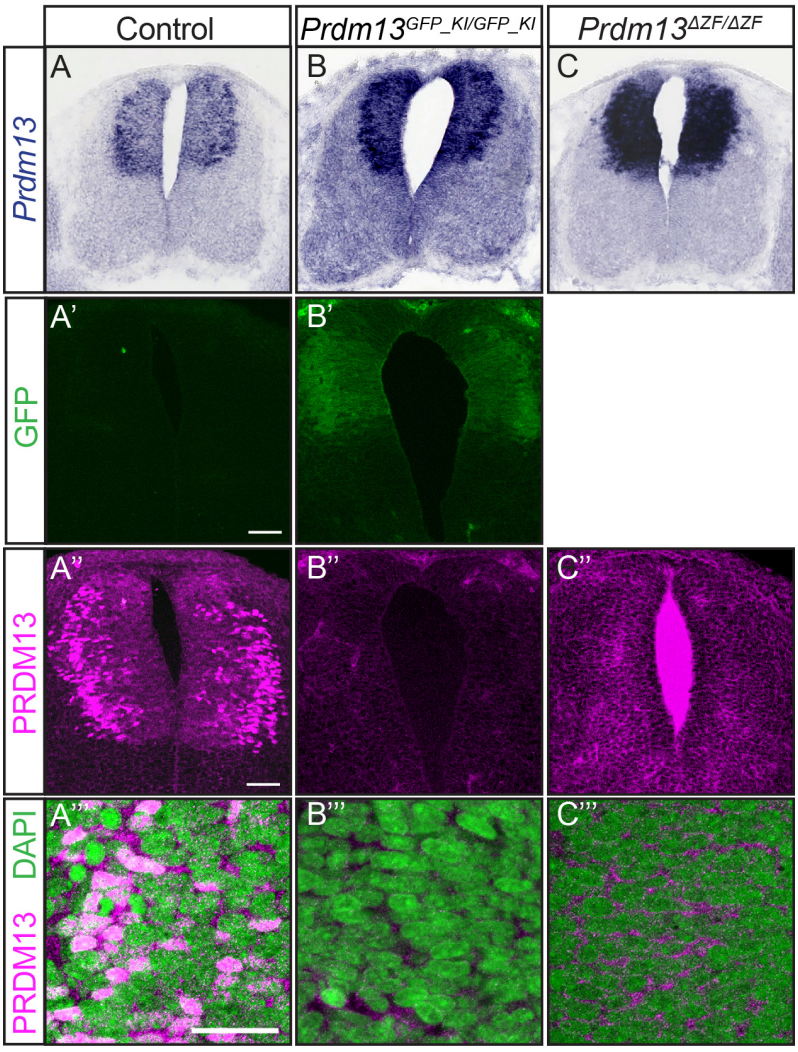

Figure 3-3. *Prdm13*$^{GFP\_KI}$ and *Prdm13*$^{\Delta ZF}$ are lack expression of PRDM13 protein
(A-C) *Prdm13*$^{GFP\_KI}$ (B) and *Prdm13*$^{\Delta ZF}$ (C) E11.5 neural tubes show increased levels of *Prdm13* mRNA transcript as compared to wild-type controls (A).
(A'-B') *Prdm13*$^{GFP\_KI}$ (B') neural tube is positive for GFP in the correct pattern. (Scale = 100μm).
(A''-C'') *Prdm13*$^{GFP\_KI}$ (B'') and *Prdm13*$^{\Delta ZF}$ (C'') show complete absence of PRDM13 protein, while controls show PRDM13 protein localized to lateral ventricular zone cells (Scale = 100μm).
(A'''-C''') 40X of PRDM13 and DAPI staining for *Prdm13*$^{GFP\_KI}$ (B''') and *Prdm13*$^{\Delta ZF}$ (C''') confirm absence of protein and show wild-type protein is localized to the cell nucleus (Scale = 20μm).

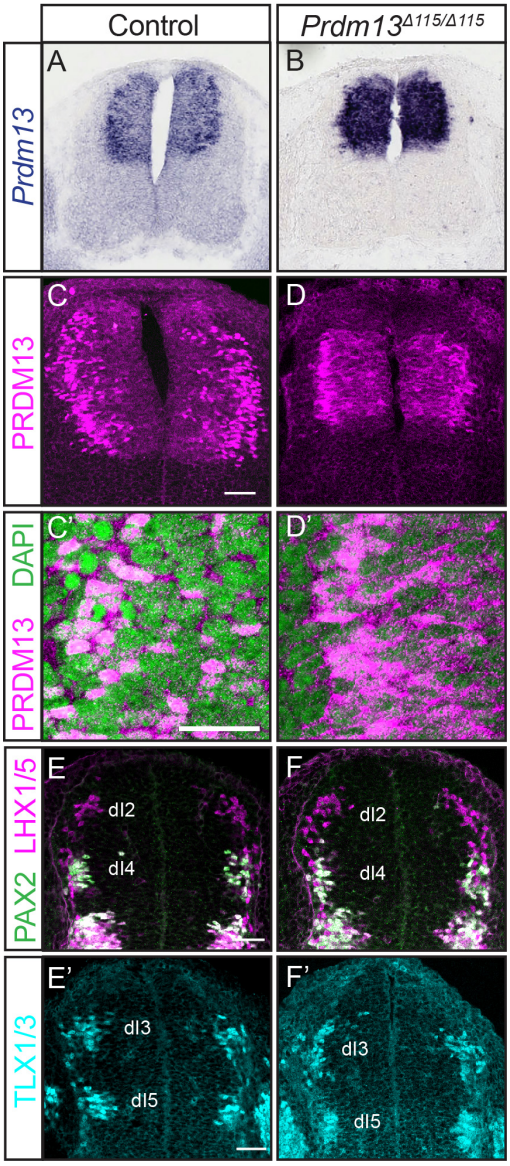

Figure 3-4. *Prdm13*$^{\Delta 115}$ is a functional hypomorph for PRDM13
(A-B) *Prdm13*$^{\Delta 115}$ (B) E11.5 neural tubes show upregulation of *Prdm13* mRNA transcript levels as compared to wild-type controls (A).
(C-D) *Prdm13*$^{\Delta 115}$ (D) shows upregulated and mislocalized expression of PRDM13 when compared to control (C) (Scale = 100μm).
(C'-D') 40X of PRDM13 and NISSL staining for *Prdm13*$^{\Delta 115}$ shows PRDM13 is expressed but localized to the cytoplasm and the nucleus, while wild-type protein is localized to the nucleus (D') (Scale = 20μm).
(E-F') E10.5 *Prdm13*$^{\Delta 115}$ neural tubes (E, E') show no changes in dI2/3/4/5 interneuron populations as compared to controls (F-F') (Scale = 50μm).

CHAPTER FOUR

PRDM13 is required for specification of the inhibitory lineage in the dorsal spinal cord

Introduction

The Class II bHLH TF PTF1A is an essential factor for specification of the inhibitory lineage within the dP4 progenitor population. These cells will ultimately give rise to the GABAergic neuronal lineage residing in the dorsal horn of the spinal cord. Its function as a specification factor has been characterized through chick electroporation experiments where ectopic expression of PTF1A leads to an increase in the PAX2+ GABAergic population of cells, accompanied by a corresponding decrease in the TLX1/3+ population. Absence of PTF1A expression found the reciprocal phenotype, in which the PAX2+ lineage is lost, while the number of TLX1/3+ increases. These data suggest absence of PTF1A protein expression causes the dP4 lineage to switch to an alternative fate. Lineage trace experiments using a *Ptf1a*$^{CRE/CRE}$ mouse line crossed to *R26R-stop-YFP*$^{+/-}$ reporter revealed the ectopic TLX1/3+ cells in the *Ptf1a* null are indeed from the *Ptf1a* lineage (Chang et al., 2013; Glasgow et al., 2005). This experiment shows PTF1A is placed in the crux of the bimodal fate decision between the excitatory/inhibitory lineages.

Overexpression studies in the spinal cord have determined PRDM13 is the factor downstream of PTF1A capable of suppressing the glutamatergic program. Epistasis experiments show PTF1A is unable to suppress the expression of TLX1/3 in the dI4 interneurons when PRDM13 is knocked down. PRDM13 is capable of antagonizing TLX3 activation by ASCL1 through the *eTlx3* enhancer where both proteins are found to bind. Additionally, this function was found to be dependent on the zinc-finger domains of the protein (Chang et al., 2013).

Here I characterize PRDM13 function *in vivo* within the spinal cord through analysis of distinct dorsal interneuron populations and their changes in the absence of PRDM13. I found at E10.5 PAX2+ population is completely lost, while the TLX1/3+ population increases within the dorsal spinal cord, phenocopying the *Ptf1a* null neural tubes. Surprisingly, at E12.5 and E16.5 I find ectopic PAX2 expression within the dorsal neural tube, a phenotype contrasting that is seen in mice that lack PTF1A protein,, where dorsal PAX2 expression is completely lost. These results are supported by ISH showing *Gad1*, a marker of inhibitory neurons, is only partially lost in the dorsal neural tube of these mutants, and indicating a subset of cells are still capable of being specified to the inhibitory fate. Lastly, the $Prdm13^{\Delta ZF}$ and $Prdm13^{\Delta GFP\_KI}$ mutants present with the same phenotype, providing strong support for these mutants as nulls for PRDM13.

Results

PRDM13 is required for production of the PAX2+ population

Although *Prdm13* has a broader expression within the dorsal neural tube than *Ptf1a*, it is enriched in the PTF1A domain and is a known downstream transcriptional target of PTF1A (Chang et al., 2013). Overexpression of PRDM13 in the chick neural tube leads to a suppression of TLX1/3 expression and a subsequent increase in PAX2. The latter is thought to be an indirect consequence of TLX1/3 function in repressing PAX2 (Chang et al., 2013; Cheng et al., 2004; Cheng et al., 2005). To determine if the mouse mutants supported similar functions for PRDM13, I evaluated the $Prdm13^{GFP\_KI}$ and $Prdm13^{\Delta ZF}$ mutant mouse models for alteration in dorsal interneuron populations (Fig. 4-1). Transverse sections at E10.5 were collected and analyzed by immunohistochemistry with antibodies against PAX2 and LHX1/5 to evaluate changes, if any, in the dI2 and dI4 dorsal interneuron populations. A complete loss of dI4

(PAX2+/LHX1/5+) in both the *Prdm13*$^{GFP\_KI/GFP\_KI}$ and *Prdm13*$^{\Delta ZF/\Delta ZF}$ neural tubes was seen. These phenotypes are similar to the *Ptf1a* null mouse (Fig. 4-1) (Glasgow et al., 2005) and are complementary to the overexpression phenotypes in the chick (Chang et al., 2013). The perturbations in cell fate specification in the E10.5 *Prdm13* mutant neural tubes are not a complete phenocopy of the *Ptf1a* mutants. One important distinction is a marked reduction of the dI2 population (LHX1/5^{+};PAX2^{-}) not seen with the *Ptf1a* mutants that indicate PRDM13 function is not restricted to the dI4/dI5 domain as reported for PTF1A (Glasgow et al., 2005).

TLX1/3+ population is expanded in the absence of PRDM13

The model for how PRDM13 function involves a direct repression of the *Tlx3* gene (Chang et al., 2013). To determine if TLX3 is increased in the *Prdm13* mutants as would be predicted from this model, I performed IHC on E10.5 neural tubes using antibodies against TLX1/3 (dI3/5). An increase in the number of TLX1/3+ cells was seen complementing the loss of PAX2. In order to define whether this increase in the TLX1/3 population is due to an expansion of the dI3, dI5 or both populations I performed IHC with antibodies against ISL1 (marking the dI3 population) and LMX1B (marking the dI5 population). Surprisingly, neither ISL1 nor LMX1B were increased in the *Prdm13* mutants suggesting differential regulation of the neuronal subtype specification factors (Fig. 4-2).

Late stage PAX2+ populations do not require PRDM13

In order to understand the contribution of PRDM13 at later stages of spinal cord development, I evaluated PAX2 expression at E12.5 and E16.5. Surprisingly, while PAX2+ neuron population is completely lost dorsally at both these stages in the *Ptf1a*$^{CRE/CRE}$ null mouse (Fig. 4-3), it is only partially lost in the *Prdm13* null (Fig. 3B''). Given the partial decrease of PAX2+ cells still seen at E16.5, one would predict a corresponding increase in the TLX1/3+

population. At this time point, the TLX1/3+ population is only partially increased in *Prdm13*$^{GFP/GFP}$. This is similar to the phenotype seen in *Ptf1a*$^{CRE/CRE}$ mice (Fig. 4-3), even though these neural tubes present a greater increase in TLX1/3+ cells that that seen in the *Prdm13* nulls. These data demonstrate a distinct requirement for PRDM13 during the early and late phases of neuronal specification in the dorsal neural tube.

PRDM13 is required to generate the correct specification of inhibitory and excitatory neurons in the dorsal spinal cord

It has been well characterized that the PAX2 lineage gives rise to the inhibitory neurons within the CNS. As shown previously (Glasgow et al., 2005) *Ptf1a*$^{CRE/CRE}$ mice show a complete loss of *Gad1* expression dorsally, which is accompanied by an increase in *Vglut2* expression, markers of inhibitory and excitatory neurons, respectively. *In situ* hybridization was performed with probes against *Gad1* and *Vglut2*, to evaluate alterations, if any, in the balance of these two neuronal populations. The *Prdm13*$^{GFP/GFP}$ mutant shows only a partial loss of *Gad1* expression dorsally presumably reflecting the inhibitory neurons derived from the E10.5 dI4 population (Fig. 4-4). Similarly, only a modest increase in *Vglut2* expression is detected in the lateral region of the domain lacking *Gad1*. Taken together, these data demonstrate *Prdm13* is required for generating the correct balance of inhibitory and excitatory neurons in the dorsal spinal cord, but this requirement is not as complete as the requirement for PTF1A in these populations.

Discussion

The analysis presented here shows absence of PRDM13 partially recapitulates the phenotypes seen in mice lacking PTF1A, with a complete loss of the PAX2+ (dI4) population and an increase of the TLX1/3+ (dI3/5) cells at E10.5. However, even at this stage there are slight differences between the requirement for these factors. The *Prdm13* mutant shows a

decrease in dI2, demonstrating PRDM13 has a role in specifying the proper cell number for this population. Additionally, although there are significantly more TLX1/3+ cells in the *Prdm13* mutant, analysis of the dI3 and dI5 populations independently through IHC against ISL1 and LMX1B respectively found a decrease in the number of cells positive for each marker when compared to the *Ptf1a* mutant. These data suggest ISL1/2 and LMX1B are regulated independently from TLX1/3. Moreover, later in development PAX2 in the dorsal spinal cord does not require PRDM13. One possible explanation for how PAX2 could become refractive to repression by PRDM13 may involve PTF1A since PTF1A directly activates transcription of *Pax2* (Borromeo et al., 2014; Meredith et al., 2013). As is reported in Chapter Five, PTF1A levels are substantially elevated in the *Prdm13* mutants.

The phenotypes for survival and for neuronal specification are consistent between $Prdm13^{GFP\_KI}$ and $Prdm13^{\Delta ZF}$. Given the lack of protein detected in these mutants and the independent strategies used to generate these animals, we consider these mutants as nulls for *Prdm13*. The $Prdm13^{\Delta ZF}$ mutants also suggest the zinc-finger domains are required *in vivo*, as previously suggested by the overexpression experiments performed in chick (Chang et al., 2013). However, due to the lack of an antibody capable of detecting the N-terminal domain of the protein, I am not able to distinguish whether this region is being produced in the $Prdm13^{\Delta ZF}$ mutant, or whether the truncated protein lacks stability and no PRDM13 product is present. This analysis would be informative given that different members of the PRDM family of proteins require the PR domain, ZF domain, or both to mediate their function. Further insight into these structure function questions may be inferred from the $Prdm13^{\Delta 2/3}$. In this mutant a majority of the PR domain must be deleted, however, the animals still survive. A careful analysis of phenotype in the neural tube in addition to determination if a ZF portion of the protein is made in these

mutants would add clarity to this question of the role of the PR domain for the dorsal neural tube specification function for PRDM13.

Interestingly, even though TLX1/3 is ectopically expressed in these mutants, there is absolutely no overlap with PAX2 at any of the developmental stages analyzed. This highlights the restrictive nature of the bimodal fate specification process. Expression of PAX2 or TLX1/3 is mutually exclusive, given that TLX1/3 completely suppresses PAX2 expression in dI3/5 (Batista and Lewis, 2008; Cheng et al., 2004; Cheng et al., 2005). These data further emphasize the significance of ASCL1, PTF1A and PRDM13 in the early specification process. While ASCL1 and PTF1A are important in the activation of their respective programs, PRDM13 is necessary to antagonize the excitatory program. It was possible that in the absence of PRDM13, PAX2 activation by PTF1A could have overcome suppression by TLX1/3, as is seen at E12.5 and E16.5 (Chapter Five). These results show this is not the case, and direct activation of PAX2 by PTF1A is not capable of overcoming the suppression by TLX1/3.. Moreover, even though later in development direct activation of PAX2 by PTF1A allows for some PAX2 expression within the dorsal spinal cord, overcoming suppression by TLX1/3, there are still no cells present that co-express TLX1/3 and PAX2. These data suggest the existence of a mechanism that restricts these cells to one fate, and does not allow specification to a "mixed fate". This seems to be true for the relationship between PAX2 and TLX1/3, but as I will show in Chapter Six, absence of PRDM13 does cause ectopic expression of OLIG2 in the dorsal neural tube. This expression overlaps with that of TLX1/3 and PTF1A. This may be due to the independent regulation of OLIG2, TLX1/3 and PTF1A by PRDM13. While previous studies and data presented here show PAX2 and TLX1/3 cross-inhibit each other's expression, these other factors seem to function independently, allowing the generation of these "mixed fate" interneurons which co-express

OLIG2 along with TLX1/3 and PTF1A, which in normal developmental conditions would generate motor, excitatory and inhibitory neurons, respectively.

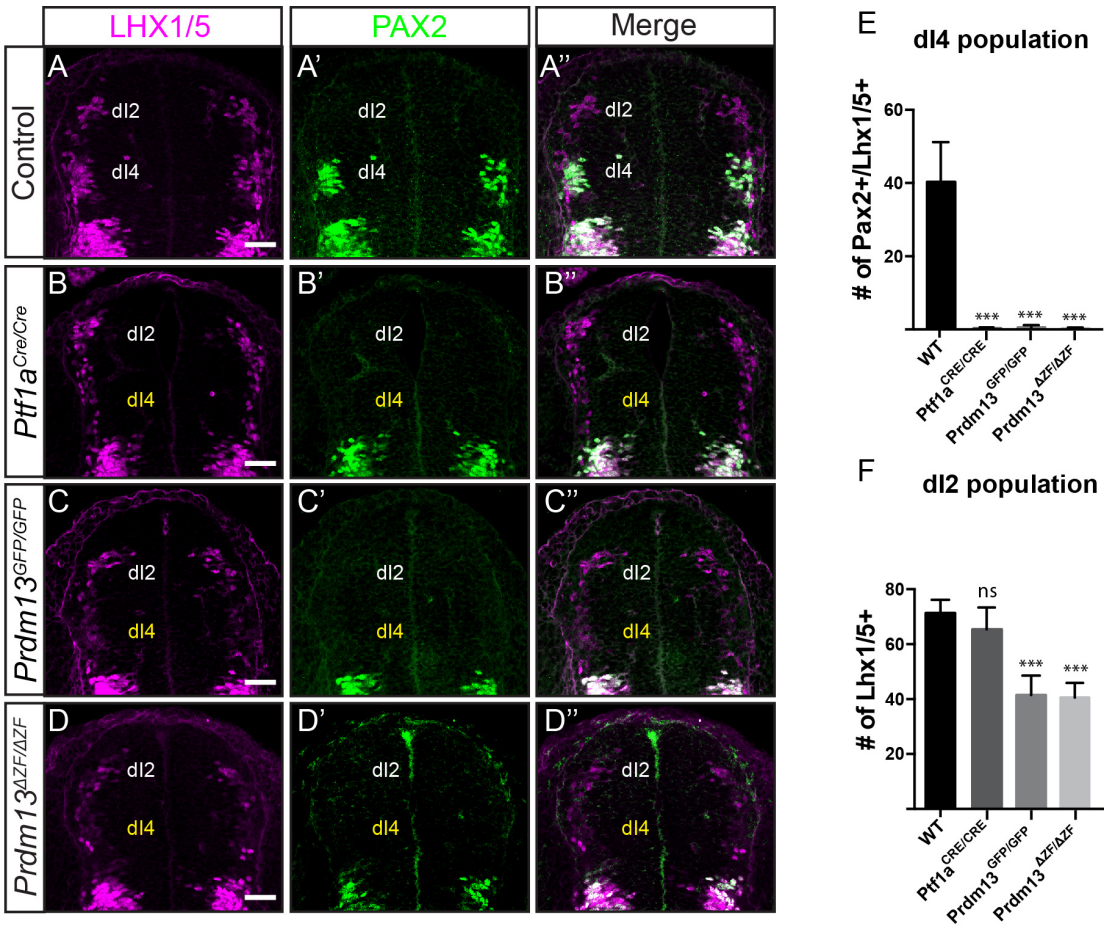

Figure 4-1. PRDM13 is required for production of the dI4 interneuron population
(A-D) At E10.5 absence of PRDM13 (C-D) leads to a slight depletion of the LHX1/5+ population when compared to *Ptf1a* null (B) and controls (A).
(A'-D') Absence of PRDM13 causes a complete loss of the dI4 PAX2+ population (C'-D'), phenocopying the *Ptf1a* null (B').
(A''-D'') Absence of PRDM13 causes a complete loss of the PAX2+/LHX1/5+ dI4 population (C''-D''), as seen in the *Ptf1a* null (B'').
(E-F) Absence of PRDM13 leads to a complete loss of the PAX2+/LHX1/5+ (dI4) population seen in the *Ptf1a* null (E), and a decrease in the PAX2-/LHX1/5+ (dI2) population (F).
(n = 6, Scale = 50μm for all).
* = 0.05, ** = 0.01, *** = 0.001

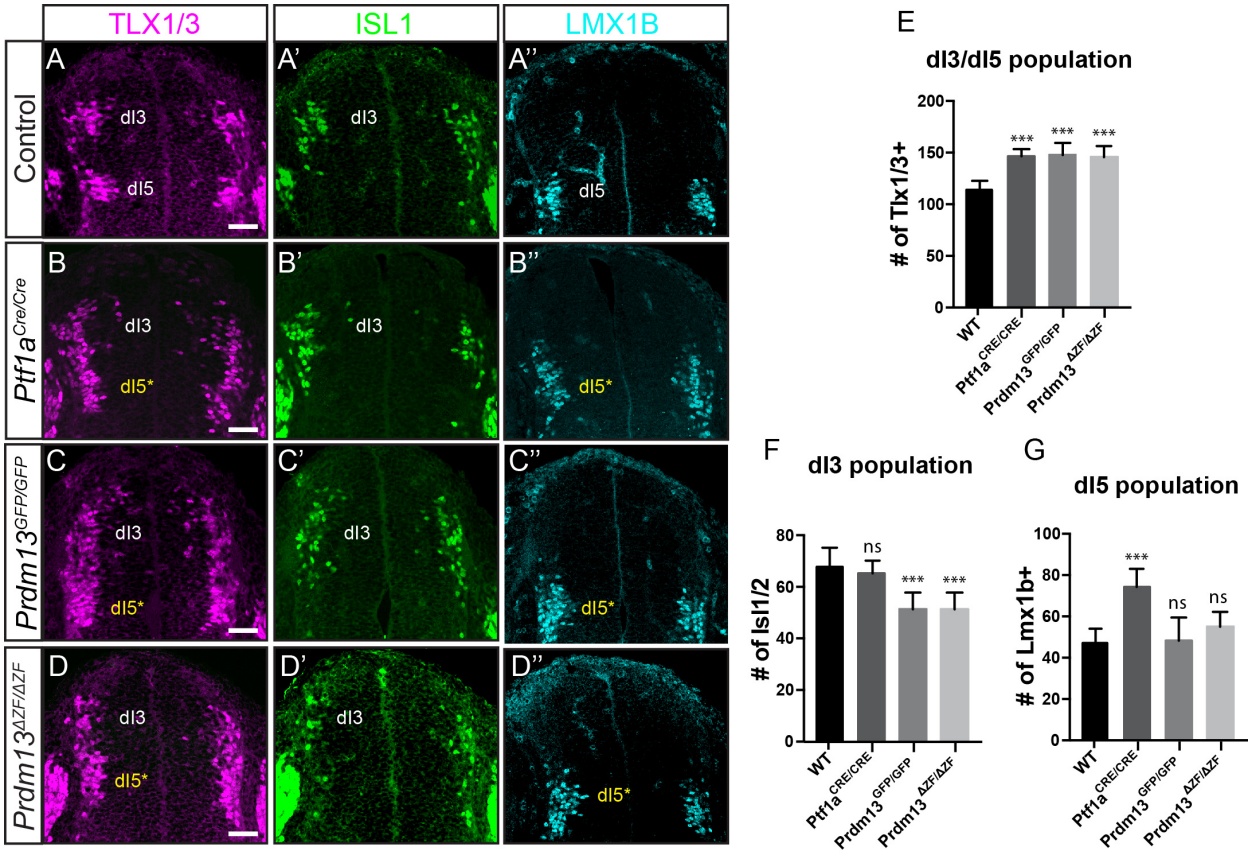

Figure 4-2. PRDM13 is required for production of the TLX1/3+ population
(A-D) At E10.5 absence of PRDM13 (C-D) leads to an increase in the TLX1/3+ population, phenocopying the *Ptf1a* null (B).
(A'-D') Absence of PRDM13 causes no change the LMX1B+ population (C'-D'), unlike the increase observed in *Ptf1a* null (B').
(A''-D'') Absence of PRDM13 causes decrease in the ISL1+ population (C''-D''), while these cells show are in similar number in the *Ptf1a* null (B'') and control (A'').
(E-G) Both *Prdm13* null neural tubes show an increase in the TLX1/3+ population, as seen in the *Ptf1a* null (E). While the number of ISL1+ cells in decreased in the *Prdm13* nulls, the LMX1B+ population shows no change (F) when compared to controls.
(n = 6, Scale = 50μm for all).
* = 0.05, ** = 0.01, *** = 0.001

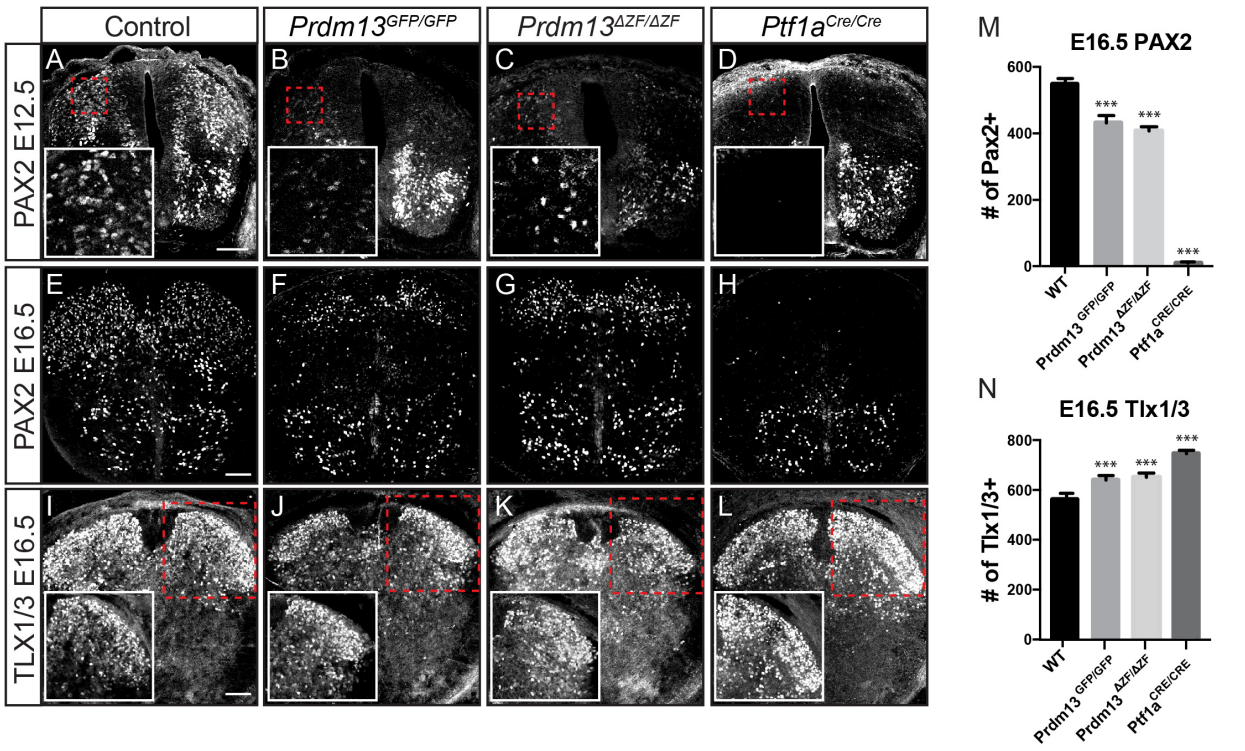

Figure 4-3. PAX2+ population is ectopically expressed in the *Prdm13* mutants at E12.5 and E16.5

(A-D) At E12.5 absence of PRDM13 (B-C) leads partial increase in the PAX2+ population, compared to the complete loss dorsally seen in the *Ptf1a* null (D). Control neural show these cells are localized throughout the developing neural tube (A) (Scale = 100μm).

(E-H) At E16.5 absence of PRDM13 (G-H) leads partial increase in the PAX2+ population, compared to the complete loss dorsally seen in the *Ptf1a* null (F). Control neural show these cells are localized throughout the developing neural tube (E) (Scale = 100μm).

(I-L) At E16.5 absence of PRDM13 (F-G) leads partial decrease in the TLX1/3+ population, compared to the large number of ectopic cells seen dorsally in the *Ptf1a* null (H). Control neural show these cells localized to the dorsal-most region of the developing neural tube (E) (Scale = 100μm).

(M-N) Absence of PTF1A causes a complete loss of PAX2+ cells dorsally and an increase in TLX1/3, while absence of PRDM13 causes partial expression of PAX2+ cells dorsally and a slight increase in TLX1/3 expression (n = 6).

* = 0.05, ** = 0.01, *** = 0.001

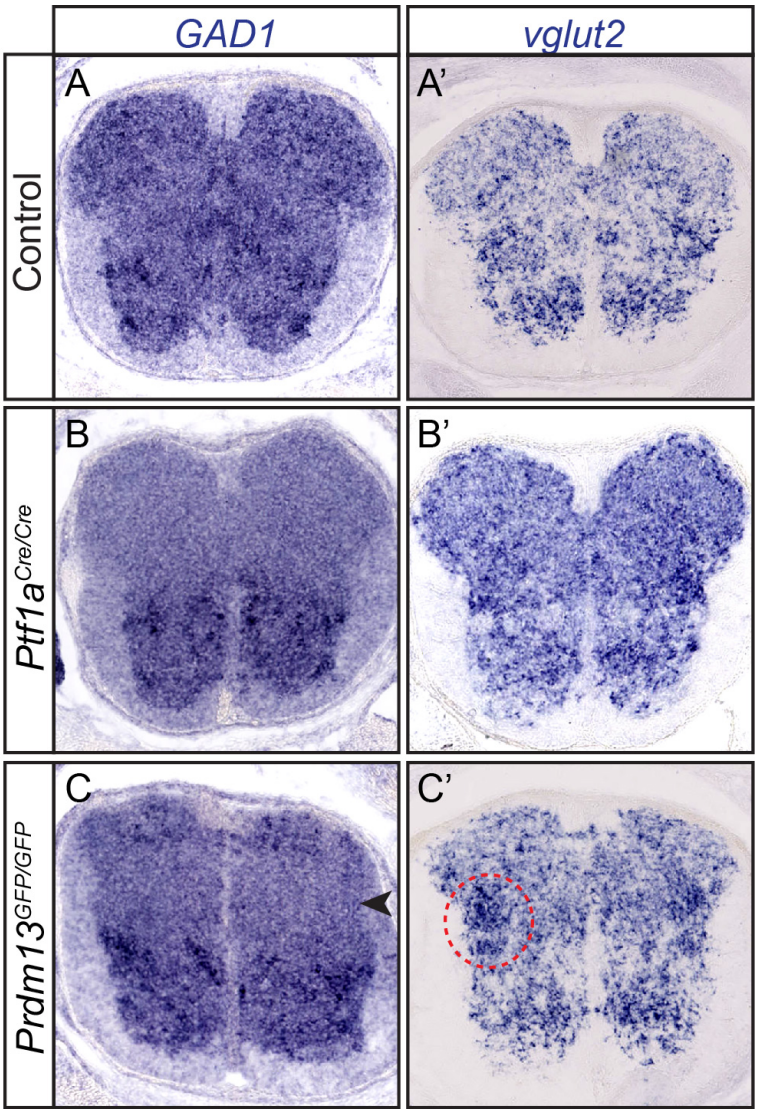

Figure 4-4. *Gad1* is partially lost at E16.5
(A-C) At E16.5 absence of PRDM13 (C) leads partial decrease of *Gad1* levels within the center of the developing neural tube, compared to the complete loss dorsally seen in the *Ptf1a* null (B). Control neural show these cells are localized throughout the developing neural tube (A). (A'-C') Absence of PRDM13 (G-H) leads partial increase of *vglut2* levels within the center of the developing neural tube, compared to the increase seen in the *Ptf1a* null (B). Control neural show these cells are localized throughout the developing neural tube (A).

CHAPTER FIVE

PRDM13 negatively feedback regulates PTF1A through *Ptf1a*'s autoregualtory enhancer

Data presented here was produced in conjunction with Bishakha Mona, a Johnson lab graduate student, Mark Borromeo, a former Johnson lab graduate student and Rahul Kollipara, research staff for the Johnson lab.

Introduction

PTF1A is expressed within the dP4 domain and is required for specification of the inhibitory lineage in the dorsal spinal cord. PTF1A is only transiently expressed in the developing neural tube as its expression is down regulated as the neurons mature. There is some understanding of the cis-regulatory elements involved in regulation of *Ptf1a* expression including the existence of an autoregulatory enhancer (Masui, Meredith). Given the transient nature of *Ptf1a* expression in the neural tube, this autoregulatory feedback mechanism must itself be interrupted.

The autoregulatory enhancer of Ptf1a utilizes the transcription activator trimer complex that consists of PTF1A, and E-protein and either RBPJ, for its function in all tissues of the CNS and pancreas, or RBPJL, for its function in the pancreas (Masui et al., 2007; Masui et al., 2010; Meredith et al., 2009). The PTF1 trimer binds in a sequence specific manner to two spatially restricted sequences, and E-box (CANNTG) and a TC box (TTCCC). These sequences must be spaced by one, two, or threee helical turns as changes in this spacing will ablate the ability of the transcription activator complex to function (Masui et al., 2007).

The autoregulatory enhancer of *Ptf1a* is a highly conserved 2.3Kb region approximately ~15Kb upstream of the transcriptional start site that features two PTF1 binding sequences. Mutation of either the E-boxes or TC boxes ablated binding of the PTF1 complex to each site, and causes a loss of enhancer activity when tested *in vitro* and *in vivo*. These enhancers were found to be able to direct reporter expression in the pancreas and the spinal cord during embryogenesis in transgenic mice, and in the chick neural tube (Masui et al., 2008; Meredith et al., 2009).

Here, I find *Ptf1a* expression in the dorsal neural tube is modulated by PRDM13. Absence of PRDM13 leads to an increase in *Ptf1a* expression within the dP4 domain. This surge in PTF1A may be responsible for the partial expression of PAX2 observed at later developmental stages. Furthermore, this regulation is mediated through the 2.3Kb autoregulatory enhancer for *Ptf1a*, revealing a feedback inhibitory mechanism by which PTF1A levels are regulated in the dorsal spinal cord.

Results

PTF1A is upregulated in *Prdm13* mutants

In order to gain further insight of the transcriptional profile in the absence of PRDM13, we performed fluorescence activated cell sorting on E11.5 $Prdm13^{GFP\_KI/+}$ versus $Prdm13^{GFP\_KI/GFP\_KI}$ neural tubes followed by RNA isolation and sequencing from these cells. This analysis allowed for an unbiased identification of differentially expressed genes between the heterozygous and homozygous *Prdm13* mutant cell populations. A number of genes were misregulated including *Ptf1a*, which was found to be upregulated 3.7 fold in the *Prdm13* mutant versus the heterozygote (Table 6-1). Upregulation of *Ptf1a* in the *Prdm13* null was confirmed by mRNA *in situ* hybridization and immunofluorescence for PTF1A. The increased levels are

localized within its endogenous domain, dP4, when compared to controls (Fig. 5-1). These data reveal a negative feedback loop between PRDM13 and PTF1A. Moreover, the increase expression of PTF1A may explain the upregulation of *Prdm13* mRNA transcript in *Prdm13* mutant mouse models.

Ectopic PAX2+ and TLX1/3+ cells at E16.5 are from the *Ptf1a* lineage

Previous studies have determined PTF1A is capable of directly activating expression of PAX2 (Meredith et al., 2013). It is somewhat surprising then, that at E10.5 while PTF1A is upregulated in the *Prdm13* mutant lines, PAX2 is decreased. This suggests the repression by TLX1/3 is sufficient to overcome direct activation of PAX2 by PTF1A. Unexpectedly, at E12.5 and E16.5 both $Prdm13^{GFP\_KI/GFP\_KI}$ and $Prdm13^{\Delta ZF/\Delta ZF}$ neural tubes show partial expression of PAX2, markedly different from the absolute loss of PAX2 observed in the $Ptf1a^{CRE/CRE}$ null (Fig. 4-3). This phenotype may be due to an accumulation of PTF1A within the burgeoning dP4 progenitors. In order to address whether the ectopic PAX2 cells seen at E16.5 are from the *Ptf1a* lineage, I traced the *Ptf1a* lineage cells in the *Prdm13* mutant background. Using Ai15 as a Cre reporter (ROSA-LSL-tdTom). I found subsets of ectopic PAX2+/TLX1/3- and ectopic PAX2-/TLX1/3+ cells present at E16.5 are from the *Ptf1a* lineage (Fig. 5-2). These results are consistent with the ectopic TLX1/3+ cells seen at E10.5 emerging from the fate switch caused by the lack of PRDM13 suppression of TLX3. Additionally, the PAX2+ population may be a product of the direct activation by PTF1A later on in development. The emerging model has the upregulation of PTF1A in the *Prdm13* mutant able to overcome TLX1/3 suppression of PAX2 to directly activate PAX2 expression at the later phase of neurogenesis.

Recruitment of PRDM13 to the *Ptf1a* autoregulatory enhancer for feedback inhibition of PTF1A

Multiple mechanisms could be at play in the regulation of *Ptf1a* by PRDM13. For example, PRDM13 could block the positive autoregulatory loop used by PTF1A (Masui et al., 2008; Meredith et al., 2009) or a secondary factor may be de-repressed in the absence of PRDM13 that functions in PTF1A regulation. To test the first model, we performed chromatin immunoprecipitation (ChIP) followed by sequencing (described in further detail in Chapter six) and looked for PRDM13 enrichment at the *Ptf1a* autoregulatory enhancer. Only modest PRDM13 enrichment was detected at the PTF1A bound sites within this enhancer region (Fig. 5-3), but it suggests PRDM13 can localize to these sites. Additional ChIPs will be needed to confirm this interaction.

Given the upregulation of PTF1A seen in the *Prdm13* mutants, I hypothesized that PRDM13 may normally disrupt the formation of the PTF1-J trimer at the autoregulatory enhancer to down-regulate *Ptf1a*. In order to explore if PRDM13 is capable of interacting with PTF1A, I overexpressed myc-PTF1A with FLAG-PRDM13 in HEK293 cells and performed a co-immunoprecipitation assay. myc-HOOK3, a coiled-coil microtubule binding protein localized to the cytosol, was used as a negative control for this assay. PRDM13 co-immunoprecipitated with PTF1A but not a negative control, similar to what has been shown for PRDM13 and ASCL1 (Fig. 5-4) (Chang et al., 2013). Because both ASCL1 and PTF1A co-immunoprecipitate with PRDM13, it is possible that this is an indirect interaction mediated through the E-protein heterodimerization factor common to both ASCL1 and PTF1A. I performed co-IP with FLAG-PRDM13 and myc-tagged versions of several E-proteins. No co-IP was detected, demonstrating PRDM13 is not capable of interacting with E-proteins under these conditions, but rather is apparently interacting with multiple class II bHLH proteins (Fig. 5-4). Further analysis of PRDM13 interaction with additional Class II bHLH proteins can be found in Appendix Three.

The localization of PRDM13 to the autoregulatory enhancer by ChIP-Seq, combined with co-IP between PRDM13 and PTF1A, is consistent with a model for PRDM13 feedback inhibiting transcription of *Ptf1a* through the autoregulatory enhancer.

PRDM13 suppresses PTF1A activation of 2.3 kb enhancer

To test the ability for PRDM13 to regulate expression through the *Ptf1a* autoregulatory enhancer, we performed *in ovo* chick electroporation assays with the GFP reporter under the control of the 2.3 kb enhancer (Meredith et al., 2009). As was previously reported, this enhancer directs GFP expression to the dorsal neural tube and co-electroporation of a PTF1A expression vector increases enhancer activity (Meredith et al., 2009) (Fig. 5-5). ASCL1 is not present at this site, therefore it was not tested in this assay. However, electroporation of a PRDM13 expression vector alone or along with that for PTF1A blocks reporter activity completely (Fig. 5-5). Taken together, a model emerges where PRDM13 directly feedback inhibits expression of *Ptf1a* by interrupting the PTF1A auto-feedback regulation through binding the autoregulatory enhancer.

Discussion

The 2.3 Kb enhancer directs PTF1A expression in all PTF1A+ domains, including the spinal cord, retina, cerebellum and pancreas, and was defined as an autoregulatory enhancer (Masui et al., 2008; Meredith et al., 2009). While autoregulation for *Ptf1a* in the pancreas makes sense, given the sustained expression of *Ptf1a* into the adult acinar lineage, it makes less sense in the nervous system where PTF1A is only transiently expressed (Beres et al., 2006; Masui et al., 2007; Masui et al., 2008; Meredith et al., 2013). As *Prdm13* is a neural-specific target of PTF1A (Borromeo et al., 2014), it provides a molecular explanation for how *Ptf1a* can be specifically downregulated in the nervous system while sparing the pancreas.

The *Prdm13*$^{GFP\_KI}$ and *Prdm13*$^{\Delta ZF}$ mutants presented elevated levels of PTF1A, revealing a negative feedback loop between PRDM13 and PTF1A. This new node within the dorsal transcriptional network only became evident upon complete lack of PRDM13 protein expression, since knockdown experiments performed through chick electroporations did not recapitulate these results (Chang et al., 2013). This regulation seems to occur through the known 2.3Kb *Ptf1a* autoregulatory enhancer, potentially through a mechanism involving direct interaction with PTF1A at this site (Masui et al., 2008; Meredith et al., 2009). These results suggest PRDM13 plays a role in maintaining the appropriate PTF1A levels within the dorsal spinal cord, adding a layer of nuance to its function in interneuron specification. While PRDM13 and PTF1A are co-expressed in other regions of the central nervous system (CNS), such as the cerebellum, it requires further study to determine whether this mechanism is conserved between the different regions.

A parallel can be drawn between PRDM13 and PRDM8, another PRDM factor capable of interaction with a bHLH TF, BHLHB5 (Ross et al., 2012). PRDM8 is specifically recruited to its target sites through interaction with BHLHB5 to form a repressor complex. Absence of PRDM8 or BHLHB5 l protein expression leads to the same phenotype in loss of proper neuronal circuitry assembly and behavior. Moreover, both factors were found to bind at genomic enhancers for genes misregulated in *Prdm8* and *Bhlhb5* mutants. Lastly, a lack of BHLHB5 expression hinders PRDM8's ability to bind to its transcriptional targets. PRDM13 can interact with both PTF1A and ASCL1. This interaction suggests a model where PRDM13 binding hinders heterodimerization of these TFs to their E-protein partners, or alternatively, PRDM13 is recruited to these bHLH TFs and forms a repressor complex to inhibit activation of their transcriptional targets. Co-IP data shown here favors PRDM13 interaction with ASCL1 and

PTF1A and, in this way, inhibits their activity. Interestingly, ChIP-Seq data discussed in Chapter Seven and further co-IP assays shown in Appendix One, also yields the possibility that PRDM13 can interact with not only additional class II bHLH TFs, but also a variety of other TFs found in the dorsal spinal cord, such as SOX, RFX and NKX factors. This flexibility in binding abilities has not been reported for any other PRDM factor, and warrants further research to confirm and to understand PRDM13's mechanism of action. Given the lack of evidence to support direct PRDM13 binding to DNA, it is possible PRDM13 is recruited to its target sites by PTF1A and ASCL1, as is seen for PRDM8 and BHLHB5, to form a repressor complex and inhibit activation of their transcriptional targets.

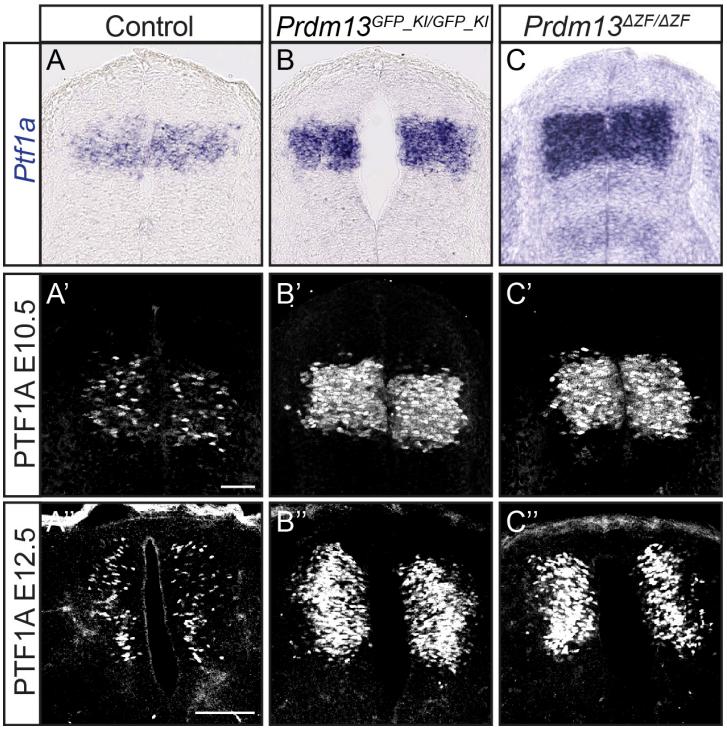

Figure 5-1. PTF1A is upregulated in *Prdm13* mutants
(A-C) At 10.5 *Ptf1a* mRNA transcript levels are upregulated within the dP4 domain in *Prdm13* mutants (B-C) when compared to control (A).
(A'-C') PTF1A is upregulated within the dP4 domain in the absence of PRDM13 (B'-C') when compared to control (A') (Scale = 50μm).
(A''-C'') At E12.5 PTF1A is upregulated within the endogenous expression domain in the absence of PRDM13 (B''-C'') when compared to control (A'') (Scale = 100μm).

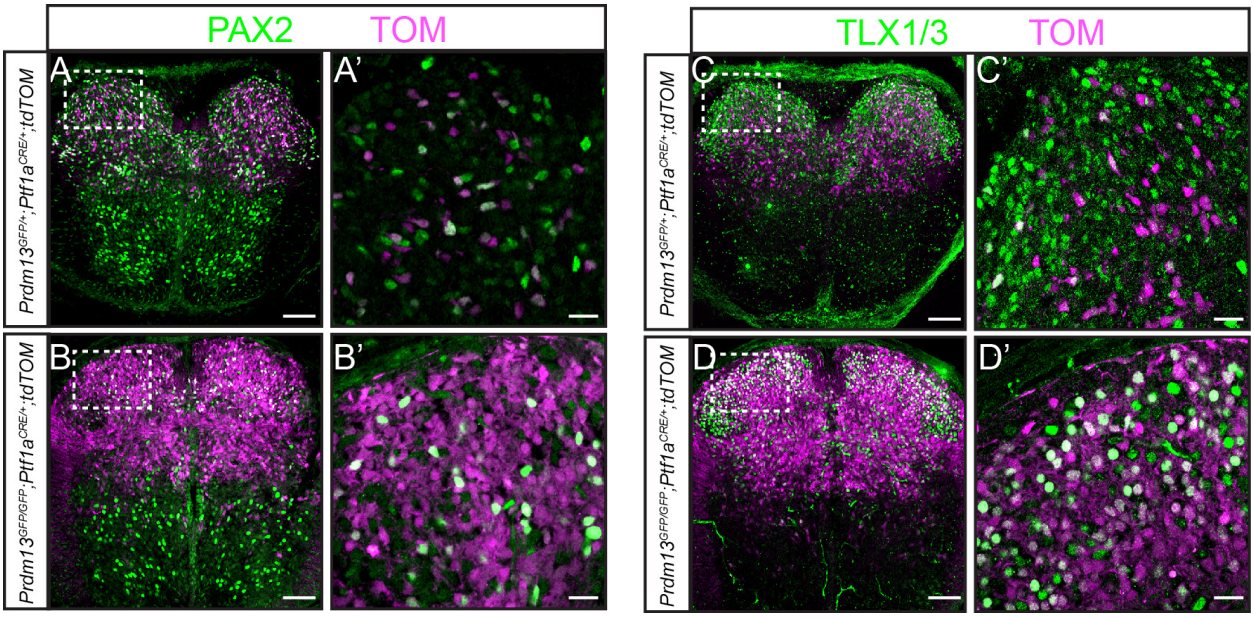

Figure 5-2. PAX2+ and TLX1/3+ cells seen at E16.5 are from the *Ptf1a* lineage
(A-A') At E16.5 tracing the *Ptf1a* lineage cells in a *Prdm13* heterozygote shows the PAX2 cells from the this lineage (A- Scale = 100μm, A'- Scale = 20μm).
(B-B') Tracing the *Ptf1a* lineage cells in a *Prdm13* mutant shows the PAX2+ cells also come from the this lineage (B- Scale = 100μm, B'- Scale = 20μm).
(C-C') At E16.5 tracing the *Ptf1a* lineage cells in a *Prdm13* heterozygote shows most of the TLX1/3+ cells do not come from this lineage (C- Scale = 100μm, C'- Scale = 20μm).
(D-D') Tracing the *Ptf1a* lineage cells in a *Prdm13* mutant shows the ectopic TLX1/3+ cells come from this lineage (D- Scale = 100μm, D'- Scale = 20μm).

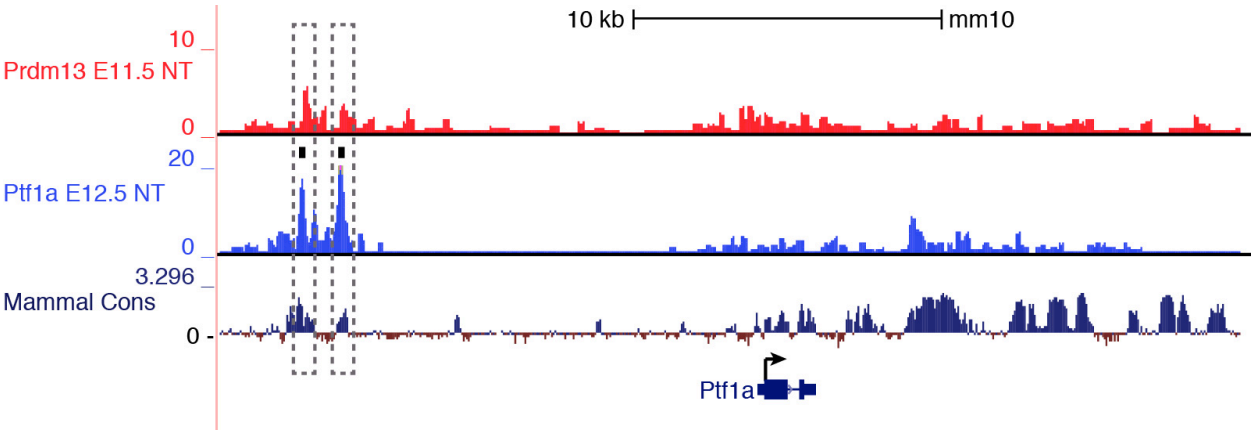

Figure 5-3. PRDM13 is moderately enriched at the 2.3 kb autoregulatory enhancer of *Ptf1a*
ChIP-Seq for PRDM13 shows this protein is moderately enriched at the 2.3 kb known as the autoregulatory enhancer for *Ptf1a* at the same genomic regions where PTF1A is bound.

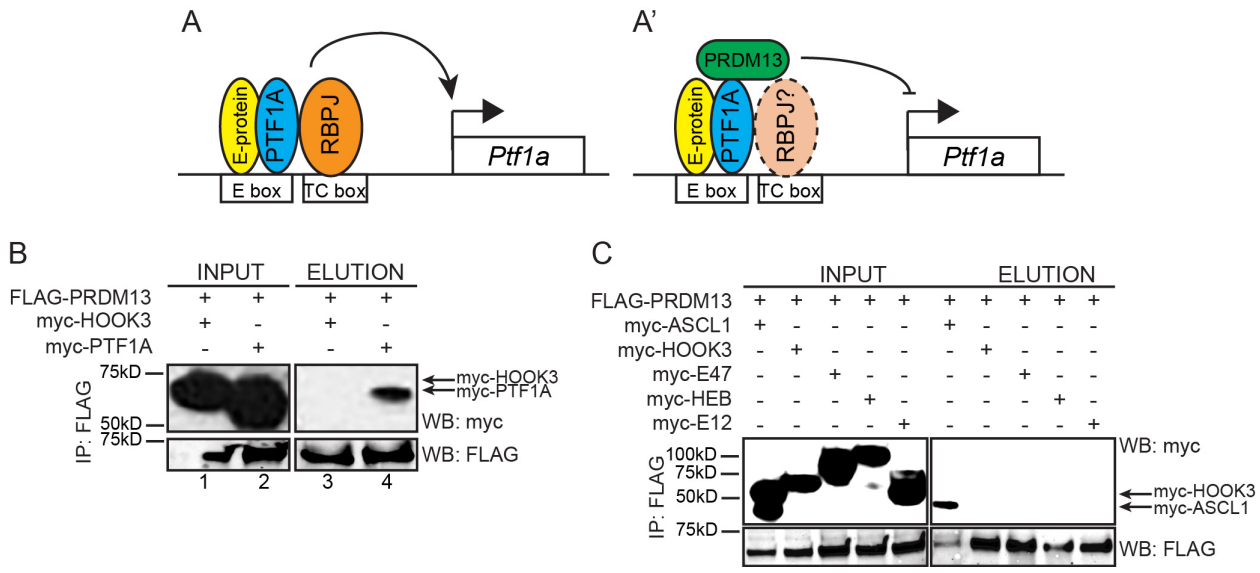

Figure 5-4. PRDM13 interacts with PTF1A *in vitro*

(A) Model for PTF1 trimer binding at the 2.3 kb autoregulatory enhancer sites to activate PTF1A expression in the absence of PRDM13.

(A') Model for PRDM13 disruption of the PTF1 trimer to suppress PTF1A expression through the 2.3 kb autoregulatory enhancer.

(B) Overexpression of FLAG-PRDM13 and/or myc-HOOK3 and myc-PTF1A in HEK293 cells shows PRDM13 interaction with PTF1A *in vitro*.

(C) Overexpression of FLAG-PRDM13 with myc-tagged E-proteins in HEK293 cells shows PRDM13 is not capable of interaction with these proteins *in vitro*.

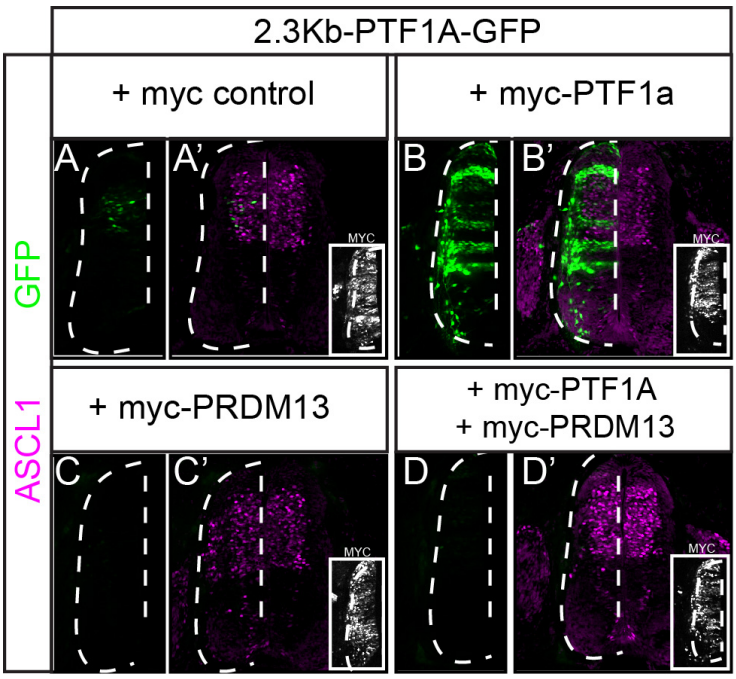

Figure 5-5. PRDM13 can suppress reporter activation by PTF1A through the 2.3 kb autoregulatory enhancer by *in ovo* chick electroporation
(A-A') 2.3 kb-PTF1A-GFP reporter expresses specifically within the dP4 domain.
(B-B') PTF1A activates 2.3Kb-PTF1A-GFP reporter when coexpressed in the dorsal neural tube.
(C-C') PRDM13 suppresses 2.3 kb-PTF1A-GFP reporter expression when coexpressed in the dorsal neural tube.
(D-D') PRDM13 can suppress PTF1A activation of 2.3 kb-PTF1A-GFP reporter expression when coexpressed in the dorsal neural tube.
Insets show IHC to myc indicating the electroporation efficiency.

CHAPTER SIX

PRDM13 suppresses ventral specification factors in the dorsal spinal cord

Data presented here was produced in conjunction with Mark Borromeo, a former Johnson lab graduate student and Rahul Kollipara, research staff for the Johnson lab.

Introduction

Data presented in previous studies and Chapter Four present PRDM13 as the essential factor in suppressing the excitatory program in the dI4 interneurons. PRDM13 is capable of interacting *in vitro* with both PTF1A and ASCL1, suggesting a mechanism by which interaction with these Class II bHLH TFs allows it to execute its function. While the interaction with ASCL1 suggests the formation of a complex on *Tlx3* regulatory enhancer to suppress its activation, the *in vivo* implications of the potential interaction with PTF1A remain unknown (Chang et al., 2013).

ASCL1 and PTF1A are expressed in distinct subsets of cells within the dorsal neural tube progenitors. While both factors are expressed within the dP4, IHC shows the majority of cells expressing PTF1A do not express ASCL1, or express very low levels of it (Borromeo et al., 2014; Glasgow et al., 2005). These data highlight the existence of a mechanism that is capable of excluding expression of one factor when the other is present.

ChIP-Seq and RNA-Seq studies have been performed exploring the mechanisms by which these two factors can differentially regulate their opposing programs (Borromeo et al., 2014). ChIP-Seq for PTF1A and ASCL1 from E12.5 mouse neural tubes found these factors bind many distinct regions, but 1588 regions are bound by both factors. Interestingly, while both are

Class II bHLH TFs that bind to E-box sequences with the canonical CANNTG, they bind to preferential core sequences, with ASCL1 enriched at CAGCTG regions and PTF1A enriched at CAGCTG/CATCTG/CAGATG regions. Moreover, the shared ASCL1/PTF1A sites were also enriched for SOX, HD, RFX and POU motifs, suggesting members of these families of factors may be co-bound to these sites, or aid in opening the chromatin regions for ASCL1 and PTF1A to bind. These motifs were also enriched in regions where ASCL1 or PTF1A bind individually without the other factor present. Cross-reference of the differentially expressed genes from the RNA-Seq from wild-type and *Ptf1a* and *Ascl1* mutant neural tubes, and the ChIP-Seq dataset, identifies putative direct targets of these factors. This analysis identified *Pax2, Lhx1* and *Lhx5* as potential direct targets of PTF1A, and *Tlx1, Tlx3, Isl1* and *Lmx1b* as putative direct targets of ASCL1 (Borromeo et al., 2014). These data are consistent with the phenotypes observed upon lack of expression of each of these TFs, and support the program each of these factors are known to regulate in the progenitor domains in which they are expressed. One surprising result revealed in this analysis was a large number of putative direct targets of both these factors were upregulated upon lack of expression of these TFs. This direct repression is counter to expectations given that both ASCL1 and PTF1A are transcriptional activators and may be due to activity of PRDM13 in these tissues (Borromeo et al., 2014).

*Tlx3 w*as identified as a direct PRDM13 target for repression but a global analysis of targets directly regulated by PRDM13 is still required to fully understand its function within the dorsal neural tube. Moreover, given that PRDM13 can interact with ASCL1 and PTF1A *in vitro*, their targets present a high value set of genes for testing potential co-regulation by PRDM13.

Here, ChIP-Seq with PRDM13 antibodies and RNA-Seq in the *Prdm13* mutants versus wild-type were performed to identify putative direct PRDM13 targets. While *de novo* motif

analysis did not identify a unique binding motif for PRDM13, it did find enrichment for E-box, SOX, RFX and NKX motifs, suggesting PRDM13 may not directly interact with DNA, but binds to sites where bHLH TFs and other TF factors are bound and may form complexes with these factors on DNA. Lastly, PRDM13 regulates a large set of genes involved in cell proliferation and neuronal fate specification. Surprisingly, a number of ventral specification factors are upregulated in the dorsal neural tube in the absence PRDM13 expression. These data suggest a novel function for PRDM13 in suppressing ventral fates within the dorsal neural tube to allow for proper neuronal specification.

Results

PRDM13 ChIP-Seq shows PRDM13 binding to 2345 genomic sites

In order to identify direct gene targets of PRDM13 and to advance the mechanistic understanding of PRDM13 function in cell fate specification, we performed ChIP-Seq with antibodies made to the zinc finger domain of PRDM13. ChIP-Seq identified 2345 PRDM13 binding sites corresponding to 2993 genes. Cross-referencing the PRDM13 bound sites with that PTF1A and ASCL1 identifies a number of sites bound by PRDM13 and either of these factors. PRDM13/PTF1A were found to bind to 407 sites, while PRDM13/ASCL1 are found at 218 sites. All three factors are found at 156 sites throughout the genome (Fig. 6-1). Indeed, ~8% of PRDM13 binding sites are co-occupied by ASCL1, ~17% by PTF1A and ~6% by both ASCL1 and PTF1A. These results propose a model in which PRDM13 may serve to repress a number of genes activated by either PTF1A or ASCL1.

De novo motif analysis was performed in an attempt to identify a unique binding motif for PRDM13. This analysis failed to identify a novel binding motif unique to PRDM13, but highlighted motifs for other TFs enriched within the developing dorsal spinal cord such as E-box

(bHLH), RFX, NKX and SOX motifs. Moreover, previous data has shown that while PTF1A and ASCL1 are enriched for binding at their known preferred E-box sites, they also show enrichment for SOX, HD, RFX and POU motifs (Fig. 6-2). Given the PRDM13 interaction with both these factors *in vitro*, it is interesting that PRDM13 is enriched at these same sites where ASCL1 and PTF1A is bound. Also, a large proportion of PRDM13 binding sites are not co-occupied by ASCL1 or PTF1A, thus, members of these other transcription factor families may serve to recruit PRDM13 to its genomic targets.

RNA-Seq identifies misregulated genes in *Prdm13* null neural tubes

In order to identify the misregulated genes in the *Prdm13* null neural tubes, I performed fluorescent activated cell sorting to isolate GFP+ cells from *Prdm13* heterozygote versus homozygote $Prdm13^{GFP\_KI}$ neural tubes. GFP+ cells from 2 neural tubes for heterozygote and 2 neural tubes for homozygote genotypes were sorted in replicate, for a total of 4 neural tubes for each genotype. From there, RNA was isolated and sequenced, followed by a comparative analysis of the changes in transcript expression between both genotypes. Examination of the cohort of differentially expressed genes from the RNA-Seq analysis predictably revealed a number of transcription factors known to play a role in dorsal neural tube specification (i.e. *Pax2, Tlx1, Tlx3, Lhx1, Lhx5, Lmx1b, Isl1*), as well as other neural related factors (Fig. 6-3, Table 6-1). Unexpectedly, several ventral transcription factors were ectopically expressed within the dorsal neural tube of the *Prdm13* mutant (i.e. *Olig2, Prdm12, Phox2a, Phox2b, Bhlhb5, Foxd3*). The latter finding is surprising since the ventral specification factors are not normally present dorsally, and are limited to the ventral neural tube. These results suggest a novel role for PRDM13 in wide spread suppression of ventral transcription factors in the dorsal neural tube.

To gain a broader view of the types of genes misregulated in the absence PRDM13, I performed gene ontology analysis to assign a function to the differentially expressed genes in the *Prdm13* heterozygotes versus homozygotes. This analysis determined the genes misregulated in the *Prdm13* null neural tubes function in cell specification, neuron differentiation and neurogenesis. These data are consistent with the phenotypes observed upon in mice lacking PRDM13, placing it as an important player in regulating neurogenesis within the dorsal spinal cord.

Prdm12, Olig2, Neurog1 and _Neurog2_ were confirmed by _in situ_ hybridization and immunohistochemistry to be upregulated in the dorsal spinal cord

As discussed above, a large number of the genes misregulated in the *Prdm13* null neural tubes are important in the specification of the ventral neural tube populations. The factors with the highest fold change included *Olig2* (1719-fold), *Olig1* (288-fold), *Prdm12* (24-fold), *En1* (5-fold), *Dbx1* (5-fold), *Bhlhb5* (3-fold) and *Sim1* (2-fold). I performed ISH or IHC to confirm upregulation and evaluate the pattern of ectopic regulation of a subset of these factors. The two factors with the highest ectopic expression are OLIG2 and *Prdm12*, confirmed by IHC and ISH respectively (Fig. 6-4). The ectopic expression of OLIG2 appears restricted to the region predicted to be dI4, while the pattern for *Prdm12* mimics the endogenous pattern of NEUROG2 and, to a certain extent, NEUROG1 (Sommer et al., 1996). Given that *Neurog1* and *Neurog2* were also increased based on RNA-Seq, I performed ISH with probes targeting *Neurog1* and *Neurog2*, and found that both these factors were upregulated in their endogenous domains. This upregulation, combined with the absence of PRDM13 expression, may serve to activate *Prdm12* dorsally (Fig. 6-4). These results suggest PTF1A and NEUROG1/2 may function as the

transcriptional activators of ventral factors in the dorsal neural tube, and PRDM13 is required to restrict their expression to the ventral domain.

Ectopic OLIG2 expression co-localizes with TLX1/3 and PTF1A

Given the dorsal expression of OLIG2 has not been reported previously, I sought out to determine whether these cells co-express any other factors expressed dorsally. The region of ectopic expression is within the endogenous domain for PTF1A and ASCL1, as well as the ectopic expression of TLX1/3 see in the *Prdm13* mutant. IHC for OLIG2 and TLX1/3 show a subset of both ectopic populations are positive for both factors. Additionally, some of the OLIG2 positive cells are also positive for PTF1A (Fig. 6-5). Interestingly, ASCL1 does not co-express with OLIG2 in the dorsal neural tube, and ASCL1 levels seem to the lower in these mutants. These data suggest PTF1A as a possible activator for the ectopic expression of OLIG2. Indeed, in double mutants of *Ptf1a* and *Prdm13*, there is no ectopic OLIG2 detected (Fig. 6-4).

Discussion

We found PRDM13 lacks a unique binding motif within the genome, suggesting it requires interaction with co-factors to form complexes on DNA. The motifs enriched at PRDM13 binding sites suggest a number of candidate factors that could be playing this role. Importantly, enrichment of E-box motifs suggests PTF1A or ASCL1 are candidates for this interaction, especially given their ability to interact with PRDM13 *in vitro*. This model has been seen previously for another PRDM family member expressed in the CNS, PRDM8, which requires interaction with BHLHB5 in order to repress its transcriptional targets. Loss of interaction with BHLHB5 hinders the ability for PRDM8 to bind to its transcriptional targets, suggesting this interaction is required for recruitment to DNA (Ross et al., 2012). Moreover, PRDM8 is the PRDM family member most closely related PRDM13, suggesting they may share

mechanistic and structural properties, making it an interesting candidate for study and understanding of PRDM13 function (Hohenauer and Moore, 2012). It will be interesting to see if other PRDM factors interact with bHLH factors representing a fundamental mechanism for the function of this class of transcription factors.

The RNA-Seq revealed a role for PRDM13 in repressing a number of ventral specification factors within the dorsal spinal cord. These genes were not expressed in the dorsal neural tube upon in the absence of PTF1A. If PTF1A is the activator of these ventral genes in the dorsal neural tube, mice lacking PTF1A/PRDM13 protein expression would present a loss of ventral TF expression in the dorsal neural tube, given that PTF1A is absent and cannot activate their expression. These data have identified a novel role for PRDM13 for suppression of these ventral specification factors within the dorsal neural tube.

These data highlight the principles laid out in two recent publications studying the role of repressive factors in ventral neural tube specification (Kutejova et al., 2016; Nishi et al., 2015). These studies used ChIP-Seq and RNA-Seq to evaluate the role of gene morphogens and transcription factors in determining the transcriptional profile of distinct cellular populations within the ventral spinal cord. Both studies bring to the forefront the role of transcriptional repressors in this process. While many genes defining specific cellular programs seem to be broadly cross-activated by multiple transcriptional activators in numerous cell populations, the precision seen in specification of the ventral neural tube domains is achieved through the activity of a network of repressors. Moreover, accurate cellular identity is not only achieved through repression of factors functioning in adjacent domains as has been understood for over a decade (Kutejova et al., 2016), but requires widespread suppression of all other alternative fates possible within that specific domain. Here we show PRDM13 plays this broad repressor role within the

dorsal spinal cord. In addition to its function in suppressing the activity of ASCL1 on the *Tlx3* enhancer, it is required for repression of the activity of ventral specification factors broadly activated within this region. Absence PRDM13 causes not only a loss of the dI4 interneuron population, but a disturbance in the cellular identity of the resulting populations through the improper expression of transcription factors within the dorsal spinal cord.

Figure 6-1. Prdm13 co-localizes with PTF1A and ASCL1 throughout the genome
Overlay of the PRDM13 ChIP-Seq data with that for PTF1A and ASCL1 shows this factor is enriched throughout the genome in regions where ASCL1 (62 sites), PTF1A (251 sites) or both (156 sites) are found to bind. The majority of PRDM13 binding sites do not show enrichment for ASCL1 or PTF1A (1876), suggesting it may interact with other factors as well to bind to DNA, or bind to DNA independently.

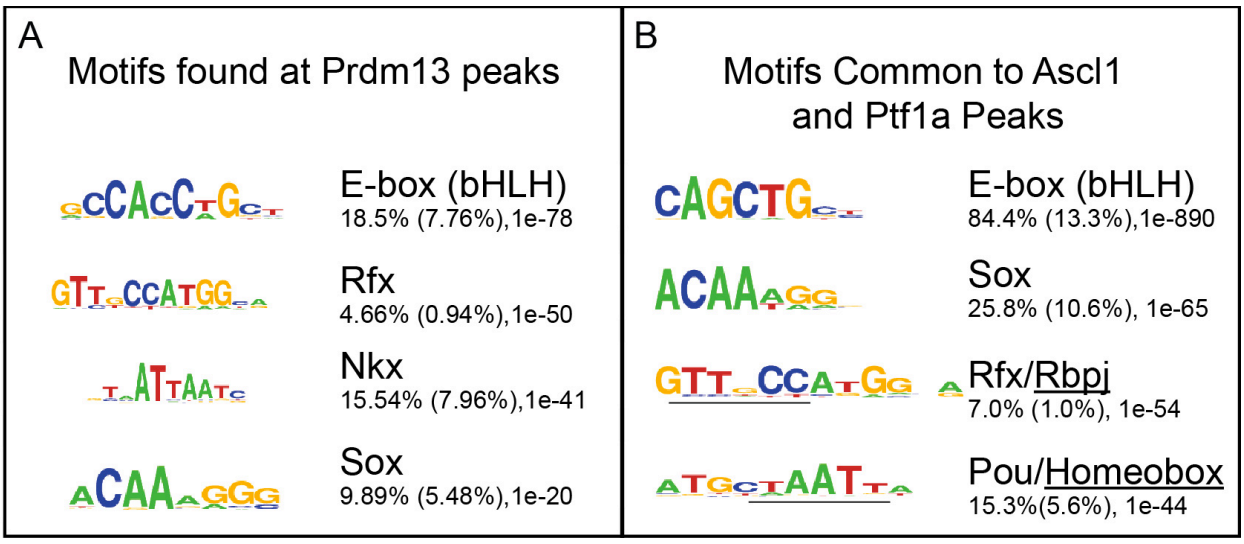

Figure 6-2. *De novo* motif analysis failed to identify a unique binding motif for PRDM13
A. *De novo* motif analysis for PRDM13 ChIP-Seq data identified no unique binding motif for this factor, but saw enrichment of E-box, RFX, NKX and SOX motifs.
B. *De novo* motif analysis for PTF1A and ASCL1 ChIP-Seq data found these factors prefer to bind at E-box motif sites, while they are modestly enriched at SOX, RFX and POU motifs.

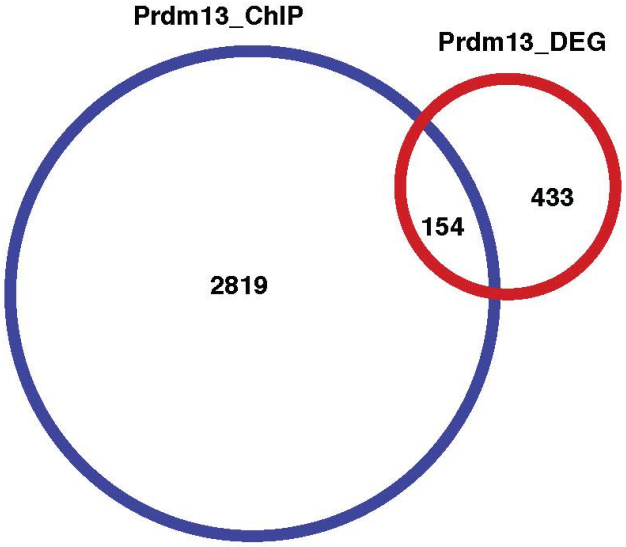

Figure 6-3. Candidate direct targets of PRDM13 are identified
ChIP-Seq identified 2973 putative PRDM13 binding sites, while RNA-Seq identified 567 differentially expressed genes (DEG) in the *Prdm13* mutant. Cross-reference of these datasets identified 154 potential direct targets of PRDM13.

TFs	Fold up in mutants	Neural Related Factors	Fold up in mutants		TFs	Fold down in mutants	Neural Related Factors	Fold down in mutants
Olig2	1710	Calb2	7.5		Hmx2	6.4	Gad2	6.2
Olig1	288	**Syt13**	5.3		**Pax2**	6.2	**Slc6a5**	5.9
Prdm12	24	**Slc1a3**	4.4		**Pax8**	5.6	**Slc32a1**	5.6
Tlx3	17	**Mfng**	4.2		**Lhx1**	5.6	Cacna2d3	5.0
Phox2b	17	**Frzb**	4.3		Hmx3	5.3	Nrxn3	5.0
Phox2a	13	Slc17a6	4.1		Lhx5	4.3	Gad1	4.6
Otp	13	Slc17a7	3.6		Gsx2	3.4	Slc30a3	4.3
Lmx1b	11	Cbln2	3.5		**Skor2**	3.2	Epha2	3.3
Tlx1	4.3	Cbln1	3.4		**Gbx2**	2.9	Robo3	2.7
Isl1	4.5	Ntrk1	3.4		Foxd3	2.7	**Npy**	2.6
Ptf1a	3.5	Slc15a2	3.2		**Mecom**	2.6	Slc7a5	2.4
Neurod4	3.7	Sncg	3.1		Pax5	2.4	**Slc7a1**	2.3
Neurog1	3.4	**Chrna4**	3.1		Gsx1	2.3		
Pou4f1	3.0	Ncald	3.0					
Pou3f1	2.9	Lgr5	3.0					
Bhlhe22	2.8	**Cacna2d1**	3.0					
Prdm13	2.6	Nefl	2.9					
Id1	2.3	**Nrn1**	2.8					
Id4	2.0	**Chrna3**	2.7					
Neurog2	1.8	Nphs1	2.6					
		Kirrel2	2.4					

Table 6-1. Select differentially expressed genes (DEG) in the dorsal neural tube of the *Prdm13* mutant

Genes with associated PRDM13 ChIP-seq peaks are bolded. A full list of the 154 candidate target genes and their fold change between mutant and wildtype is shown in Appendix Four.

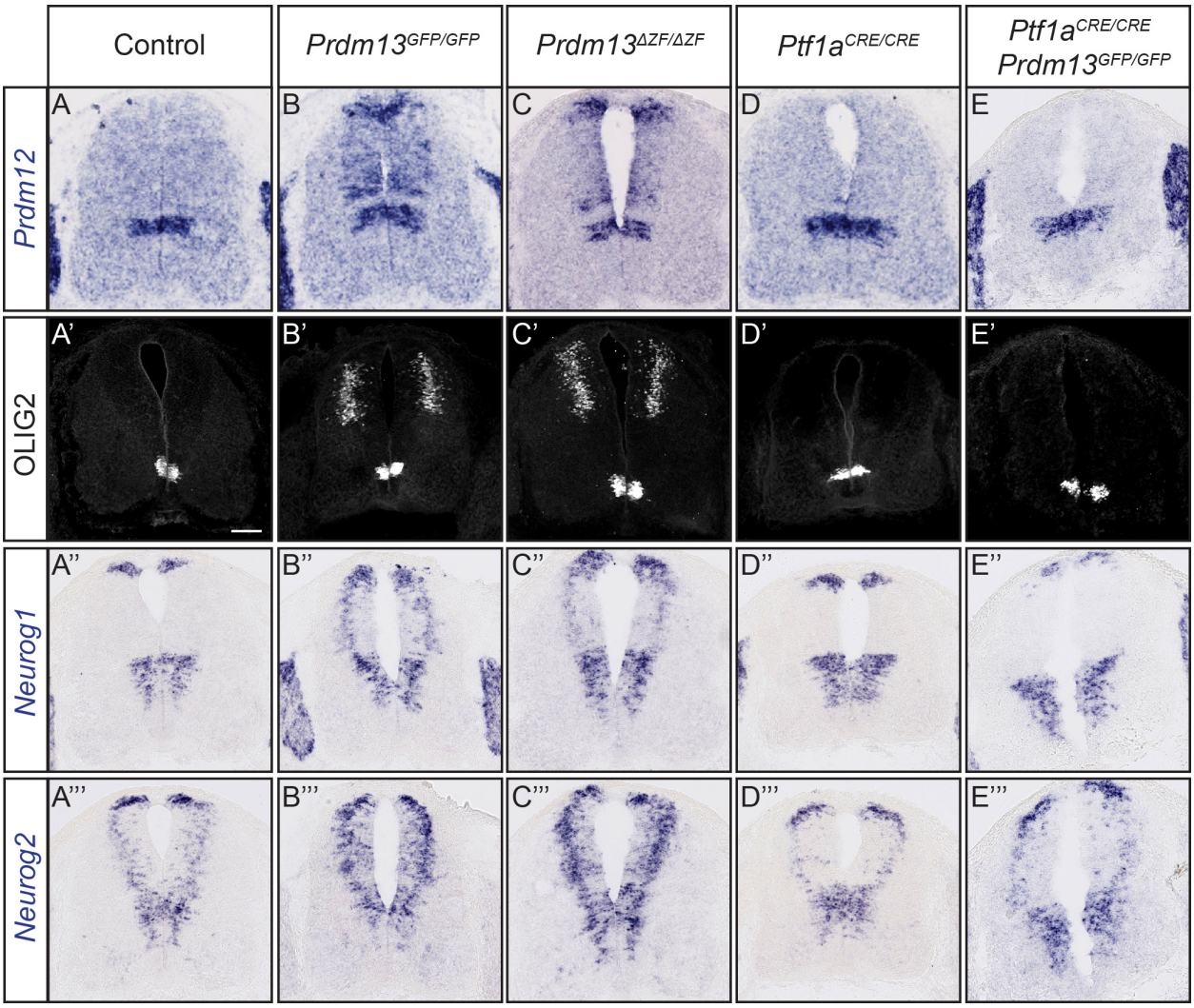

Figure 6-4. *Prdm12*, OLIG2, *Neurog1* and *Neurog2* are ectopically expressed in the dorsal neural tube of *Prdm13* mutants

(A-A''') Endogenous expression patterns of *Prdm12*, OLIG2, *Neurog1* and *Neurog2* in control neural tubes.

(B-C''') Absence PRDM13 leads to ectopic expression of *Prdm12*, OLIG2, *Neurog1* and *Neurog2* in the dorsal neural tube. Note that *Prdm12* and OLIG2 are normally restricted to the ventral neural tube.

(D-D''') Absence PTF1A expression causes no change in expression of *Prdm12*, OLIG2, *Neurog1* and *Neurog2*.

(E-E''') Double mutants for *Ptf1a* and *Prdm13* show no change in expression of *Prdm12*, OLIG2, *Neurog1* and *Neurog2*, indicating PTF1A is required for the ectopic expression of these factors.

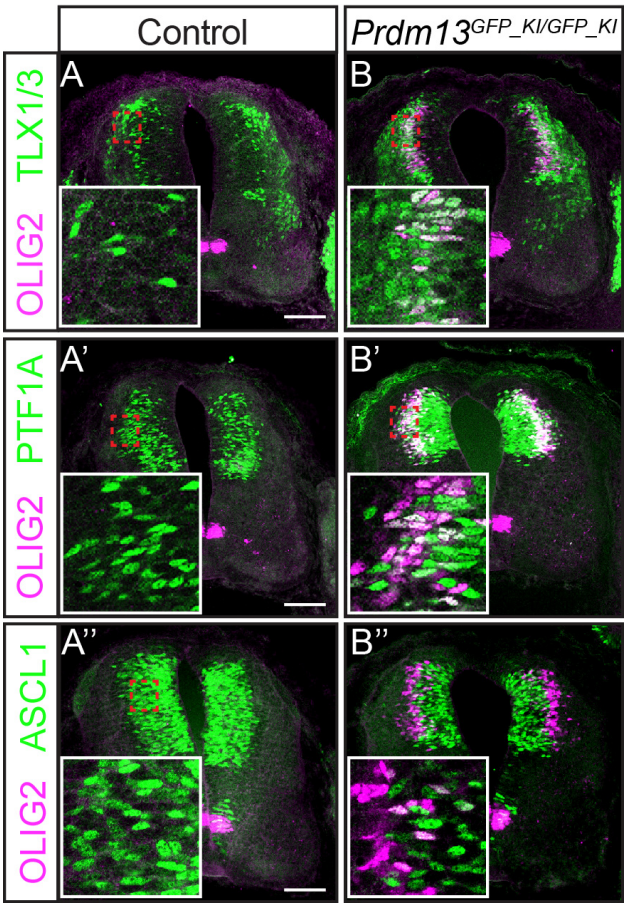

Figure 6-5. Dorsal ectopic expression of OLIG2 co-localizes with expression of TLX1/3 and PTF1A

(A-A'') Control neural tubes show no dorsal expression of OLIG2 and, therefore, no co-localization with TLX1/3, PTF1A or ASCL1.

(B-B'') Absence of PRDM13 leads to ectopic expression of OLIG2 in the dorsal neural tube. The ectopic OLIG2 co-localizes with ectopic expression of TLX1/3 and PTF1A in a subset of cells. There is no co-localization with dorsal ASCL1.

(Scale = 100μm)

CHAPTER SEVEN

PRDM13 mechanism for suppression of *Prdm12*

Data presented here was produced in conjunction with Bishakha Mona, a Johnson lab graduate student.

Introduction

In the previous Chapters I have discussed the inroads made in understanding the function of PRDM13 in the dorsal neural tube. I have found PRDM13 not only functions in specification of the dI4 interneurons, but also serves to repress expression of ventral factors in the dorsal neural tube. One aspect of PRDM13 that remains elusive is the mechanism by which it functions. PRDM13 can antagonize ASCL1 activity through *eTlx3* and, by inhibiting activation of TLX3, allows expression of PAX2 in the dI4. Given that both ASCL1 and PRDM13 are bound to this enhancer, it is clear that while ASCL1 functions to activate this gene, PRDM13 serves to repress its expression in the dP4. Loss of TLX3 repression of PAX2, in turn allows its expression in the dI4 (Chang et al., 2013). Here, I have shown PRDM13 is also capable of interacting with PTF1A, a potential activator of the ventral genes in the dorsal neural tube. Moreover, given the lack of evidence supporting direct interaction between PRDM13 and DNA, the data presented in Chapter six, recruitment by another co-factor seems more likely to be the mode for PRDM13 genomic targeting. These data support the model where PRDM13 is recruited to its genomic targets through interaction with these bHLH TFs.

Given the variety of mechanisms by which the PRDM proteins function, I sought out to gain further understanding of how PRDM13 may function to repress its transcriptional targets.

Here, PRDM13 is found to suppress *Prdm12* by localizing to specific genomic enhancers and antagonize activation by other TFs.

Results

PRDM13 directly binds to enhancer regions for *Prdm12*

In order to gain insight on how some ventral factors are ectopically expressed in the absence of PRDM13, I focused on one of the genes with a dramatic ectopic expression, *Prdm12*. This factor is normally restricted to ventral progenitor domain 1 (p1) and is essential in specification of the v1 population (Thelie et al., 2015).

Prdm12 appears to be a direct target of PRDM13. PRDM13 is bound at one site upstream of the *Prdm12* transcriptional start site and a second site within the first intron (Fig. 7-1). I used these sites to probe the mechanism by which PRDM13 represses this ventral TF. Because many PRDM13 bound regions contain the binding motif for bHLH factors, we determined whether each PRDM13 bound site might also be bound by ASCL1, PTF1A, or both. Here, I found PTF1A binds to the enhancer region within the first intron of *Prdm12,* overlapping with PRDM13 binding at this site. Additionally, no ASCL1 binding was detected at either of the PRDM13 bound sites around *Prdm12*, excluding it as the activator of *Prdm12* expression through these enhancers.

PRDM13 suppresses activity of an enhancer for *Prdm12*

Given PTF1A and PRDM13 show overlapping binding sites at genomic regions surrounding these cells (Fig. 7-1), and PTF1A functions as a transcriptional activator, I probed whether absence of PTF1A in the PRDM13 null background caused a loss in activation of *Prdm12* and OLIG2 in the dorsal neural tube. Interestingly, neural tubes null for both *Prdm13*

and *Ptf1a* lose ectopic expression of *Prdm12* and *Olig2*, suggesting PTF1A, or a downstream target, may function as the dorsal activator for both these factors. In addition, the pattern of ectopic *Prdm12* expression within the dorsal neural tube mimics that of endogenous *Neurog1* and *Neurog2*, both of which are also upregulated in the *Prdm13* null (Fig. 6-4). These data place NEUROG1 and NEUROG2 as two additional candidates for the activators of *Prdm12* expression in the dorsal neural tube.

The region around *Prdm12* yielded two PRDM13 binding sites, *e1Prdm12*, which has an overlapping binding site for PTF1A, and *e2Prdm12,* which showed no PTF1A or ASCL1 binding (Fig. 7-1). Both enhancers contain E-box motifs near the apex of the ChIP-Seq peak. We used chick electroporation system to test the activity of the identified enhancers for *Prdm12*. Electroporation of *e1Prdm12-GFP* in chick neural tubes showed enhancer activity in a localized intermediate region within the neural tube. Co-electroporation with myc-PRDM13 suppressed GFP expression completely, while co-electroporation with myc-PTF1A localized reporter expression to the post-mitotic cells of the ventricular zone, but was not capable of further activating its expression throughout the neural tube (Fig. 7-2). Further analysis revealed that while *e1Prdm12* has multiple E-box sequences, it lacks a corresponding TC box in the appropriate spacing to form a functional PTF1 trimer complex. Therefore, it is possible that the presence of PTF1A may function to recruit PRDM13 to this site, but is not an activator itself for *Prdm12*. These results along with the potential interaction between PRDM13 and PTF1A, suggest a model where PTF1A mediates PRDM13 interaction with DNA for excluding *Prdm12* from the dorsal neural tube. Given that the ectopic expression pattern of *Prdm12* in the dorsal neural tube mimics that of endogenous NEUROG2, we performed overexpression of NEUROG2 in this assay. Overexpression of NEUROG2 directed reporter expression to the postmitotic cells

of the developing spinal cord, while not being able to direct further ectopic expression throughout the spinal cord, demonstrating it is not likely to be the dorsal activator for *Prdm12*.

Electroporation of *e2Prdm12-GFP* directed broader expression of the GFP reporter, and this expression is moderately suppressed by myc-PRDM13. Previous studies have identified PAX6 as an activator of *Prdm12* expression within the ventral spinal cord through binding at *e2Prdm12* (Thelie et al., 2015). To test the ability of PAX6 to activate the GFP reporter through *e2Prdm12* within the spinal cord, we electroporated of PAX6 along with the *e2Prdm12*-GFP. PAX6 was not sufficient to activate GFP expression (Fig. 7-3). Given this observation the ectopic *Prdm12* expression mimics that of endogenous NEUROG1 and NEUROG2, we tested the ability for these TFs to activate *Prdm12* expression through *e2Prdm12*. Testing of NEUROG2 was not successful, given that all samples died after electroporation due to factors outside our control. NEUROG1 was not capable of activating reporter expression, and directed its expression to the postmitotic cells, indicating it is not the dorsal activator of *Prdm12* expression in the absence of PRDM13. Taken together, these data indicate that while PRDM13 represses expression of *Prdm12* in the dorsal neural tube, serving to restricting its expression to the ventral neural tube, the dorsal activator of *Prdm12* remains unknown.

Discussion

In Chapter Six I presented data demonstrating the role of PRDM13 as a repressor of ventral specification factors in the dorsal neural tube. Given that PRDM13 functions as a transcriptional repressor (Chang et al., 2013), we used chick electroporation assays not only to test its ability to control reporter expression through putative *Prdm12* regulatory sites, but to identify the transcriptional activators for this gene within the dorsal spinal cord, providing a more comprehensive model for PRDM13 function. Given that *Prdm13* null neural tubes show

ectopic *Prdm12* expression, we sought to identify the dorsal activator of this factor through chick electroporation assays. We found that neither PTF1A, NEUROG1 or NEUROG2 were capable of activating reporter expression. This was surprising given the overlapping binding of PTF1A and PRDM13 at *e2Prdm12* and the loss of *Prdm12* expression dorsally in the absence of both PTF1A and PRDM13 expression. While PRDM13 seems to be recruited to specific genomic regions to suppress expression of targets such as *Prdm12*, the mechanism of how it targets these sites remains unknown. PTF1A and ASCL1 are candidates for this role, given their ability to interact with PRDM13 *in vitro*.

PRDM8 is to date the only family member known to be recruited to DNA through interaction with a bHLH protein, BHLHB5 (Ross et al., 2012). Loss of BHLHB5 expression hinders the ability for PRDM8 to interact with DNA and form a repressor complex to regulate its transcriptional targets. Given the structural similarities between PRDM8 and PRDM13, it is interesting that both these proteins are able to interact with bHLH proteins. It will be important to identify the regions of these two proteins capable of interacting with bHLH factors, and analyze the similarities between the two to gain further insight on how they function mechanistically.

The existing data for PRDM13 function support a model where PRDM13 is recruited in a site-specific manner to its genomic targets by co-factors. The ChIP-Seq data place several classes of proteins as candidate co-factors. Interestingly, E-box sites are enriched for PRDM13 binding, supporting ASCL1 and PTF1A as candidates. Moreover, the *in vitro* data for PRDM13 interaction with these two factors supports potential complex formation *in vivo*. Moreover, given the lack of *in vivo* confirmation for intrinsic HMT activity for PRDM13, it will be necessary to assess whether this function is relevant *in vivo* or if PRDM13 is capable of interacting with

histone modifying factors to exert its repressive function. Indeed, PRDM family members that lack intrinsic HMT activity function in this manner (Di Zazzo et al., 2013). This would suggest a model where PRDM13 is specifically recruited to its target sites by co-factors, such as PTF1A and ASCL1, and recruits a histone-modifying factor to modify the chromatin structure and suppress target activation.

Overall, these data show the repressive activity of PRDM13 is required not only for suppression of the excitatory gene program driven by ASCL1, but also for restriction of a number of transcription factors to the ventral spinal cord. PRDM13 seems to exert its repressive function by recruitment to its genetic targets by other transcription factors, such as PTF1A. Given the ability for PRDM13 to directly suppress activity of ASCL1 and PTF1A, it will be interesting to further probe its repressive ability with respect to the activity of other bHLH factors, given the variety of these factors expressed throughout the CNS. Additional *in vitro* experiments found PRDM13 is also capable of interacting with other class II bHLH factors such as MYOD and ATOH1 (Appendix 3). The most pressing question is how PRDM13 can potentially be recruited by bHLH TFs in a specific manner, since PRDM13 expression in the dorsal NT expands from dI2-dI6. Arguments laid out here present evidence for the existence of other *Prdm13* isoforms, but the protein conformation, encoding exons, regulatory control and functional relevance of these isoforms are unknown. It will be important in the future to determine whether of these different PRDM13 materializations play different roles dependent on developmental context and tissue specificity.

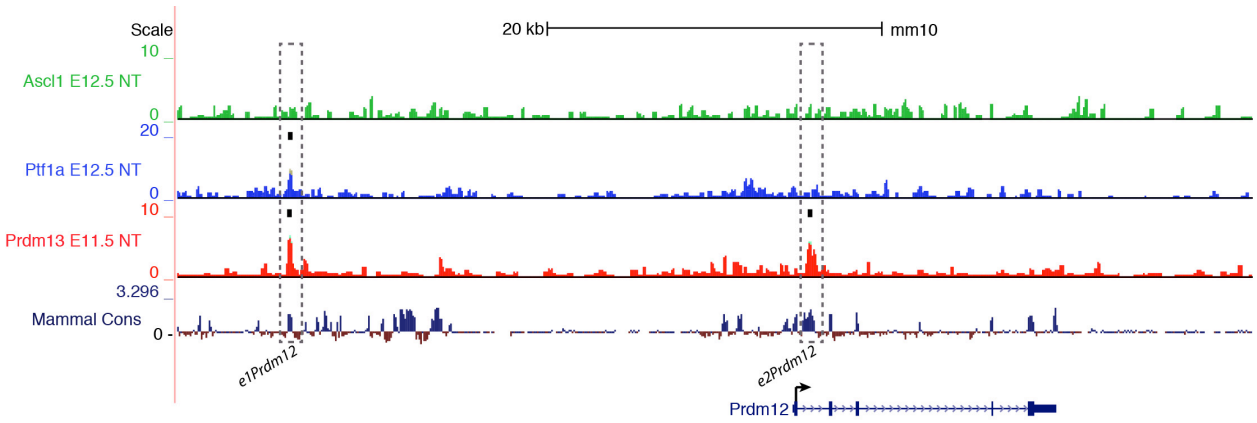

Figure 7-1. Two PRDM13 binding sites around *Prdm12*
ChIP-Seq identified two sites round *Prdm12* where PRDM13 is enriched, *e1Prdm12* and *e2Prdm12*. While *e1Prdm12* also shows a binding site for PTF1A, *e2Prdm12* shows no binding of ASCL1 or PTF1A.

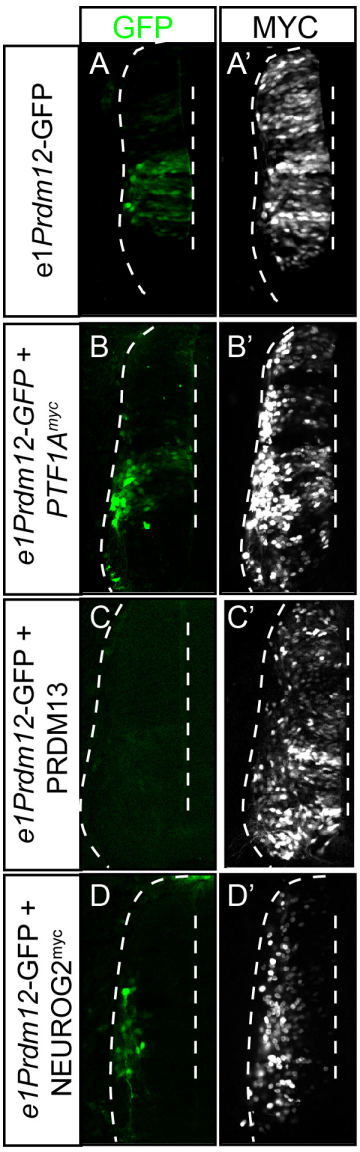

Figure 7-2. PRDM13 suppresses *e1Prdm12* reporter expression
(A) *e1Prdm12* directs reporter expression to the central region of the developing neural tube.
(B) PTF1A localizes reporter expression to the post-mitotic neurons within the ventricular zone, but does not further activate its expression throughout the neural tube.
(C) PRDM13 completely represses reporter expression throughout the developing neural tube.
(D) NEUROG2, like PTF1A (B), localizes reporter expression to the post-mitotic neurons within the ventricular zone, but does not further activate its expression throughout the neural tube.
(A'-D') myc expression indicates the electroporation efficiency across the dorsal/ventral axis of the neural tube.

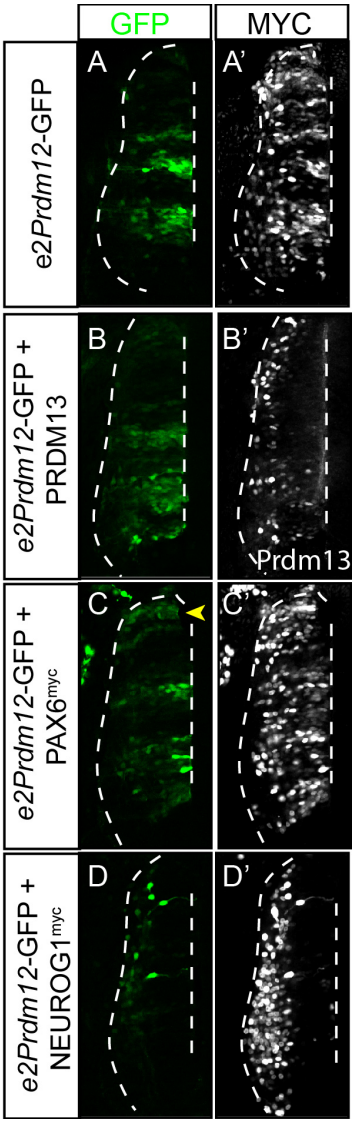

Figure 7-3. PRDM13 restricts *e2Prdm12* reporter expression
(A) *e2Prdm12* directs reporter expression to the central region of the developing neural tube.
(B) PRDM13 somewhat represses reporter expression throughout the developing neural tube.
(C) PAX6 activates reporter expression to the dorsal-most region of the developing neural tube.
(D) NEUROG1 localizes reporter expression to the post-mitotic neurons within the ventricular zone, but does not further activate its expression throughout the neural tube.
(A'-D') myc expression indicates the electroporation efficiency across the dorsal/ventral axis of the neural tube.

CHAPTER EIGHT

Future Directions

The data presented here has served to elucidate several aspects of PRDM13 function within the dorsal spinal cord. I confirm PRDM13 functions to specify the dI4 interneuron population by suppressing the excitatory neuronal program. Through the generation of *Prdm13* null mice, I identified a novel feedback loop for PRDM13 repression of PTF1A through the 2.3Kb *Ptf1a* autoregulatory enhancer. Moreover, PRDM13 is required for repression of ventral transcription factors in the dorsal neural tube and, in this way, mediates proper specification of the dorsal interneuron populations through wide spread suppression of alternative fates. Lastly, PRDM13 is capable of suppressing activity of several class II bHLH factors, possibly through forming complexes on DNA to inhibit activation of their targets.

While these findings help advance the understanding of PRDM13 in the context of neurogenesis, several questions remain. Chick electroporation experiments demonstrated that when overexpressed the zinc-finger domains are sufficient for PRDM13's function in neuronal specification (Chang et al., 2013). Although the ZF mutation generated in mouse seem to confirm this finding, the lack of antibodies detecting the N-terminus of the protein does not allow a firm conclusion on this point. Also, Prdm13$^{\Delta 115}$ is predicted to produce a truncated protein product lacking the PR domain, however, these mice still produce the C-terminus of the protein and the animals survive. It will be necessary to analyse the neural tubes of the Prdm13delta2/3 mutant that deletes the PR domain in order to assess the *in vivo* contributions of this protein domain to PRDM13 function.

PRDM13 regulation of PTF1A may serve as a mechanism to modulate PTF1A levels within the dorsal spinal cord. Moreover, the lack of PRDM13 expression in the pancreas may

allow for persistent PTF1A expression in this tissue and not in the spinal cord. PRDM13 and PTF1A are co-expressed in several regions of the CNS such as the retina and cerebellum. While some understanding of PRDM13 function in the retina has emerged, its role in the cerebellum within the context of PTF1A remains unknown. Given that PTF1A is also transiently expressed in these two neural tissues, it will be important to determine whether PRDM13 modulates PTF1A expression within these tissues as well (Dong et al., 2008; Dullin et al., 2007; Fujitani et al., 2006; Glasgow et al., 2005; Hoshino et al., 2005; Masui et al., 2007; Meredith et al., 2009; Nakhai et al., 2007).

The experiments presented here support a model where PRDM13 requires binding to a co-factor in order to interact with DNA. The lack of a unique binding motif, along with PRDM13 enrichment at several motifs including E-boxes, and its ability to interact with bHLH TFs *in vitro* suggest these factors are capable of complexing with PRDM13 and bind to DNA. ChIP-Seq data for PTF1A and ASCL1 found they bind to many of the sites where PRDM13 is found *in vivo*. Given PRDM13 can antagonize several class II factors expressed within the dorsal neural tube, one of the questions remaining is how it can be specifically recruited to particular sites by these different bHLH factors. This is particularly intriguing within the dP4 domain, where both PTF1A and ASCL1 are expressed. Additionally, motifs for SOX, RFX and NKX factors were also enriched in the ChIP-Seq data for PRDM13, suggesting it may be able to interact with these factors to modulate other gene targets. Understanding of these interactions will provide further insight on PRDM13 function and shed light on how PRDM13 can be targeted to a wide variety of genomic sites.

The RNA-Seq data also identified a number of other neural factors that are misregulated in the absence of PRDM13. Understanding the role of these genes may reveal further functions

of PRDM13 within the dorsal interneuron populations. Specifically, the results presented here find the dI2 interneuron population is depleted in mice lacking PRDM13 protein expression. It is necessary to gain understanding of how PRDM13 may function to specify this population. Additionally, the differential regulation of LMB1X and ISL1 independently from TLX1/3 is a novel function for PRDM13 that is not yet fully understood. The mechanism by which PRDM13 can be recruited to a variety of genomic targets and independently regulate their expression will be necessary to answer some of these pending questions.

Another issue that remains is whether PRDM13 possesses intrinsic HMT activity and the significance of this function *in vivo*. Indeed, previous data suggests PRDM13 does have intrinsic HMT activity, although this was not addressed in a purified system or confirmed *in vivo* (Hanotel et al., 2014). The mouse models described here will serve as informative tools to determine whether this activity is relevant *in vivo*. Further work in determining the protein products made from some of these mouse models will aid in defining the essential domains for PRDM13 function. If the PR domain proves to be expendable it is unlikely PRDM13 has intrinsic HMT activity. If PRDM13 is proven to lack HMT activity, it will be essential to identify novel co-factors recruited to allow for PRDM13 to repress its targets. The PRDM family members that lack endogenous HMT activity are known to recruit histone modifying factors to exert their function. Therefore, it will be informative to determine whether this is the alternative mechanism by which PRDM13 functions.

Given the essential role PRDM13 plays in proper specification of the dorsal interneuron populations, addressing the outstanding questions presented here will be paramount to understanding its mechanism of function. Since the PRDM factors have been implicated in a broad range of developmental decisions and disease models, it is important to gain understanding

of the mechanisms by which they function individually and as a family. Defining the developmental contributions of the distinct protein domains within this family can also be important in understanding how they may function in different contexts. For example, insights from PRDM16 and PRDM3 have shown loss of the PR domain contributes to their function in acute myeloid leukemia, but may have no relevance for normal developmental function (Cohen et al., 2014; Deluche et al., 2008; Duhoux et al., 2012; Harms et al., 2015; Kajimura et al., 2009). Interestingly, data discussed here poses the possibility of distinct PRDM13 domains expresses in different regions in the CNS. This would add to the number of PRDM family members that are differentially expressed in different developmental contexts. Although how this is occurring in PRDM13 is still not understood, other PRDM family members express different isoforms through use alternative start sites or alternative splicing. Given that PRDM13 has been implicated in diseases such as North Carolina macular dystrophy and age-associated changes in sleep quality, it is still necessary to define how PRDM13 functions in these contexts as well. The models and mechanistic inroads presented here will overall contribute to the broader understanding of this family of factors, which continue to place themselves as essential contributors to a variety of developmental processes.

APPENDIX ONE

Generation and characterization of GFP-Prdm13-FUS mice

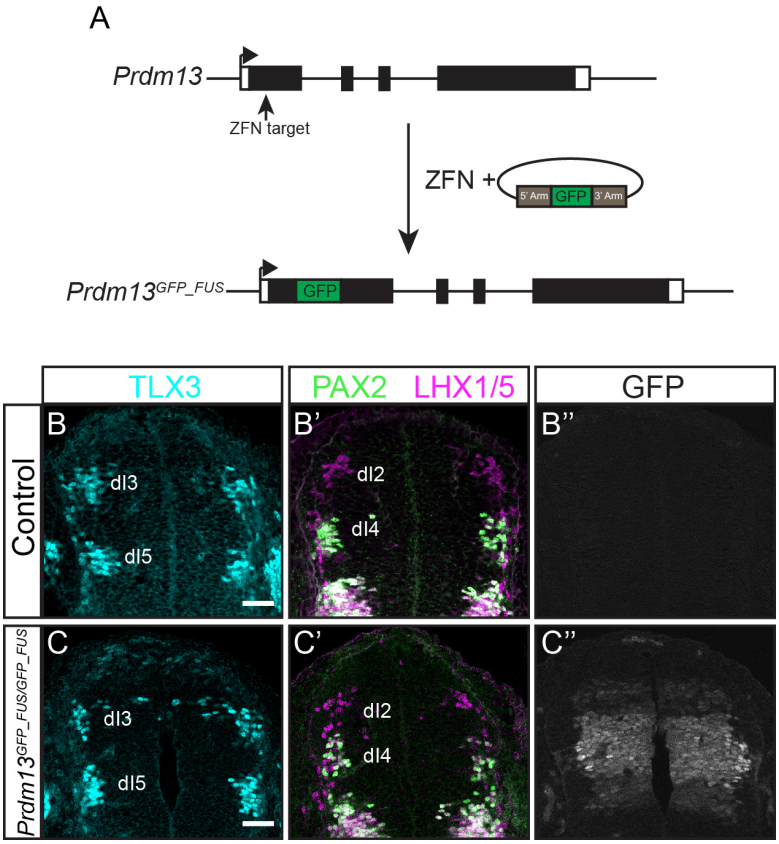

APPENDIX TWO

Generation and characterization of Prdm13-V5 tagged mice

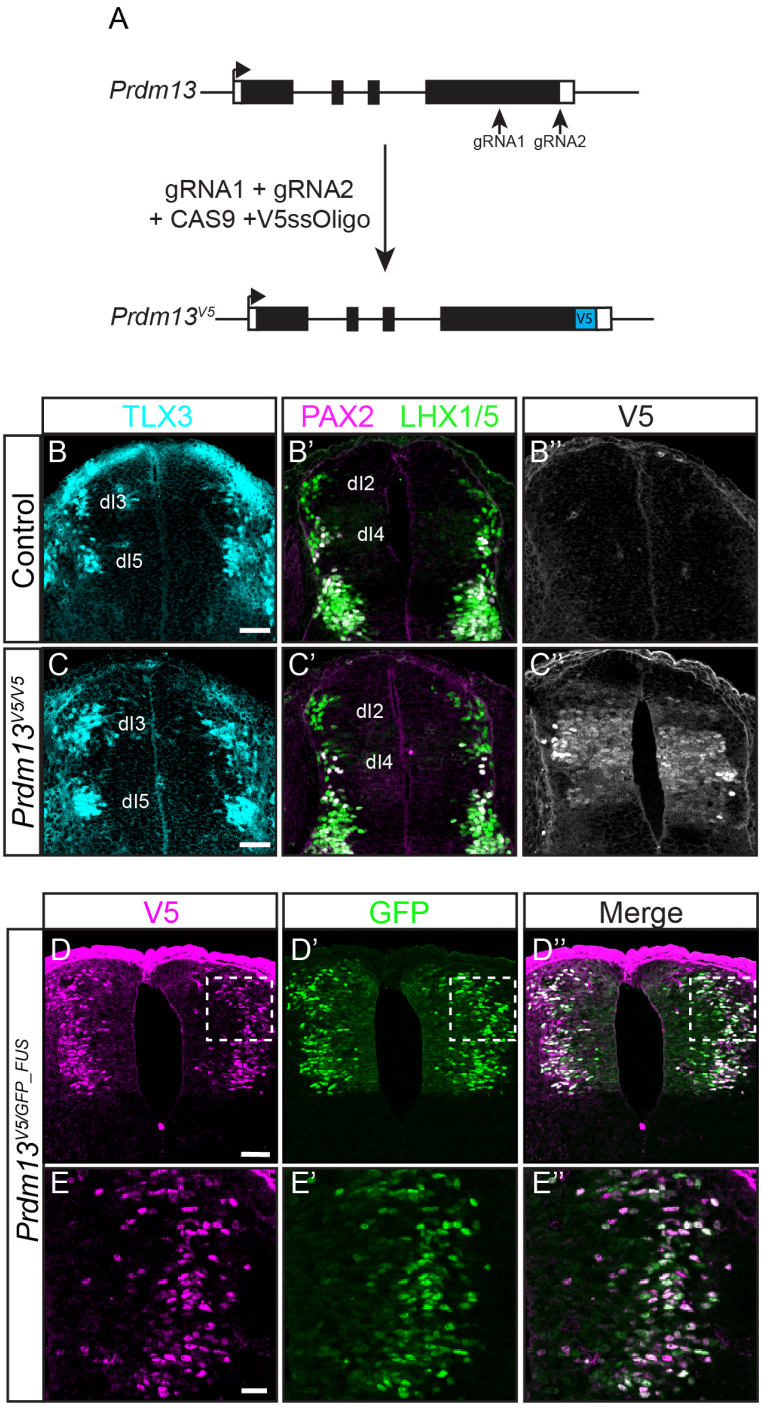

APPENDIX THREE

PRDM13/bHLH interaction analysis

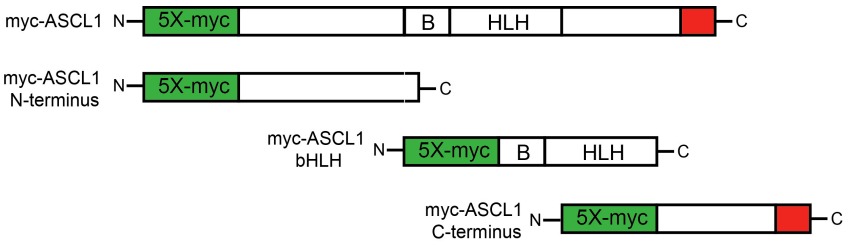

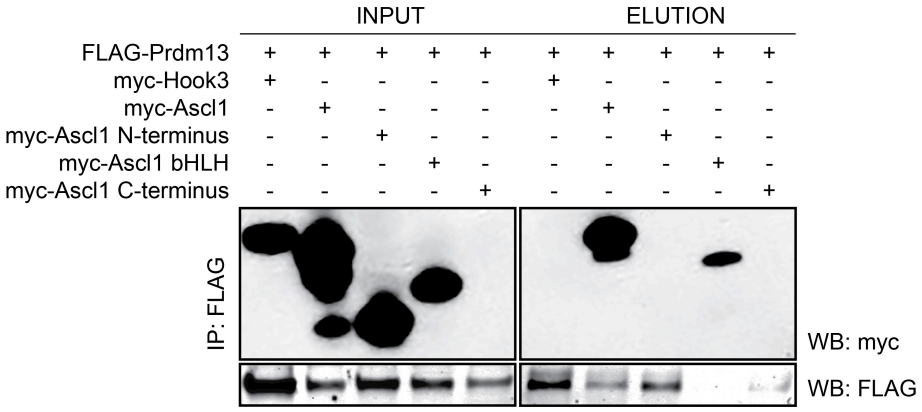

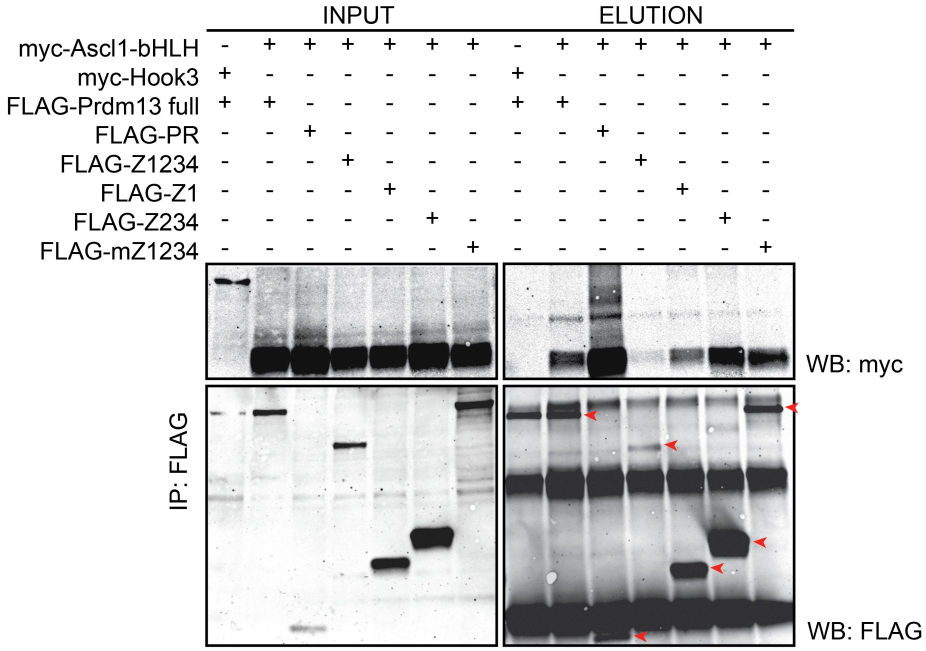

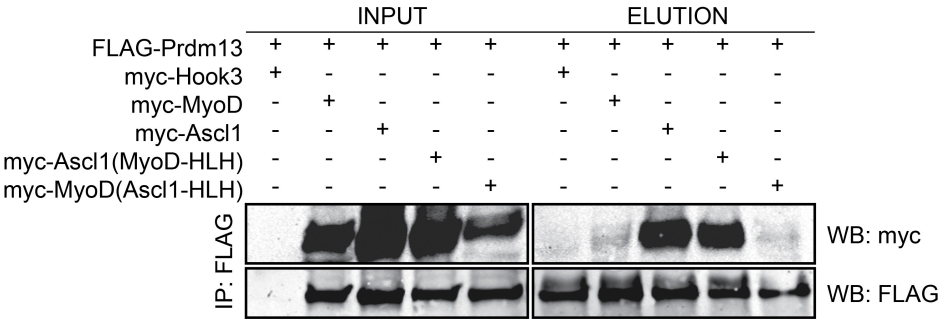
INPUT
ELUTION
FLAG-Prdm13 + + + + + + + + + +
myc-Hook3 + - - - - + - - - -
myc-MyoD - + - - - - + - - -
myc-Ascl1 - - + - - - - + - -
myc-Ascl1(MyoD-HLH) - - - + - - - - + -
myc-MyoD(Ascl1-HLH) - - - - + - - - - +
IP: FLAG
WB: myc
WB: FLAG

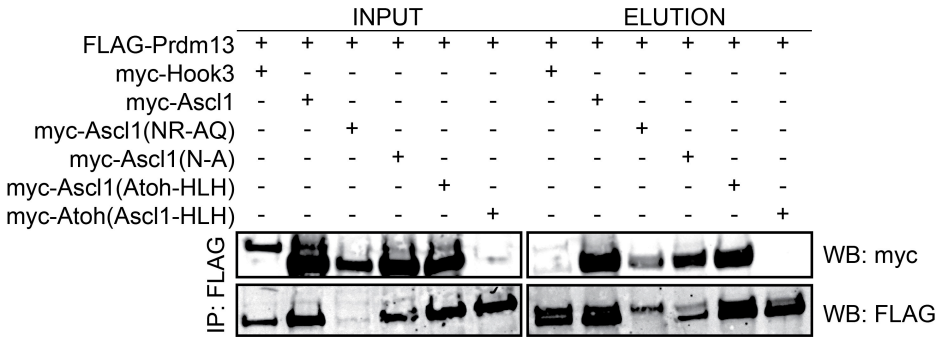
INPUT
ELUTION
FLAG-Prdm13 + + + + + + + + + + + +
myc-Hook3 + - - - - - + - - - - -
myc-Ascl1 - + - - - - - + - - - -
myc-Ascl1(NR-AQ) - - + - - - - - + - - -
myc-Ascl1(N-A) - - - + - - - - - + - -
myc-Ascl1(Atoh-HLH) - - - - + - - - - - + -
myc-Atoh(Ascl1-HLH) - - - - - + - - - - - +
IP: FLAG
WB: myc
WB: FLAG

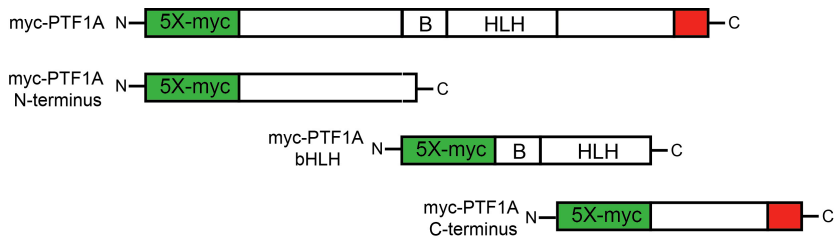
myc-PTF1A N 5X-myc B HLH C
myc-PTF1A N-terminus N 5X-myc C
myc-PTF1A bHLH N 5X-myc B HLH C
myc-PTF1A C-terminus N 5X-myc C

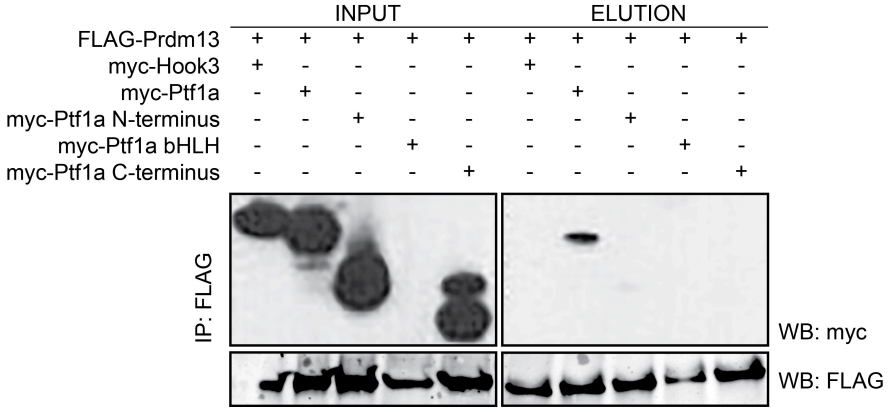
INPUT
ELUTION
FLAG-Prdm13 + + + + + + + + + +
myc-Hook3 + - - - - + - - - -
myc-Ptf1a - + - - - - + - - -
myc-Ptf1a N-terminus - - + - - - - + - -
myc-Ptf1a bHLH - - - + - - - - + -
myc-Ptf1a C-terminus - - - - + - - - - +
IP: FLAG
WB: myc
WB: FLAG

APPENDIX FOUR

Putative direct targets of PRDM13

Gene	Prdm13 Het NT Rep1	Prdm13 Het NT Rep2	Prdm13 Homo NT Rep1	Prdm13 Homo NT Rep2	Prdm13 Het Average	Prdm13 Homo Average	FC(Homo/ Het)
Olig2	0.0	0.0	17.0	21.3	0.0	19.2	1710.5
Olig1	0.0	0.1	10.7	11.0	0.0	10.9	288.1
Prdm12	0.6	0.6	13.4	15.4	0.6	14.4	24.2
Tlx3	4.6	5.6	86.2	94.1	5.1	90.1	17.6
Phox2b	1.6	1.6	26.5	27.8	1.6	27.2	17.3
Otp	2.0	2.9	31.4	37.0	2.5	34.2	13.9
Shox2	0.4	0.5	5.9	6.0	0.5	6.0	12.8
Lmx1b	1.8	1.9	22.2	20.9	1.9	21.6	11.6
Kcnn3	0.1	0.1	1.1	1.0	0.1	1.0	8.5
Hip1r	5.4	6.0	42.2	43.9	5.7	43.1	7.6
Ccbe1	1.6	1.7	11.9	11.6	1.7	11.8	7.0
Adamts5	0.5	0.4	3.3	3.2	0.5	3.3	6.8
Syt13	1.5	1.8	8.2	8.9	1.6	8.5	5.3
Dbx1	0.2	0.4	1.4	1.6	0.3	1.5	5.2
Dlx3	0.6	0.6	3.0	3.1	0.6	3.0	5.2
Adcyap1	2.0	1.7	9.5	9.7	1.9	9.6	5.1
Mgat4c	0.3	0.3	1.6	1.6	0.3	1.6	5.1
Hoxd10	0.1	0.2	0.7	0.9	0.2	0.8	5.0
Cyp26a1	0.2	0.2	1.2	0.9	0.2	1.1	4.9
Kcnh7	0.2	0.2	0.8	0.8	0.2	0.8	4.8
Isl1	1.7	1.7	7.8	7.4	1.7	7.6	4.5
Slc1a3	2.6	2.8	12.4	11.4	2.7	11.9	4.4
Tlx1	0.9	0.9	3.8	4.1	0.9	4.0	4.3
Frzb	9.2	9.8	40.9	39.9	9.5	40.4	4.3
Mfng	13.0	16.1	59.4	64.0	14.6	61.7	4.2
Tnfsf13b	0.1	0.2	0.5	0.5	0.1	0.5	4.1
Tmem163	4.5	4.8	17.0	18.0	4.6	17.5	3.8
Neurod4	6.3	6.3	24.2	23.4	6.3	23.8	3.8
Grp	0.2	0.1	0.8	0.3	0.2	0.6	3.7
Ddc	0.5	0.3	1.4	1.3	0.4	1.4	3.6
Crabp1	292.4	301.8	1040.4	1092.6	297.1	1066.5	3.6
Neurog1	9.9	12.5	35.3	42.0	11.2	38.7	3.5
Sox8	2.6	3.1	9.0	9.5	2.9	9.3	3.2
Cacng5	0.2	0.4	1.0	0.8	0.3	0.9	3.2
Rapgef4	0.5	0.4	1.3	1.4	0.4	1.3	3.2

Chrna4	45.2	44.7	134.0	141.0	44.9	137.5	3.1
Vstm2l	6.0	6.2	18.0	19.2	6.1	18.6	3.1
Pou4f1	16.9	18.1	52.9	52.7	17.5	52.8	3.0
Cacna2d1	3.1	2.9	9.3	8.8	3.0	9.1	3.0
Fam84b	1.0	1.1	3.2	3.1	1.1	3.2	3.0
Adcyap1r1	8.6	8.5	24.7	26.2	8.5	25.5	3.0
Dkk3	2.8	2.5	7.5	7.6	2.7	7.6	2.8
Mboat1	1.3	1.1	3.4	3.4	1.2	3.4	2.8
Nrn1	6.0	5.3	14.9	16.7	5.7	15.8	2.8
Kcnk2	2.1	1.7	5.2	5.4	1.9	5.3	2.8
Chrna3	19.3	17.9	50.7	51.1	18.6	50.9	2.7
Oacyl	1.0	0.8	2.1	2.7	0.9	2.4	2.7
Sim1	0.3	0.3	0.7	0.7	0.3	0.7	2.7
Prdm13	113.9	126.8	309.5	324.5	120.4	317.0	2.6
Chrnb4	4.1	4.3	10.9	10.3	4.2	10.6	2.5
Peg10	23.1	23.0	56.7	57.8	23.0	57.2	2.5
Thbs1	0.6	0.6	1.4	1.5	0.6	1.5	2.5
A930009A 15Rik	0.6	0.3	1.0	1.2	0.4	1.1	2.5
Tnfrsf19	5.3	5.7	13.4	13.5	5.5	13.4	2.4
Hspb1	1.7	1.2	3.3	3.9	1.5	3.6	2.4
3110082J2 4Rik	1.7	2.3	4.5	5.3	2.0	4.9	2.4
Gca	0.5	0.6	1.3	1.2	0.5	1.3	2.4
Shb	5.8	6.1	13.1	15.2	6.0	14.1	2.4
Tmtc1	0.6	0.5	1.2	1.4	0.6	1.3	2.4
Cxcl14	0.5	0.3	0.8	1.0	0.4	0.9	2.3
Tchh	1.1	0.9	2.3	2.3	1.0	2.3	2.3
Nefm	37.8	35.9	87.6	83.3	36.8	85.4	2.3
Slc8a2	23.0	26.9	55.6	59.9	24.9	57.7	2.3
Prr15	0.3	0.3	0.6	0.7	0.3	0.7	2.3
Elfn1	2.5	3.2	6.2	6.8	2.8	6.5	2.3
Id1	46.4	53.8	107.9	122.3	50.1	115.1	2.3
Gap43	61.4	60.6	138.1	141.7	61.0	139.9	2.3
Lhx2	0.6	0.7	1.4	1.5	0.7	1.5	2.2
Cck	0.1	0.3	0.5	0.4	0.2	0.5	2.2
Cystm1	0.3	1.0	1.0	1.8	0.6	1.4	2.2
Fgfbp3	7.6	8.0	17.0	17.5	7.8	17.2	2.2
Dcn	0.2	0.2	0.4	0.6	0.2	0.5	2.2
Sp8	1.9	1.8	4.1	4.1	1.9	4.1	2.2
Ephb1	1.9	2.0	4.1	4.4	2.0	4.3	2.2
Casz1	2.1	2.4	4.6	5.1	2.2	4.8	2.2

Rtn4r	3.2	4.0	7.7	7.6	3.6	7.7	2.1
Mbp	2.7	2.2	5.1	5.3	2.4	5.2	2.1
Fbxl7	3.0	3.1	6.3	6.5	3.0	6.4	2.1
Arg1	3.0	4.1	7.4	7.9	3.6	7.6	2.1
Pipox	1.4	1.9	3.6	3.5	1.7	3.6	2.1
Rbp2	0.3	0.2	0.3	0.8	0.3	0.5	2.1
Grb14	0.4	0.4	0.7	0.8	0.4	0.7	2.1
Id4	60.0	61.3	125.8	122.7	60.7	124.2	2.0
Stk17b	7.9	7.9	16.5	15.7	7.9	16.1	2.0
Ifi35	0.3	0.2	0.5	0.6	0.3	0.6	2.0
Veph1	1.3	1.3	2.6	2.6	1.3	2.6	2.0
Adamts9	1.7	1.5	0.8	0.8	1.6	0.8	0.5
Cttnbp2	5.2	5.7	2.6	2.8	5.4	2.7	0.5
Nkx1-1	3.7	4.5	1.7	2.3	4.1	2.0	0.5
Sez6	12.4	14.0	6.2	6.8	13.2	6.5	0.5
Rnf144b	5.7	5.4	2.5	2.9	5.6	2.7	0.5
Lrrtm4	1.2	0.9	0.4	0.6	1.1	0.5	0.5
Tex26	1.1	0.8	0.6	0.3	1.0	0.4	0.5
Hmcn1	0.5	0.5	0.2	0.2	0.5	0.2	0.5
Anks1b	1.7	1.7	0.7	0.9	1.7	0.8	0.5
Plcb4	8.1	7.7	3.6	3.4	7.9	3.5	0.4
Opcml	0.6	0.5	0.2	0.3	0.6	0.2	0.4
Nkain3	1.3	1.4	0.7	0.5	1.3	0.6	0.4
Ptprd	14.8	14.0	6.5	6.1	14.4	6.3	0.4
Mc4r	1.8	2.2	0.9	0.8	2.0	0.9	0.4
Fgf12	0.6	0.6	0.3	0.2	0.6	0.3	0.4
Cap2	2.6	2.6	1.2	1.0	2.6	1.1	0.4
Chsy3	1.7	2.2	0.8	0.8	1.9	0.8	0.4
Slc7a11	0.8	0.7	0.3	0.3	0.8	0.3	0.4
Egfem1	1.0	1.2	0.3	0.6	1.1	0.5	0.4
Prss12	1.0	0.7	0.4	0.3	0.9	0.3	0.4
Npy	10.8	8.6	3.2	4.3	9.7	3.7	0.4
Mecom	3.8	3.3	1.4	1.3	3.5	1.3	0.4
Lypd1	0.5	0.5	0.2	0.2	0.5	0.2	0.4
Gbx2	74.1	77.7	27.3	25.8	75.9	26.5	0.3
Bcas1	2.3	2.1	0.7	0.8	2.2	0.8	0.3
Dok6	0.3	1.0	0.3	0.1	0.7	0.2	0.3
Eno1b	14.9	13.9	4.8	4.9	14.4	4.8	0.3
Cntn1	2.2	2.6	0.9	0.7	2.4	0.8	0.3
Rftn1	2.0	2.2	0.6	0.7	2.1	0.7	0.3
Skor2	8.3	9.7	2.9	2.6	9.0	2.8	0.3

Rph3a	3.2	3.6	0.9	0.9	3.4	0.9	0.3
Cartpt	24.2	24.0	6.7	5.8	24.1	6.3	0.3
Nxph1	2.8	2.9	0.6	0.7	2.8	0.7	0.2
Zfp385b	0.6	0.5	0.2	0.1	0.6	0.1	0.2
Lamp5	95.2	95.5	20.4	20.1	95.4	20.3	0.2
Tfeb	1.9	1.7	0.3	0.4	1.8	0.4	0.2
Prok1	0.6	0.1	0.1	0.0	0.4	0.1	0.2
4-Mar	9.3	10.4	1.8	1.9	9.8	1.8	0.2
Nrxn3	7.9	8.1	1.5	1.4	8.0	1.5	0.2
Olfm4	0.6	1.1	0.3	0.0	0.8	0.2	0.2
Slc32a1	34.3	36.6	6.1	6.6	35.4	6.3	0.2
Lhx1	120.6	131.1	22.3	22.5	125.9	22.4	0.2
Pax8	53.3	54.2	9.3	9.9	53.8	9.6	0.2
Slc6a5	21.0	19.7	3.1	3.8	20.3	3.4	0.2
Pax2	106.4	119.2	17.7	18.6	112.8	18.2	0.2
Esrrb	0.5	0.5	0.1	0.1	0.5	0.1	0.2
Cacng3	2.3	1.8	0.4	0.2	2.0	0.3	0.1
Kcnk9	1.0	1.5	0.3	0.1	1.2	0.2	0.1
Rpp25	10.8	10.7	1.5	0.8	10.7	1.2	0.1
Fam135b	0.5	0.5	0.0	0.0	0.5	0.0	0.1
Col6a4	1.4	1.1	0.1	0.1	1.3	0.1	0.1

RNA-Seq data obtained from FACS sorting of GFP+ cells from *Prdm13*$^{GFP\_KI/GFP\_KI}$ or *Prdm13*$^{GFP\_KI/+}$ cells, extraction and isolation of RNA, followed by sequencing of RNA transcripts.

REFERENCES

Ahn, S., and Joyner, A.L. (2005). In vivo analysis of quiescent adult neural stem cells responding to Sonic hedgehog. Nature *437*, 894-897.

Andzelm, M.M., Cherry, T.J., Harmin, D.A., Boeke, A.C., Lee, C., Hemberg, M., Pawlyk, B., Malik, A.N., Flavell, S.W., Sandberg, M.A., *et al.* (2015). MEF2D drives photoreceptor development through a genome-wide competition for tissue-specific enhancers. Neuron *86*, 247-263.

Ashe, H.L., and Briscoe, J. (2006). The interpretation of morphogen gradients. Development *133*, 385-394.

Balaskas, N., Ribeiro, A., Panovska, J., Dessaud, E., Sasai, N., Page, K.M., Briscoe, J., and Ribes, V. (2012). Gene regulatory logic for reading the Sonic Hedgehog signaling gradient in the vertebrate neural tube. Cell *148*, 273-284.

Barth, K.A., Kishimoto, Y., Rohr, K.B., Seydler, C., Schulte-Merker, S., and Wilson, S.W. (1999). Bmp activity establishes a gradient of positional information throughout the entire neural plate. Development *126*, 4977-4987.

Batista, M.F., and Lewis, K.E. (2008). Pax2/8 act redundantly to specify glycinergic and GABAergic fates of multiple spinal interneurons. Dev Biol *323*, 88-97.

Beres, T.M., Masui, T., Swift, G.H., Shi, L., Henke, R.M., and MacDonald, R.J. (2006). PTF1 is an organ-specific and Notch-independent basic helix-loop-helix complex containing the mammalian Suppressor of Hairless (RBP-J) or its paralogue, RBP-L. Mol Cell Biol *26*, 117-130.

Bertrand, V. (2016). beta-catenin-driven binary cell fate decisions in animal development. Wiley Interdiscip Rev Dev Biol *5*, 377-388.

Biesiada, E., Hamamori, Y., Kedes, L., and Sartorelli, V. (1999). Myogenic basic helix-loop-helix proteins and Sp1 interact as components of a multiprotein transcriptional complex required for activity of the human cardiac alpha-actin promoter. Mol Cell Biol *19*, 2577-2584.

Bikoff, E.K., Morgan, M.A., and Robertson, E.J. (2009). An expanding job description for Blimp-1/PRDM1. Curr Opin Genet Dev *19*, 379-385.

Blackwell, T.K., and Weintraub, H. (1990). Differences and similarities in DNA-binding preferences of MyoD and E2A protein complexes revealed by binding site selection. Science *250*, 1104-1110.

Borromeo, M.D., Meredith, D.M., Castro, D.S., Chang, J.C., Tung, K.C., Guillemot, F., and Johnson, J.E. (2014). A transcription factor network specifying inhibitory versus excitatory neurons in the dorsal spinal cord. Development *141*, 2803-2812.

Briscoe, J., and Small, S. (2015). Morphogen rules: design principles of gradient-mediated embryo patterning. Development *142*, 3996-4009.

Brzezinski, J.A.t., Lamba, D.A., and Reh, T.A. (2010). Blimp1 controls photoreceptor versus bipolar cell fate choice during retinal development. Development *137*, 619-629.

Brzezinski, J.A.t., Uoon Park, K., and Reh, T.A. (2013). Blimp1 (Prdm1) prevents re-specification of photoreceptors into retinal bipolar cells by restricting competence. Dev Biol *384*, 194-204.

Burlison, J.S., Long, Q., Fujitani, Y., Wright, C.V., and Magnuson, M.A. (2008). Pdx-1 and Ptf1a concurrently determine fate specification of pancreatic multipotent progenitor cells. Dev Biol *316*, 74-86.

Castro, D.S., Martynoga, B., Parras, C., Ramesh, V., Pacary, E., Johnston, C., Drechsel, D., Lebel-Potter, M., Garcia, L.G., Hunt, C.*, et al.* (2011). A novel function of the proneural factor Ascl1 in progenitor proliferation identified by genome-wide characterization of its targets. Genes Dev *25*, 930-945.
Castro, D.S., Skowronska-Krawczyk, D., Armant, O., Donaldson, I.J., Parras, C., Hunt, C., Critchley, J.A., Nguyen, L., Gossler, A., Gottgens, B.*, et al.* (2006). Proneural bHLH and Brn proteins coregulate a neurogenic program through cooperative binding to a conserved DNA motif. Dev Cell *11*, 831-844.
Cau, E., and Blader, P. (2009). Notch activity in the nervous system: to switch or not switch? Neural Dev *4*, 36.
Cauthen, C.A., Berdougo, E., Sandler, J., and Burrus, L.W. (2001). Comparative analysis of the expression patterns of Wnts and Frizzleds during early myogenesis in chick embryos. Mech Dev *104*, 133-138.
Chan, S.S., and Kyba, M. (2013). What is a Master Regulator? J Stem Cell Res Ther *3*.
Chang, J.C., Meredith, D.M., Mayer, P.R., Borromeo, M.D., Lai, H.C., Ou, Y.H., and Johnson, J.E. (2013). Prdm13 mediates the balance of inhibitory and excitatory neurons in somatosensory circuits. Dev Cell *25*, 182-195.
Cheng, L., Arata, A., Mizuguchi, R., Qian, Y., Karunaratne, A., Gray, P.A., Arata, S., Shirasawa, S., Bouchard, M., Luo, P.*, et al.* (2004). Tlx3 and Tlx1 are post-mitotic selector genes determining glutamatergic over GABAergic cell fates. Nat Neurosci *7*, 510-517.
Cheng, L., Samad, O.A., Xu, Y., Mizuguchi, R., Luo, P., Shirasawa, S., Goulding, M., and Ma, Q. (2005). Lbx1 and Tlx3 are opposing switches in determining GABAergic versus glutamatergic transmitter phenotypes. Nat Neurosci *8*, 1510-1515.
Chi, J., and Cohen, P. (2016). The Multifaceted Roles of PRDM16: Adipose Biology and Beyond. Trends Endocrinol Metab *27*, 11-23.
Chiang, C., Litingtung, Y., Lee, E., Young, K.E., Corden, J.L., Westphal, H., and Beachy, P.A. (1996). Cyclopia and defective axial patterning in mice lacking Sonic hedgehog gene function. Nature *383*, 407-413.
Chittka, A., Nitarska, J., Grazini, U., and Richardson, W.D. (2012). Transcription factor positive regulatory domain 4 (PRDM4) recruits protein arginine methyltransferase 5 (PRMT5) to mediate histone arginine methylation and control neural stem cell proliferation and differentiation. J Biol Chem *287*, 42995-43006.
Clyde, D.E., Corado, M.S., Wu, X., Pare, A., Papatsenko, D., and Small, S. (2003). A self-organizing system of repressor gradients establishes segmental complexity in Drosophila. Nature *426*, 849-853.
Cockell, M., Stevenson, B.J., Strubin, M., Hagenbuchle, O., and Wellauer, P.K. (1989). Identification of a cell-specific DNA-binding activity that interacts with a transcriptional activator of genes expressed in the acinar pancreas. Mol Cell Biol *9*, 2464-2476.
Cohen, P., Levy, J.D., Zhang, Y., Frontini, A., Kolodin, D.P., Svensson, K.J., Lo, J.C., Zeng, X., Ye, L., Khandekar, M.J.*, et al.* (2014). Ablation of PRDM16 and beige adipose causes metabolic dysfunction and a subcutaneous to visceral fat switch. Cell *156*, 304-316.
Costamagna, D., Quattrocelli, M., Duelen, R., Sahakyan, V., Perini, I., Palazzolo, G., and Sampaolesi, M. (2014). Fate choice of post-natal mesoderm progenitors: skeletal versus cardiac muscle plasticity. Cell Mol Life Sci *71*, 615-627.
Dalton, S. (2013). Signaling networks in human pluripotent stem cells. Curr Opin Cell Biol *25*, 241-246.

Davis, R.L., Weintraub, H., and Lassar, A.B. (1987). Expression of a single transfected cDNA converts fibroblasts to myoblasts. Cell *51*, 987-1000.
de la Serna, I.L., Carlson, K.A., and Imbalzano, A.N. (2001). Mammalian SWI/SNF complexes promote MyoD-mediated muscle differentiation. Nat Genet *27*, 187-190.
Deluche, L., Joha, S., Corm, S., Daudignon, A., Geffroy, S., Quief, S., Villenet, C., Kerckaert, J.P., Lai, J.L., Preudhomme, C.*, et al.* (2008). Cryptic and partial deletions of PRDM16 and RUNX1 without t(1;21)(p36;q22) and/or RUNX1-PRDM16 fusion in a case of progressive chronic myeloid leukemia: a complex chromosomal rearrangement of underestimated frequency in disease progression? Genes Chromosomes Cancer *47*, 1110-1117.
Di Zazzo, E., De Rosa, C., Abbondanza, C., and Moncharmont, B. (2013). PRDM Proteins: Molecular Mechanisms in Signal Transduction and Transcriptional Regulation. Biology (Basel) *2*, 107-141.
Dong, P.D., Provost, E., Leach, S.D., and Stainier, D.Y. (2008). Graded levels of Ptf1a differentially regulate endocrine and exocrine fates in the developing pancreas. Genes Dev *22*, 1445-1450.
Driever, W., and Nusslein-Volhard, C. (1988). A gradient of bicoid protein in Drosophila embryos. Cell *54*, 83-93.
Du, Y., Jenkins, N.A., and Copeland, N.G. (2005). Insertional mutagenesis identifies genes that promote the immortalization of primary bone marrow progenitor cells. Blood *106*, 3932-3939.
Duhoux, F.P., Ameye, G., Montano-Almendras, C.P., Bahloula, K., Mozziconacci, M.J., Laibe, S., Wlodarska, I., Michaux, L., Talmant, P., Richebourg, S.*, et al.* (2012). PRDM16 (1p36) translocations define a distinct entity of myeloid malignancies with poor prognosis but may also occur in lymphoid malignancies. Br J Haematol *156*, 76-88.
Dullin, J.P., Locker, M., Robach, M., Henningfeld, K.A., Parain, K., Afelik, S., Pieler, T., and Perron, M. (2007). Ptf1a triggers GABAergic neuronal cell fates in the retina. BMC Dev Biol *7*, 110.
Dyson, S., and Gurdon, J.B. (1998). The interpretation of position in a morphogen gradient as revealed by occupancy of activin receptors. Cell *93*, 557-568.
Eom, G.H., Kim, K., Kim, S.M., Kee, H.J., Kim, J.Y., Jin, H.M., Kim, J.R., Kim, J.H., Choe, N., Kim, K.B.*, et al.* (2009). Histone methyltransferase PRDM8 regulates mouse testis steroidogenesis. Biochem Biophys Res Commun *388*, 131-136.
Eram, M.S., Bustos, S.P., Lima-Fernandes, E., Siarheyeva, A., Senisterra, G., Hajian, T., Chau, I., Duan, S., Wu, H., Dombrovski, L.*, et al.* (2014). Trimethylation of histone H3 lysine 36 by human methyltransferase PRDM9 protein. J Biol Chem *289*, 12177-12188.
Ericson, J., Briscoe, J., Rashbass, P., van Heyningen, V., and Jessell, T.M. (1997). Graded sonic hedgehog signaling and the specification of cell fate in the ventral neural tube. Cold Spring Harb Symp Quant Biol *62*, 451-466.
Ferrell, J.E., Jr. (1999). Building a cellular switch: more lessons from a good egg. Bioessays *21*, 866-870.
Fitzgerald, M. (2005). The development of nociceptive circuits. Nat Rev Neurosci *6*, 507-520.
Fog, C.K., Galli, G.G., and Lund, A.H. (2012). PRDM proteins: important players in differentiation and disease. Bioessays *34*, 50-60.
Fruhbeck, G., Sesma, P., and Burrell, M.A. (2009). PRDM16: the interconvertible adipo-myocyte switch. Trends Cell Biol *19*, 141-146.

Fujitani, Y., Fujitani, S., Luo, H., Qiu, F., Burlison, J., Long, Q., Kawaguchi, Y., Edlund, H., MacDonald, R.J., Furukawa, T.*, et al.* (2006). Ptf1a determines horizontal and amacrine cell fates during mouse retinal development. Development *133*, 4439-4450.
Fukuda, A., Kawaguchi, Y., Furuyama, K., Kodama, S., Horiguchi, M., Kuhara, T., Kawaguchi, M., Terao, M., Doi, R., Wright, C.V.*, et al.* (2008). Reduction of Ptf1a gene dosage causes pancreatic hypoplasia and diabetes in mice. Diabetes *57*, 2421-2431.
Glasgow, S.M., Henke, R.M., Macdonald, R.J., Wright, C.V., and Johnson, J.E. (2005). Ptf1a determines GABAergic over glutamatergic neuronal cell fate in the spinal cord dorsal horn. Development *132*, 5461-5469.
Graham, T.G., Tabei, S.M., Dinner, A.R., and Rebay, I. (2010). Modeling bistable cell-fate choices in the Drosophila eye: qualitative and quantitative perspectives. Development *137*, 2265-2278.
Green, J.B., and Smith, J.C. (1991). Growth factors as morphogens: do gradients and thresholds establish body plan? Trends Genet *7*, 245-250.
Gustafsson, M.K., Pan, H., Pinney, D.F., Liu, Y., Lewandowski, A., Epstein, D.J., and Emerson, C.P., Jr. (2002). Myf5 is a direct target of long-range Shh signaling and Gli regulation for muscle specification. Genes Dev *16*, 114-126.
Hanotel, J., Bessodes, N., Thelie, A., Hedderich, M., Parain, K., Van Driessche, B., Brandao Kde, O., Kricha, S., Jorgensen, M.C., Grapin-Botton, A.*, et al.* (2014). The Prdm13 histone methyltransferase encoding gene is a Ptf1a-Rbpj downstream target that suppresses glutamatergic and promotes GABAergic neuronal fate in the dorsal neural tube. Dev Biol *386*, 340-357.
Harms, M.J., Ishibashi, J., Wang, W., Lim, H.W., Goyama, S., Sato, T., Kurokawa, M., Won, K.J., and Seale, P. (2014). Prdm16 is required for the maintenance of brown adipocyte identity and function in adult mice. Cell Metab *19*, 593-604.
Harms, M.J., Lim, H.W., Ho, Y., Shapira, S.N., Ishibashi, J., Rajakumari, S., Steger, D.J., Lazar, M.A., Won, K.J., and Seale, P. (2015). PRDM16 binds MED1 and controls chromatin architecture to determine a brown fat transcriptional program. Genes Dev *29*, 298-307.
Heinz, S., Benner, C., Spann, N., Bertolino, E., Lin, Y.C., Laslo, P., Cheng, J.X., Murre, C., Singh, H., and Glass, C.K. (2010). Simple combinations of lineage-determining transcription factors prime cis-regulatory elements required for macrophage and B cell identities. Mol Cell *38*, 576-589.
Helms, A.W., Battiste, J., Henke, R.M., Nakada, Y., Simplicio, N., Guillemot, F., and Johnson, J.E. (2005). Sequential roles for Mash1 and Ngn2 in the generation of dorsal spinal cord interneurons. Development *132*, 2709-2719.
Helms, A.W., and Johnson, J.E. (2003). Specification of dorsal spinal cord interneurons. Curr Opin Neurobiol *13*, 42-49.
Henke, R.M., Meredith, D.M., Borromeo, M.D., Savage, T.K., and Johnson, J.E. (2009). Ascl1 and Neurog2 form novel complexes and regulate Delta-like3 (Dll3) expression in the neural tube. Dev Biol *328*, 529-540.
Hohenauer, T., and Moore, A.W. (2012). The Prdm family: expanding roles in stem cells and development. Development *139*, 2267-2282.
Hollyday, M., McMahon, J.A., and McMahon, A.P. (1995). Wnt expression patterns in chick embryo nervous system. Mech Dev *52*, 9-25.
Hori, K., Cholewa-Waclaw, J., Nakada, Y., Glasgow, S.M., Masui, T., Henke, R.M., Wildner, H., Martarelli, B., Beres, T.M., Epstein, J.A.*, et al.* (2008). A nonclassical bHLH Rbpj transcription

factor complex is required for specification of GABAergic neurons independent of Notch signaling. Genes Dev *22*, 166-178.
Hoshino, M., Nakamura, S., Mori, K., Kawauchi, T., Terao, M., Nishimura, Y.V., Fukuda, A., Fuse, T., Matsuo, N., Sone, M.*, et al.* (2005). Ptf1a, a bHLH transcriptional gene, defines GABAergic neuronal fates in cerebellum. Neuron *47*, 201-213.
Huang, S., Shao, G., and Liu, L. (1998). The PR domain of the Rb-binding zinc finger protein RIZ1 is a protein binding interface and is related to the SET domain functioning in chromatin-mediated gene expression. J Biol Chem *273*, 15933-15939.
Iida, S., Chen, W., Nakadai, T., Ohkuma, Y., and Roeder, R.G. (2015). PRDM16 enhances nuclear receptor-dependent transcription of the brown fat-specific Ucp1 gene through interactions with Mediator subunit MED1. Genes Dev *29*, 308-321.
Inoue, M., Kuroda, T., Honda, A., Komabayashi-Suzuki, M., Komai, T., Shinkai, Y., and Mizutani, K. (2014). Prdm8 regulates the morphological transition at multipolar phase during neocortical development. PLoS One *9*, e86356.
Johnson, J.E., Birren, S.J., and Anderson, D.J. (1990). Two rat homologues of Drosophila achaete-scute specifically expressed in neuronal precursors. Nature *346*, 858-861.
Johnson, J.E., Birren, S.J., Saito, T., and Anderson, D.J. (1992). DNA binding and transcriptional regulatory activity of mammalian achaete-scute homologous (MASH) proteins revealed by interaction with a muscle-specific enhancer. Proc Natl Acad Sci U S A *89*, 3596-3600.
Jung, C.C., Atan, D., Ng, D., Ploder, L., Ross, S.E., Klein, M., Birch, D.G., Diez, E., and McInnes, R.R. (2015). Transcription factor PRDM8 is required for rod bipolar and type 2 OFF-cone bipolar cell survival and amacrine subtype identity. Proc Natl Acad Sci U S A *112*, E3010-3019.
Junker, J.P., Peterson, K.A., Nishi, Y., Mao, J., McMahon, A.P., and van Oudenaarden, A. (2014). A predictive model of bifunctional transcription factor signaling during embryonic tissue patterning. Dev Cell *31*, 448-460.
Kageyama, R., Ohtsuka, T., Hatakeyama, J., and Ohsawa, R. (2005). Roles of bHLH genes in neural stem cell differentiation. Exp Cell Res *306*, 343-348.
Kajimura, S., Seale, P., Kubota, K., Lunsford, E., Frangioni, J.V., Gygi, S.P., and Spiegelman, B.M. (2009). Initiation of myoblast to brown fat switch by a PRDM16-C/EBP-beta transcriptional complex. Nature *460*, 1154-1158.
Kajimura, S., Seale, P., Tomaru, T., Erdjument-Bromage, H., Cooper, M.P., Ruas, J.L., Chin, S., Tempst, P., Lazar, M.A., and Spiegelman, B.M. (2008). Regulation of the brown and white fat gene programs through a PRDM16/CtBP transcriptional complex. Genes Dev *22*, 1397-1409.
Katoh, K., Omori, Y., Onishi, A., Sato, S., Kondo, M., and Furukawa, T. (2010). Blimp1 suppresses Chx10 expression in differentiating retinal photoreceptor precursors to ensure proper photoreceptor development. J Neurosci *30*, 6515-6526.
Kawaguchi, Y., Cooper, B., Gannon, M., Ray, M., MacDonald, R.J., and Wright, C.V. (2002). The role of the transcriptional regulator Ptf1a in converting intestinal to pancreatic progenitors. Nat Genet *32*, 128-134.
Kim, D., Pertea, G., Trapnell, C., Pimentel, H., Kelley, R., and Salzberg, S.L. (2013). TopHat2: accurate alignment of transcriptomes in the presence of insertions, deletions and gene fusions. Genome Biol *14*, R36.

Kim, E.J., Battiste, J., Nakagawa, Y., and Johnson, J.E. (2008). Ascl1 (Mash1) lineage cells contribute to discrete cell populations in CNS architecture. Mol Cell Neurosci *38*, 595-606.
Kinameri, E., Inoue, T., Aruga, J., Imayoshi, I., Kageyama, R., Shimogori, T., and Moore, A.W. (2008). Prdm proto-oncogene transcription factor family expression and interaction with the Notch-Hes pathway in mouse neurogenesis. PLoS One *3*, e3859.
Knoepfler, P.S., Bergstrom, D.A., Uetsuki, T., Dac-Korytko, I., Sun, Y.H., Wright, W.E., Tapscott, S.J., and Kamps, M.P. (1999). A conserved motif N-terminal to the DNA-binding domains of myogenic bHLH transcription factors mediates cooperative DNA binding with pbx-Meis1/Prep1. Nucleic Acids Res *27*, 3752-3761.
Krapp, A., Knofler, M., Frutiger, S., Hughes, G.J., Hagenbuchle, O., and Wellauer, P.K. (1996). The p48 DNA-binding subunit of transcription factor PTF1 is a new exocrine pancreas-specific basic helix-loop-helix protein. EMBO J *15*, 4317-4329.
Krapp, A., Knofler, M., Ledermann, B., Burki, K., Berney, C., Zoerkler, N., Hagenbuchle, O., and Wellauer, P.K. (1998). The bHLH protein PTF1-p48 is essential for the formation of the exocrine and the correct spatial organization of the endocrine pancreas. Genes Dev *12*, 3752-3763.
Kraut, R., and Levine, M. (1991). Mutually repressive interactions between the gap genes giant and Kruppel define middle body regions of the Drosophila embryo. Development *111*, 611-621.
Kutejova, E., Sasai, N., Shah, A., Gouti, M., and Briscoe, J. (2016). Neural Progenitors Adopt Specific Identities by Directly Repressing All Alternative Progenitor Transcriptional Programs. Dev Cell *36*, 639-653.
Lai, H.C., Klisch, T.J., Roberts, R., Zoghbi, H.Y., and Johnson, J.E. (2011). In vivo neuronal subtype-specific targets of Atoh1 (Math1) in dorsal spinal cord. J Neurosci *31*, 10859-10871.
Lai, K., Kaspar, B.K., Gage, F.H., and Schaffer, D.V. (2003). Sonic hedgehog regulates adult neural progenitor proliferation in vitro and in vivo. Nat Neurosci *6*, 21-27.
Langmead, B., and Salzberg, S.L. (2012). Fast gapped-read alignment with Bowtie 2. Nat Methods *9*, 357-359.
Lewis, J., Slack, J.M., and Wolpert, L. (1977). Thresholds in development. J Theor Biol *65*, 579-590.
Li, H., Handsaker, B., Wysoker, A., Fennell, T., Ruan, J., Homer, N., Marth, G., Abecasis, G., Durbin, R., and Genome Project Data Processing, S. (2009). The Sequence Alignment/Map format and SAMtools. Bioinformatics *25*, 2078-2079.
Liang, H.L., Nien, C.Y., Liu, H.Y., Metzstein, M.M., Kirov, N., and Rushlow, C. (2008). The zinc-finger protein Zelda is a key activator of the early zygotic genome in Drosophila. Nature *456*, 400-403.
Liao, Y., Smyth, G.K., and Shi, W. (2014). featureCounts: an efficient general purpose program for assigning sequence reads to genomic features. Bioinformatics *30*, 923-930.
Litingtung, Y., and Chiang, C. (2000). Specification of ventral neuron types is mediated by an antagonistic interaction between Shh and Gli3. Nat Neurosci *3*, 979-985.
Liu, F., Morrison, A.H., and Gregor, T. (2013). Dynamic interpretation of maternal inputs by the Drosophila segmentation gene network. Proc Natl Acad Sci U S A *110*, 6724-6729.
Liu, Y., and Ma, Q. (2011). Generation of somatic sensory neuron diversity and implications on sensory coding. Curr Opin Neurobiol *21*, 52-60.

Lo, L.C., Johnson, J.E., Wuenschell, C.W., Saito, T., and Anderson, D.J. (1991). Mammalian achaete-scute homolog 1 is transiently expressed by spatially restricted subsets of early neuroepithelial and neural crest cells. Genes Dev *5*, 1524-1537.
Machold, R., Hayashi, S., Rutlin, M., Muzumdar, M.D., Nery, S., Corbin, J.G., Gritli-Linde, A., Dellovade, T., Porter, J.A., Rubin, L.L.*, et al.* (2003). Sonic hedgehog is required for progenitor cell maintenance in telencephalic stem cell niches. Neuron *39*, 937-950.
Marro, S., Pang, Z.P., Yang, N., Tsai, M.C., Qu, K., Chang, H.Y., Sudhof, T.C., and Wernig, M. (2011). Direct lineage conversion of terminally differentiated hepatocytes to functional neurons. Cell Stem Cell *9*, 374-382.
Masui, T., Long, Q., Beres, T.M., Magnuson, M.A., and MacDonald, R.J. (2007). Early pancreatic development requires the vertebrate Suppressor of Hairless (RBPJ) in the PTF1 bHLH complex. Genes Dev *21*, 2629-2643.
Masui, T., Swift, G.H., Deering, T., Shen, C., Coats, W.S., Long, Q., Elsasser, H.P., Magnuson, M.A., and MacDonald, R.J. (2010). Replacement of Rbpj with Rbpjl in the PTF1 complex controls the final maturation of pancreatic acinar cells. Gastroenterology *139*, 270-280.
Masui, T., Swift, G.H., Hale, M.A., Meredith, D.M., Johnson, J.E., and Macdonald, R.J. (2008). Transcriptional autoregulation controls pancreatic Ptf1a expression during development and adulthood. Mol Cell Biol *28*, 5458-5468.
McLean, C.Y., Bristor, D., Hiller, M., Clarke, S.L., Schaar, B.T., Lowe, C.B., Wenger, A.M., and Bejerano, G. (2010). GREAT improves functional interpretation of cis-regulatory regions. Nat Biotechnol *28*, 495-501.
Megason, S.G., and McMahon, A.P. (2002). A mitogen gradient of dorsal midline Wnts organizes growth in the CNS. Development *129*, 2087-2098.
Mekki-Dauriac, S., Agius, E., Kan, P., and Cochard, P. (2002). Bone morphogenetic proteins negatively control oligodendrocyte precursor specification in the chick spinal cord. Development *129*, 5117-5130.
Meredith, D.M., Borromeo, M.D., Deering, T.G., Casey, B.H., Savage, T.K., Mayer, P.R., Hoang, C., Tung, K.C., Kumar, M., Shen, C.*, et al.* (2013). Program specificity for Ptf1a in pancreas versus neural tube development correlates with distinct collaborating cofactors and chromatin accessibility. Mol Cell Biol *33*, 3166-3179.
Meredith, D.M., Masui, T., Swift, G.H., MacDonald, R.J., and Johnson, J.E. (2009). Multiple transcriptional mechanisms control Ptf1a levels during neural development including autoregulation by the PTF1-J complex. J Neurosci *29*, 11139-11148.
Merkle, F.T., and Alvarez-Buylla, A. (2006). Neural stem cells in mammalian development. Curr Opin Cell Biol *18*, 704-709.
Millen, K.J., Steshina, E.Y., Iskusnykh, I.Y., and Chizhikov, V.V. (2014). Transformation of the cerebellum into more ventral brainstem fates causes cerebellar agenesis in the absence of Ptf1a function. Proc Natl Acad Sci U S A *111*, E1777-1786.
Mizuguchi, R., Kriks, S., Cordes, R., Gossler, A., Ma, Q., and Goulding, M. (2006). Ascl1 and Gsh1/2 control inhibitory and excitatory cell fate in spinal sensory interneurons. Nat Neurosci *9*, 770-778.
Molkentin, J.D., Black, B.L., Martin, J.F., and Olson, E.N. (1995). Cooperative activation of muscle gene expression by MEF2 and myogenic bHLH proteins. Cell *83*, 1125-1136.
Muroyama, Y., Fujihara, M., Ikeya, M., Kondoh, H., and Takada, S. (2002). Wnt signaling plays an essential role in neuronal specification of the dorsal spinal cord. Genes Dev *16*, 548-553.

Murre, C., Bain, G., van Dijk, M.A., Engel, I., Furnari, B.A., Massari, M.E., Matthews, J.R., Quong, M.W., Rivera, R.R., and Stuiver, M.H. (1994). Structure and function of helix-loop-helix proteins. Biochim Biophys Acta *1218*, 129-135.
Nakada, Y., Hunsaker, T.L., Henke, R.M., and Johnson, J.E. (2004). Distinct domains within Mash1 and Math1 are required for function in neuronal differentiation versus neuronal cell-type specification. Development *131*, 1319-1330.
Nakhai, H., Sel, S., Favor, J., Mendoza-Torres, L., Paulsen, F., Duncker, G.I., and Schmid, R.M. (2007). Ptf1a is essential for the differentiation of GABAergic and glycinergic amacrine cells and horizontal cells in the mouse retina. Development *134*, 1151-1160.
Nishi, Y., Zhang, X., Jeong, J., Peterson, K.A., Vedenko, A., Bulyk, M.L., Hide, W.A., and McMahon, A.P. (2015). A direct fate exclusion mechanism by Sonic hedgehog-regulated transcriptional repressors. Development *142*, 3286-3293.
Nishikata, I., Sasaki, H., Iga, M., Tateno, Y., Imayoshi, S., Asou, N., Nakamura, T., and Morishita, K. (2003). A novel EVI1 gene family, MEL1, lacking a PR domain (MEL1S) is expressed mainly in t(1;3)(p36;q21)-positive AML and blocks G-CSF-induced myeloid differentiation. Blood *102*, 3323-3332.
Novitch, B.G., Chen, A.I., and Jessell, T.M. (2001). Coordinate regulation of motor neuron subtype identity and pan-neuronal properties by the bHLH repressor Olig2. Neuron *31*, 773-789.
Obata, J., Yano, M., Mimura, H., Goto, T., Nakayama, R., Mibu, Y., Oka, C., and Kawaichi, M. (2001). p48 subunit of mouse PTF1 binds to RBP-Jkappa/CBF-1, the intracellular mediator of Notch signalling, and is expressed in the neural tube of early stage embryos. Genes Cells *6*, 345-360.
Ohno, H., Shinoda, K., Spiegelman, B.M., and Kajimura, S. (2012). PPARgamma agonists induce a white-to-brown fat conversion through stabilization of PRDM16 protein. Cell Metab *15*, 395-404.
Oosterveen, T., Kurdija, S., Alekseenko, Z., Uhde, C.W., Bergsland, M., Sandberg, M., Andersson, E., Dias, J.M., Muhr, J., and Ericson, J. (2012). Mechanistic differences in the transcriptional interpretation of local and long-range Shh morphogen signaling. Dev Cell *23*, 1006-1019.
Palma, V., Lim, D.A., Dahmane, N., Sanchez, P., Brionne, T.C., Herzberg, C.D., Gitton, Y., Carleton, A., Alvarez-Buylla, A., and Ruiz i Altaba, A. (2005). Sonic hedgehog controls stem cell behavior in the postnatal and adult brain. Development *132*, 335-344.
Parr, B.A., Shea, M.J., Vassileva, G., and McMahon, A.P. (1993). Mouse Wnt genes exhibit discrete domains of expression in the early embryonic CNS and limb buds. Development *119*, 247-261.
Pascual, M., Abasolo, I., Mingorance-Le Meur, A., Martinez, A., Del Rio, J.A., Wright, C.V., Real, F.X., and Soriano, E. (2007). Cerebellar GABAergic progenitors adopt an external granule cell-like phenotype in the absence of Ptf1a transcription factor expression. Proc Natl Acad Sci U S A *104*, 5193-5198.
Peterson, K.A., Nishi, Y., Ma, W., Vedenko, A., Shokri, L., Zhang, X., McFarlane, M., Baizabal, J.M., Junker, J.P., van Oudenaarden, A.*, et al.* (2012). Neural-specific Sox2 input and differential Gli-binding affinity provide context and positional information in Shh-directed neural patterning. Genes Dev *26*, 2802-2816.
Pimanda, J.E., Ottersbach, K., Knezevic, K., Kinston, S., Chan, W.Y., Wilson, N.K., Landry, J.R., Wood, A.D., Kolb-Kokocinski, A., Green, A.R.*, et al.* (2007). Gata2, Fli1, and Scl form a

recursively wired gene-regulatory circuit during early hematopoietic development. Proc Natl Acad Sci U S A *104*, 17692-17697.
Pinheiro, I., Margueron, R., Shukeir, N., Eisold, M., Fritzsch, C., Richter, F.M., Mittler, G., Genoud, C., Goyama, S., Kurokawa, M.*, et al.* (2012). Prdm3 and Prdm16 are H3K9me1 methyltransferases required for mammalian heterochromatin integrity. Cell *150*, 948-960.
Puri, P.L., Avantaggiati, M.L., Balsano, C., Sang, N., Graessmann, A., Giordano, A., and Levrero, M. (1997). p300 is required for MyoD-dependent cell cycle arrest and muscle-specific gene transcription. EMBO J *16*, 369-383.
Rea, S., Eisenhaber, F., O'Carroll, D., Strahl, B.D., Sun, Z.W., Schmid, M., Opravil, S., Mechtler, K., Ponting, C.P., Allis, C.D.*, et al.* (2000). Regulation of chromatin structure by site-specific histone H3 methyltransferases. Nature *406*, 593-599.
Robinson, M.D., McCarthy, D.J., and Smyth, G.K. (2010). edgeR: a Bioconductor package for differential expression analysis of digital gene expression data. Bioinformatics *26*, 139-140.
Robinson, M.D., and Oshlack, A. (2010). A scaling normalization method for differential expression analysis of RNA-seq data. Genome Biol *11*, R25.
Rose, S.D., and MacDonald, R.J. (1997). Integration of tetracycline regulation into a cell-specific transcriptional enhancer. J Biol Chem *272*, 4735-4739.
Rose, S.D., Swift, G.H., Peyton, M.J., Hammer, R.E., and MacDonald, R.J. (2001). The role of PTF1-P48 in pancreatic acinar gene expression. J Biol Chem *276*, 44018-44026.
Ross, S.E. (2011). Pain and itch: insights into the neural circuits of aversive somatosensation in health and disease. Curr Opin Neurobiol *21*, 880-887.
Ross, S.E., McCord, A.E., Jung, C., Atan, D., Mok, S.I., Hemberg, M., Kim, T.K., Salogiannis, J., Hu, L., Cohen, S.*, et al.* (2012). Bhlhb5 and Prdm8 form a repressor complex involved in neuronal circuit assembly. Neuron *73*, 292-303.
Rudnicki, M.A., Schnegelsberg, P.N., Stead, R.H., Braun, T., Arnold, H.H., and Jaenisch, R. (1993). MyoD or Myf-5 is required for the formation of skeletal muscle. Cell *75*, 1351-1359.
Seale, P., Bjork, B., Yang, W., Kajimura, S., Chin, S., Kuang, S., Scime, A., Devarakonda, S., Conroe, H.M., Erdjument-Bromage, H.*, et al.* (2008). PRDM16 controls a brown fat/skeletal muscle switch. Nature *454*, 961-967.
Seale, P., Conroe, H.M., Estall, J., Kajimura, S., Frontini, A., Ishibashi, J., Cohen, P., Cinti, S., and Spiegelman, B.M. (2011). Prdm16 determines the thermogenic program of subcutaneous white adipose tissue in mice. J Clin Invest *121*, 96-105.
Seale, P., Kajimura, S., Yang, W., Chin, S., Rohas, L.M., Uldry, M., Tavernier, G., Langin, D., and Spiegelman, B.M. (2007). Transcriptional control of brown fat determination by PRDM16. Cell Metab *6*, 38-54.
Sellick, G.S., Barker, K.T., Stolte-Dijkstra, I., Fleischmann, C., Coleman, R.J., Garrett, C., Gloyn, A.L., Edghill, E.L., Hattersley, A.T., Wellauer, P.K.*, et al.* (2004). Mutations in PTF1A cause pancreatic and cerebellar agenesis. Nat Genet *36*, 1301-1305.
Sellick, G.S., Garrett, C., and Houlston, R.S. (2003). A novel gene for neonatal diabetes maps to chromosome 10p12.1-p13. Diabetes *52*, 2636-2638.
Shimizu, K., and Gurdon, J.B. (1999). A quantitative analysis of signal transduction from activin receptor to nucleus and its relevance to morphogen gradient interpretation. Proc Natl Acad Sci U S A *96*, 6791-6796.
Shing, D.C., Trubia, M., Marchesi, F., Radaelli, E., Belloni, E., Tapinassi, C., Scanziani, E., Mecucci, C., Crescenzi, B., Lahortiga, I.*, et al.* (2007). Overexpression of sPRDM16 coupled with loss of p53 induces myeloid leukemias in mice. J Clin Invest *117*, 3696-3707.

Sommer, L., Ma, Q., and Anderson, D.J. (1996). neurogenins, a novel family of atonal-related bHLH transcription factors, are putative mammalian neuronal determination genes that reveal progenitor cell heterogeneity in the developing CNS and PNS. Mol Cell Neurosci *8*, 221-241.
Stamataki, D., Ulloa, F., Tsoni, S.V., Mynett, A., and Briscoe, J. (2005). A gradient of Gli activity mediates graded Sonic Hedgehog signaling in the neural tube. Genes Dev *19*, 626-641.
Struhl, G., Struhl, K., and Macdonald, P.M. (1989). The gradient morphogen bicoid is a concentration-dependent transcriptional activator. Cell *57*, 1259-1273.
Sunadome, K., Suzuki, T., Usui, M., Ashida, Y., and Nishida, E. (2014). Antagonism between the master regulators of differentiation ensures the discreteness and robustness of cell fates. Mol Cell *54*, 526-535.
Tapscott, S.J. (2005). The circuitry of a master switch: Myod and the regulation of skeletal muscle gene transcription. Development *132*, 2685-2695.
Tavares, I., and Lima, D. (2007). From neuroanatomy to gene therapy: searching for new ways to manipulate the supraspinal endogenous pain modulatory system. J Anat *211*, 261-268.
Teboul, L., Summerbell, D., and Rigby, P.W. (2003). The initial somitic phase of Myf5 expression requires neither Shh signaling nor Gli regulation. Genes Dev *17*, 2870-2874.
Thayer, M.J., Tapscott, S.J., Davis, R.L., Wright, W.E., Lassar, A.B., and Weintraub, H. (1989). Positive autoregulation of the myogenic determination gene MyoD1. Cell *58*, 241-248.
Thelie, A., Desiderio, S., Hanotel, J., Quigley, I., Van Driessche, B., Rodari, A., Borromeo, M.D., Kricha, S., Lahaye, F., Croce, J.*, et al.* (2015). Prdm12 specifies V1 interneurons through cross-repressive interactions with Dbx1 and Nkx6 genes in Xenopus. Development *142*, 3416-3428.
Trompouki, E., Bowman, T.V., Lawton, L.N., Fan, Z.P., Wu, D.C., DiBiase, A., Martin, C.S., Cech, J.N., Sessa, A.K., Leblanc, J.L.*, et al.* (2011). Lineage regulators direct BMP and Wnt pathways to cell-specific programs during differentiation and regeneration. Cell *147*, 577-589.
Tutak, E., Satar, M., Yapicioglu, H., Altintas, A., Narli, N., Herguner, O., and Bayram, Y. (2009). A Turkish newborn infant with cerebellar agenesis/neonatal diabetes mellitus and PTF1A mutation. Genet Couns *20*, 147-152.
Vallstedt, A., Muhr, J., Pattyn, A., Pierani, A., Mendelsohn, M., Sander, M., Jessell, T.M., and Ericson, J. (2001). Different levels of repressor activity assign redundant and specific roles to Nkx6 genes in motor neuron and interneuron specification. Neuron *31*, 743-755.
Verma-Kurvari, S., Savage, T., Gowan, K., and Johnson, J.E. (1996). Lineage-specific regulation of the neural differentiation gene MASH1. Dev Biol *180*, 605-617.
Vierbuchen, T., Ostermeier, A., Pang, Z.P., Kokubu, Y., Sudhof, T.C., and Wernig, M. (2010). Direct conversion of fibroblasts to functional neurons by defined factors. Nature *463*, 1035-1041.
Wang, S., Sengel, C., Emerson, M.M., and Cepko, C.L. (2014). A gene regulatory network controls the binary fate decision of rod and bipolar cells in the vertebrate retina. Dev Cell *30*, 513-527.
Wapinski, O.L., Vierbuchen, T., Qu, K., Lee, Q.Y., Chanda, S., Fuentes, D.R., Giresi, P.G., Ng, Y.H., Marro, S., Neff, N.F.*, et al.* (2013). Hierarchical mechanisms for direct reprogramming of fibroblasts to neurons. Cell *155*, 621-635.

Watanabe, S., Sanuki, R., Sugita, Y., Imai, W., Yamazaki, R., Kozuka, T., Ohsuga, M., and Furukawa, T. (2015). Prdm13 regulates subtype specification of retinal amacrine interneurons and modulates visual sensitivity. J Neurosci *35*, 8004-8020.
Weintraub, H., Davis, R., Tapscott, S., Thayer, M., Krause, M., Benezra, R., Blackwell, T.K., Turner, D., Rupp, R., Hollenberg, S.*, et al.* (1991). The myoD gene family: nodal point during specification of the muscle cell lineage. Science *251*, 761-766.
Wijgerde, M., McMahon, J.A., Rule, M., and McMahon, A.P. (2002). A direct requirement for Hedgehog signaling for normal specification of all ventral progenitor domains in the presumptive mammalian spinal cord. Genes Dev *16*, 2849-2864.
Wildner, H., Muller, T., Cho, S.H., Brohl, D., Cepko, C.L., Guillemot, F., and Birchmeier, C. (2006). dILA neurons in the dorsal spinal cord are the product of terminal and non-terminal asymmetric progenitor cell divisions, and require Mash1 for their development. Development *133*, 2105-2113.
Wilson, P.A., Lagna, G., Suzuki, A., and Hemmati-Brivanlou, A. (1997). Concentration-dependent patterning of the Xenopus ectoderm by BMP4 and its signal transducer Smad1. Development *124*, 3177-3184.
Wine-Lee, L., Ahn, K.J., Richardson, R.D., Mishina, Y., Lyons, K.M., and Crenshaw, E.B., 3rd (2004). Signaling through BMP type 1 receptors is required for development of interneuron cell types in the dorsal spinal cord. Development *131*, 5393-5403.
Wolpert, L. (1996). One hundred years of positional information. Trends Genet *12*, 359-364.
Wu, H., Mathioudakis, N., Diagouraga, B., Dong, A., Dombrovski, L., Baudat, F., Cusack, S., de Massy, B., and Kadlec, J. (2013). Molecular basis for the regulation of the H3K4 methyltransferase activity of PRDM9. Cell Rep *5*, 13-20.
Wu, Y., Ferguson, J.E., 3rd, Wang, H., Kelley, R., Ren, R., McDonough, H., Meeker, J., Charles, P.C., Wang, H., and Patterson, C. (2008). PRDM6 is enriched in vascular precursors during development and inhibits endothelial cell proliferation, survival, and differentiation. J Mol Cell Cardiol *44*, 47-58.
Xinh, P.T., Tri, N.K., Nagao, H., Nakazato, H., Taketazu, F., Fujisawa, S., Yagasaki, F., Chen, Y.Z., Hayashi, Y., Toyoda, A.*, et al.* (2003). Breakpoints at 1p36.3 in three MDS/AML(M4) patients with t(1;3)(p36;q21) occur in the first intron and in the 5' region of MEL1. Genes Chromosomes Cancer *36*, 313-316.
Xu, Z., Chen, H., Ling, J., Yu, D., Struffi, P., and Small, S. (2014). Impacts of the ubiquitous factor Zelda on Bicoid-dependent DNA binding and transcription in Drosophila. Genes Dev *28*, 608-621.
Yang, C.M., and Shinkai, Y. (2013). Prdm12 is induced by retinoic acid and exhibits anti-proliferative properties through the cell cycle modulation of P19 embryonic carcinoma cells. Cell Struct Funct *38*, 197-206.
Zannino, D.A., Downes, G.B., and Sagerstrom, C.G. (2014). prdm12b specifies the p1 progenitor domain and reveals a role for V1 interneurons in swim movements. Dev Biol *390*, 247-260.
Zecca, M., Basler, K., and Struhl, G. (1996). Direct and long-range action of a wingless morphogen gradient. Cell *87*, 833-844.
Zecchin, E., Mavropoulos, A., Devos, N., Filippi, A., Tiso, N., Meyer, D., Peers, B., Bortolussi, M., and Argenton, F. (2004). Evolutionary conserved role of ptf1a in the specification of exocrine pancreatic fates. Dev Biol *268*, 174-184.